Rennebohm Hall Building Simulation and Analysis of Energy Monitoring Potential

by

Katherine Rosenau Edwards

A thesis submitted in partial fulfillment of

the requirements for the degree of

Master of Science

(Mechanical Engineering)

at the

UNIVERSITY OF WISCONSIN-MADISON

2006

Approved by

Professor Sanford A. Klein

May 26, 2006

Abstract

This project explores energy saving opportunities for Rennebohm Hall, a campus research facility on the University of Wisconsin-Madison. Building simulation, fault detection, and energy monitoring were investigated as potential tools for saving building energy. The findings of the project underscore the benefits of archiving BAS data to support conducting a systematic monthly review of building energy systems. While the focus here was on a single campus building, some of the findings may be generalized to other facilities.

A systematic review of data collected by the Rennebohm Hall building automation system detected building operational faults that, if not repaired over the course of a year, represent approximately 8% of the estimated annual building heating and cooling energy (4.984E10 Btu, est. $726,000). The methods employed for the data review did not require building simulation and are suggested as a possible energy monitoring strategy for campus facilities. The effects of increasing the building discharge air temperature on energy usage and occupant comfort were explored using building simulation. The energy savings resulting from this control change were estimated at more than 25% of the current building heating and cooling energy requirements. The implications for zone relative humidity levels with the higher discharge air temperature not conclusive and suggest the need for further investigation.

Acknowledgements

I would like to thank my advisors, Professors Sanford Klein and Douglas Reindl. Your guidance, support, and patience have been greatly appreciated. I am very fortunate to have worked with the two of you. You have both my gratitude and my respect.

I am grateful to the University of Wisconsin Physical Plant for its support of this research. In particular I'd like to thank Dan Dudley for his support. I'd like to thank Steve Thiele for archiving the building data every month for a year and for patiently answering my many questions. And, thanks to Kevin Corcoran for his help in locating drawings and equipment information and also for answering my many questions.

Thank you to David Bradley of TESS for your TRNSYS advice and help. I am also grateful to SEL TRNSYS engineers Diego Arias and Michaël Kummert for your help in setting up and trouble shooting the model.

I would also like to thank Professors Timothy Shedd and Greg Nellis for their support and insight. In addition, I owe thanks to Professor John Mitchell for his advice and interest.

I owe many thanks to all the members of the Solar Energy Lab who made the last two years so enjoyable. Diego, Andrea, Curtis, Adam, Terry, Rodrigo, Angie, John, Rory, and all the other students on the 13th floor, thank you.

Thank you to my mother, Marion Rosenau. Your example proved to me that it is indeed possible to return to school, start a new career, and to still care for a family.

Thank you to my husband, Mark Edwards, for encouraging me to pursue a dream.

To my children, Alan, Rebecca, and Elenora Edwards, I owe the most thanks. Thank you for coming with me to lecture when you were home sick from school. Thank you for understanding when homework and research took my time away from you. You mean the world to me and I love you all dearly.

I would like to dedicate this work to the memory of my father, John R. Rosenau, Ph.D., P.E., who started his engineering education here at the University of Wisconsin-Madison. I wish you were here when I learned that I share your passion for engineering.

This work was funded by the John C. Nelson Fellowship and the Chester E. & Flora Jane LeRoy Fellowship.

Table of Contents

List of Figures

List of Tables

Abbreviations and Nomenclature

AHU	Air Handling Unit
BAS	Building Automation System
Btu	British Thermal Unit
CAV	Constant Air Volume
cfm	cubic feet per minute
c_p	Specific Heat at Constant Pressure
HRM	Heat Recovery Module
HRT	Heat
$\dot{m}$	Mass Flow Rate
MER	Mechanical Equipment Room
OA	Outside Air
SA	Supply Air
$\dot{V}$	Volumetric Air Flow Rate
VAV	Variable Air Volume
VFD	Variable Frequency Driv

Chapter 1: Background and Motivation

The energy used in buildings represents a substantial portion of the world's energy consumption and there is a greater potential for energy savings in buildings than in any other energy use sector. Equipment upgrades to existing buildings and energy efficient design of new buildings represent a large potential savings in building energy. However, even buildings designed for energy efficient operation have the potential for significant energy savings when their energy consumption patterns are monitored.

1.1 Building Energy Consumption Trends

Buildings consume a large portion of the world's energy. In the United States, with our diverse climate and our expectations for indoor comfort, the combined residential and commercial building sectors consumed 38.70 quadrillion Btu (11.34 trillion kWh) of energy in 2004, which is 38.8% of the country's annual gross energy consumption (EIA, 2004). With a global energy consumption of 421.5 quadrillion Btu in 2003, the combined sectors of U.S. residential and commercial buildings are responsible for 9 percent of the world's total annual energy use, and serve 5 percent of the world's population (EIA, 2003).

For comparison, the 25 countries of the European Union (EU) report 18.65 quadrillion Btu used by the residential and services sectors (European Commission, 2005). There are some differences in the energy reporting standards between the European data and the US data. For example, the European data separate the energy lost in the conversion of primary fuels to electrical energy and report the final energy consumption of electricity, petroleum products, coal, and natural gas by sector. When electrical losses are similarly

removed from the US data, the combination of residential and commercial sectors is reduced to 19.32 quadrillion Btu, see Figure 1.1 and Figure 1.2. While these values are very similar, especially when some degree of difference in data reported and classification is assumed, the EU has a larger population than the United States (456.4 million people in 2004 versus 290.8 million people in 2003). If the total building energy end use (residential and commercial) is divided by population, the resulting per capita building energy is approximately 40.9 million Btu for the EU, and 66.4 million Btu for the US. (EIA, 2004; European Commission, 2005)

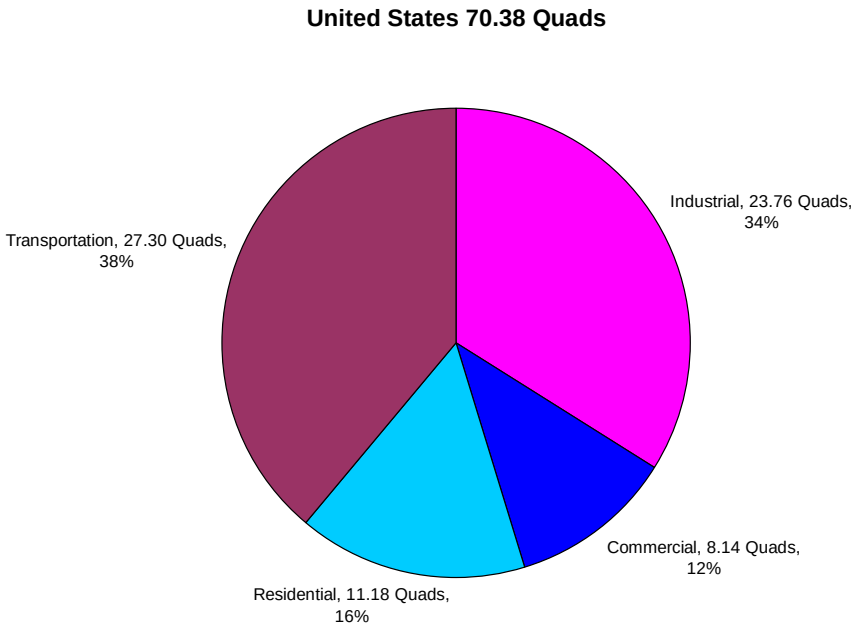

Figure 1.1: Final End Use Energy Consumption for the United States, 2003, in Quadrillion Btu

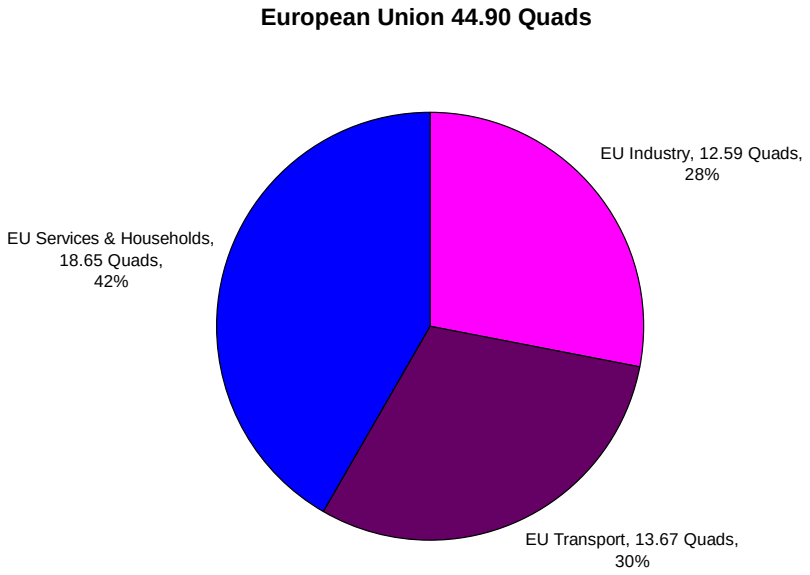

Figure 1.2: Final End Use Energy Consumption for the European Union (25 countries), 2003, in Quadrillion Btu

1.2 Building Energy Conservation Regulations and Initiatives

In 1999 President Clinton signed an executive order extending the United States Code (USC) requirement for energy efficiency in Federal buildings. The USC required U.S. Federal buildings to use 10% less energy per square foot by fiscal year1995 and 20% less energy per square foot by fiscal year 2000 compared to a 1985 baseline (42 USC sec.8235). The 1999 executive order (Executive Order 99-13123) extended this conservation requirement to 30% less energy per square foot in Federal buildings by 2005 and 35% less by 2010 relative to the 1985 baseline. For industrial and laboratory facilities, this executive order requires reductions of energy consumption per square foot, or per unit of production, of 20% by fiscal year 2005 and 25% by 2010 compared to a 1990 baseline. All the reductions,

for all building types, are to be made through life-cycle cost-effective energy measures. The order also contains requirements for the reduction of petroleum usage, green house gas emissions, and the expansion of renewable energy usage.

Many government agencies have opted to meet these efficiency requirements by contracting with private companies in what is termed an Energy Saving Performance Contract (ESPC). In an ESPC, a private contractor agrees to incur all the costs for energy efficiency upgrades in exchange for all or some of the energy savings for up to 25 years, depending on the contract. In this way, the government agency avoids the need for initial capital investment (Energy Policy Act of 1992, P.L. 102-486). However, the total cost of the project is generally more expensive than if it had been financed and performed by the agency itself (GAO, 2005).

A Government Accountability Office (GAO) report to the U.S. Congress found that ESPCs are potentially beneficial to the government interests, but that vigilance and independent auditing is necessary. Most agencies have not performed audits of their ESPCs, but those that have found several cases where the ESPC costs were not covered by the energy savings. In one example, an audit uncovered $96 million in costs that would not be covered over the 18 year project. The primary reason for this particular discrepancy involved an inflated baseline energy level determined by the contractor (GAO, 2005). Other discrepancies have come through inaccurate assumptions in energy savings calculations with the result that actual measured savings did not match calculated savings. Auditing ESPCs is not necessarily a simple undertaking – facilities often are not equipped with adequate metering to assess the actual energy consumed in the building, and it is often difficult to determine the actual energy cost.

The Energy Policy Act of 2005, signed by President George W. Bush, requires that new Federal buildings be designed to be 30% more efficient than the levels established in the American Society of Heating, Refrigeration, and Air-conditioning Engineers (ASHRAE) standard 90.1 -2004 or the 2004 International Energy Conservation Code (IECC), if it is life-cycle cost effective. ASHRAE 90.1 for commercial buildings, and the IECC for both residential and commercial buildings, are industry accepted standards and both are written into many local and state building codes.

Federal buildings are required to be more efficient than the industry standards of ASHRAE 90.1 and the IECC, when cost effective. However, there is no such federal mandate for other buildings in the United States. As a potential motivator to increase the energy efficiency of other commercial buildings, an independent council, the U.S. Green Building Council (USGBC), developed a rating system designed to promote environmentally responsible buildings called the Leadership in Energy and Environmental Design (LEED) Green Building Rating System. This system involves the award of points for environmental and energy saving design features and construction practices. There are four levels of certification: Platinum at the top, followed by Gold, Silver, and finally, Certified. The number of points earned determines the level of certification. This voluntary system has grown dramatically in its use and acceptance since its commencement in 2000. As of November, 2005 there were 359 LEED projects that had attained some level of certification, and 3000 projects , totaling 391 million square feet of building space were registered and awaiting certification (Holowka, 2005).

An additional voluntary program designed to promote energy efficiency in buildings is the ENERGY STAR program, a partnership between the U.S. Department of Energy

(DOE), the US Environmental Protection Agency (EPA) and industry. This program offers its own rating system for residential buildings and for commercial buildings. In addition, it provides a rating system for appliances and heating and air conditioning mechanical equipment (ENERGY STAR, 2005).

The European Union has taken the regulation of building energy efficiency further than the voluntary programs in position in the US. In 2002 the EU passed a directive to come into effect in 2006 that requires all new buildings and existing buildings undergoing substantial renovation to meet minimum energy consumption standards. In addition, buildings must have an energy certificate when they are constructed, sold, or rented. While each member state is free to develop its own certification methodology, the certificate should compare the building's energy usage with similar structures or benchmarks (European Parliament and the Council of the European Union, 2003).

In Wisconsin, the state has an ESPC with two separate contractors, one of which is responsible for upgrading the energy efficiency of state buildings in the southern half of the state, the other for state buildings in the northern half of the state. This program, titled the Wisconsin Energy Initiative, was instituted in 1992, and is nearing its completion. A number of efficiency upgrades have been completed under this program, such as installing new energy efficient lighting, temperature controls, and motors. This program has not been independently audited (Hall, 2005).

1.3 Energy Use at the University of Wisconsin

The annual University of Wisconsin (UW) system utility expenditure is approaching 80 million dollars (see Figure 1.3). And, the system has been operating with a shortfall in revenue appropriation since 1999 (Lang, 2004).

While electricity costs are similar to the sum of all the fossil fuel costs ($34,512,740 for electricity and $39,613,864 for fossil fuels in fiscal year 2003-2004), the actual usage amounts are quite different. In Fiscal year 2003-2004, the entire UW system used more than three times the amount of energy from fossil fuels than electrical energy with total usage levels at 7.327 x 10^{12} Btu (2,147,417 MW) for fossil fuels and 2.227 x 10^{12} Btu (652,802 MW) for electricity (DOA, 2005).

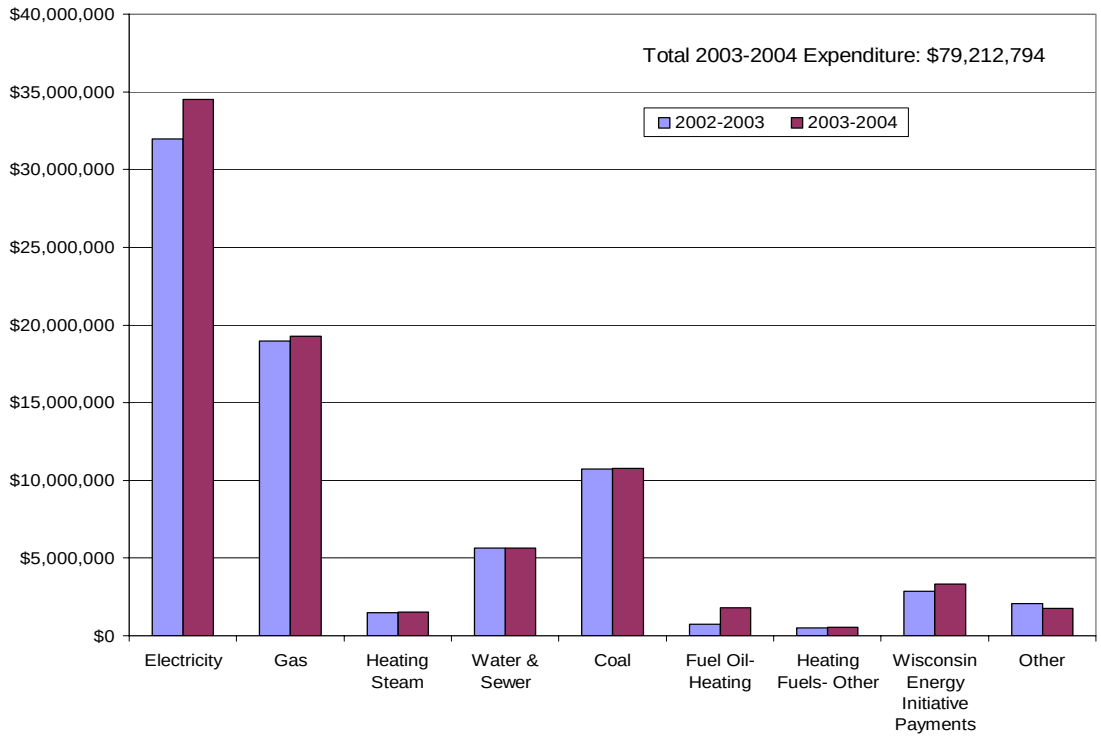

Figure 1.3: UW System Utility Expenditures

The UW system consists of 13 campuses located across the state. The total utility usage varies dramatically by location, as illustrated in Figure 1.4 (DOA, 2005).

The Madison campus is by far the largest UW campus in terms of student population and building gross square footage. But, even when campus energy usage is normalized by building square footage as shown in Figure 1.5, the Madison campus buildings use significantly more energy per gross square foot of building space (DOA, 2005).

One explanation for higher energy consumption rates at the Madison campus is the greater number of research facilities on this campus compared with other UW campuses. In general, research facilities consume more energy per gross square foot than office and classroom buildings.

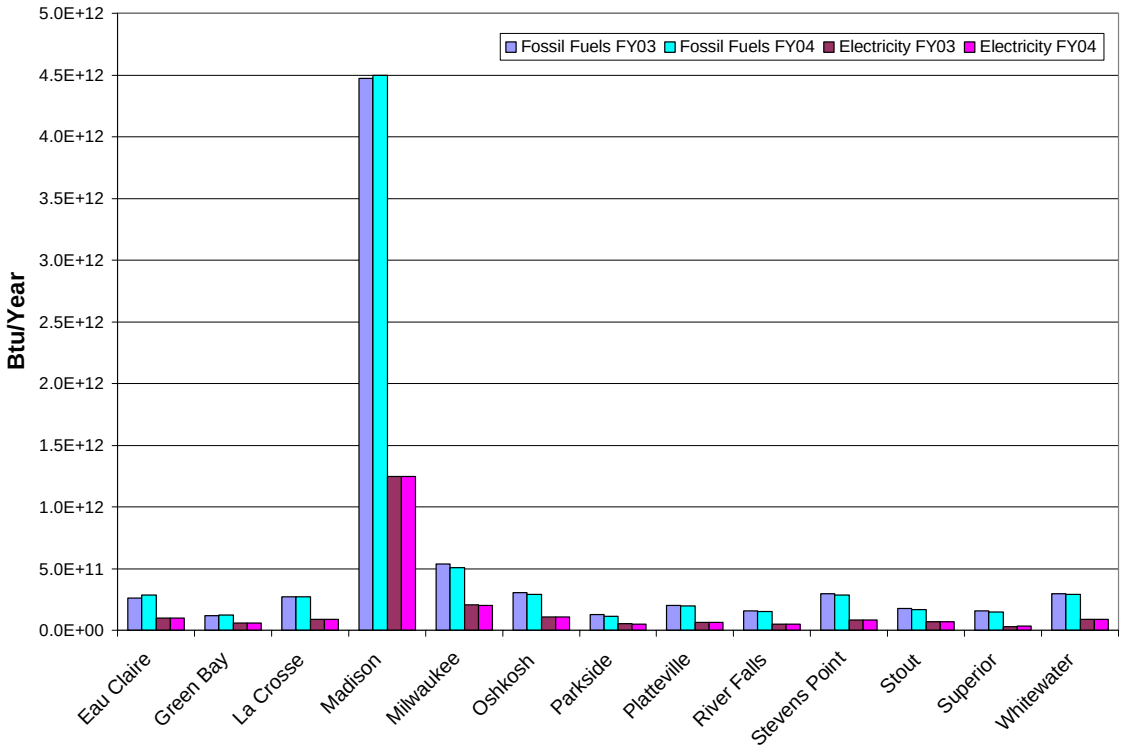

Figure 1.4: Total Energy Usage by UW Campus

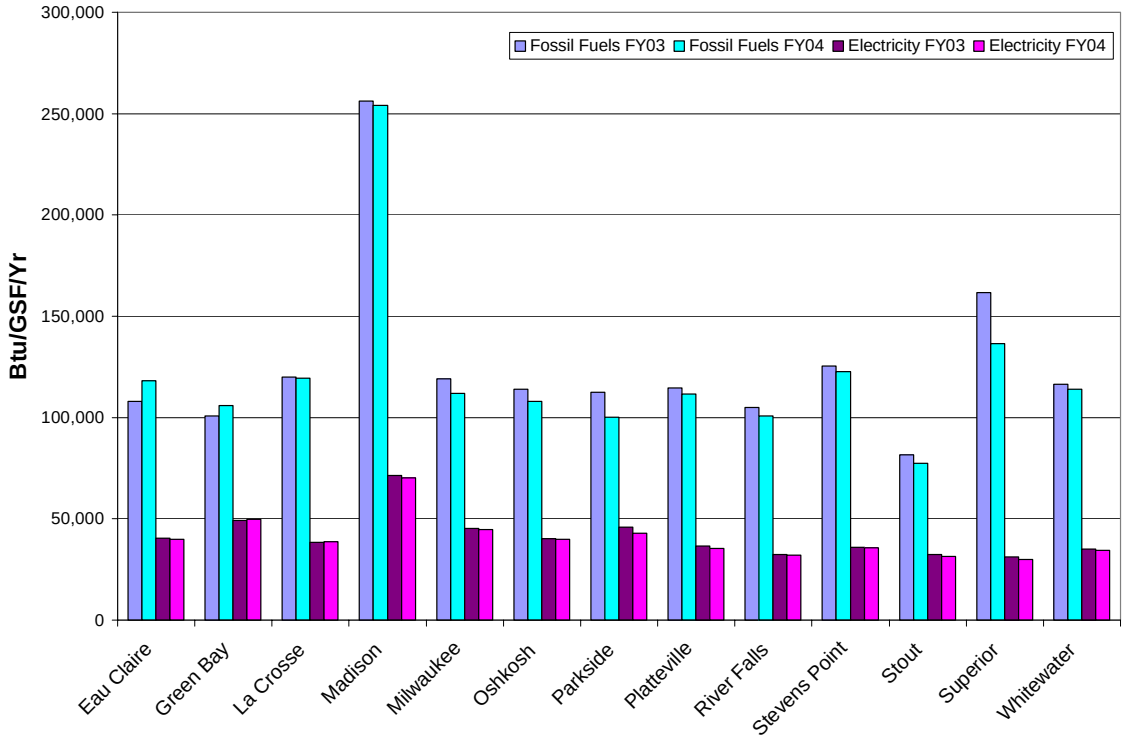

Figure 1.5: Energy Usage per Gross Square Foot of Building Space by UW Campus

1.4 Energy Usage in Research Facilities

There are three primary reasons for high energy usage rates in research facilities: the required control of particulate and fume flow, high internal heat gains from equipment, and the need for continuous space conditioning.

Laboratories, hospitals, and other research facilities require large amounts of fresh outside air to control particulate flow in the building. For example, hospitals use high ventilation rates and directional control of air flows to lessen the spread of bacteria and viruses. Laboratories exhaust air to the outside without recirculation to remove toxic fumes from occupied spaces and thus require large quantities of outside air. In addition, research facilities may include equipment with high heat loads requiring additional space conditioning

such as magnetic resonance machines, steam cage washers, and equipment sterilizers. Further, many of these facilities need to maintain these air flows 24 hours a day, 365 days per year – particularly facilities such as vivariums and hospital patient rooms.

On the UW Madison campus, data on steam and chilled water usage by building type is not available, but electrical data are available. Presumably these energy flows are related however, as a larger than average electrical draw per square foot likely stems from large equipment loads and from high fan energies. Both equipment gains and large ventilation rates imply large steam and chilled water usage.

Excluding the electricity draws from the heating plants themselves (averaging 369.75 kWh/GSF), the electricity usage per square foot of building space on the UW Madison campus is presented in Figure 1.6 (Werre, 2003).

The average research laboratory consumption is quite similar to that of the hospital buildings on campus, however, the total electricity expenditures by facility type illustrate the difference in the amount of floor space dedicated to each building type, see Figure 1.7. These expenditures are calculated based on the average 2002-2003 electricity cost (including demand charges) of $0.04971 per kWh (Werre, 2003).

Figures 1.6 and 1.6 present the average electricity usage per gross square foot in campus buildings. However as shown in Figure 1.8, this number varies widely among the research facilities depending on the nature of the research space housed in the building (Werre, 2003).

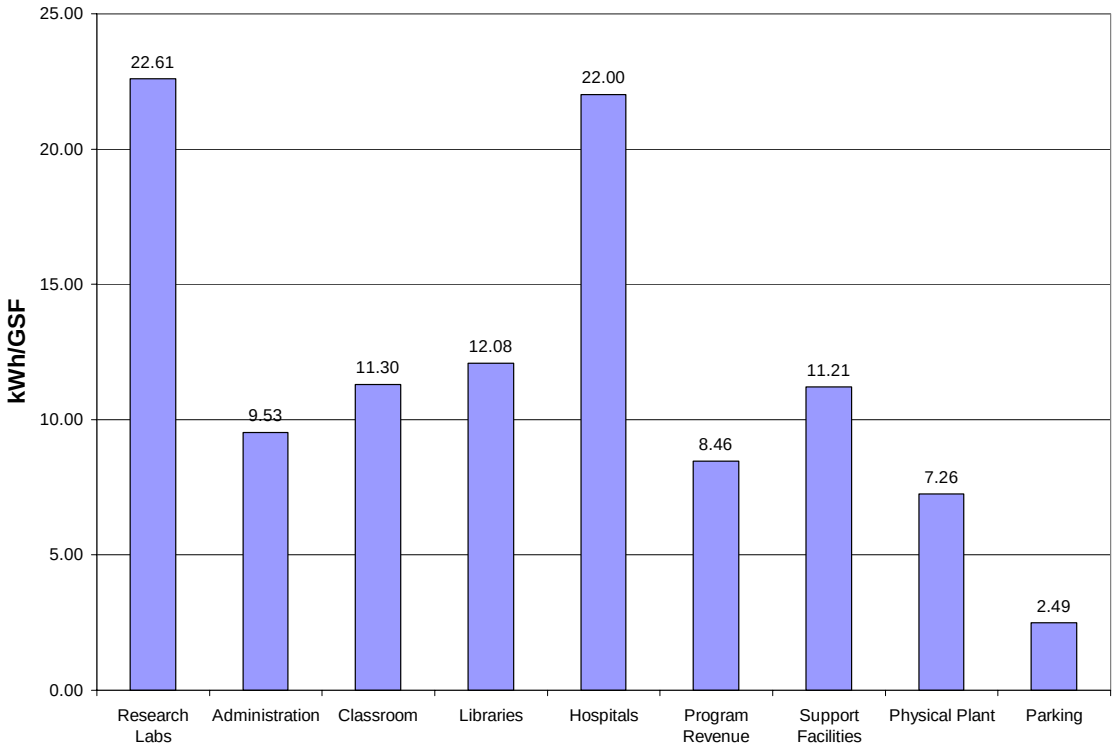

Figure 1.6: Electricity Usage per Gross Square Foot by Building Function

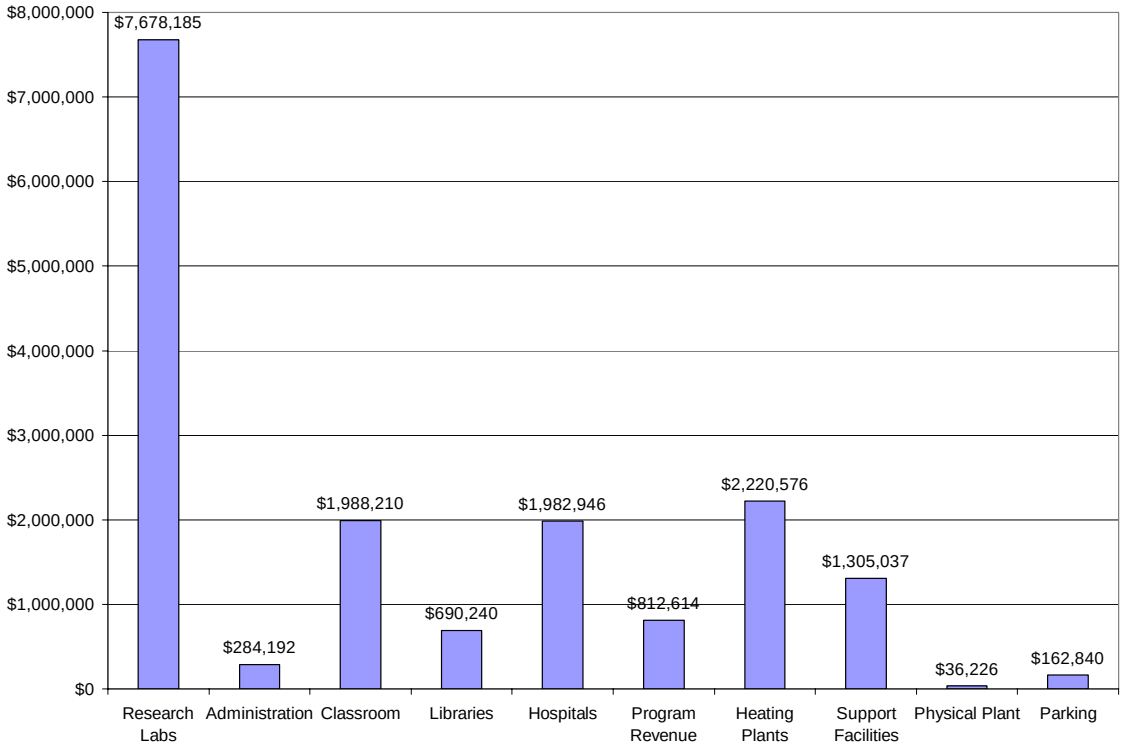

Figure 1.7: Electricity Expenditures by Building Function

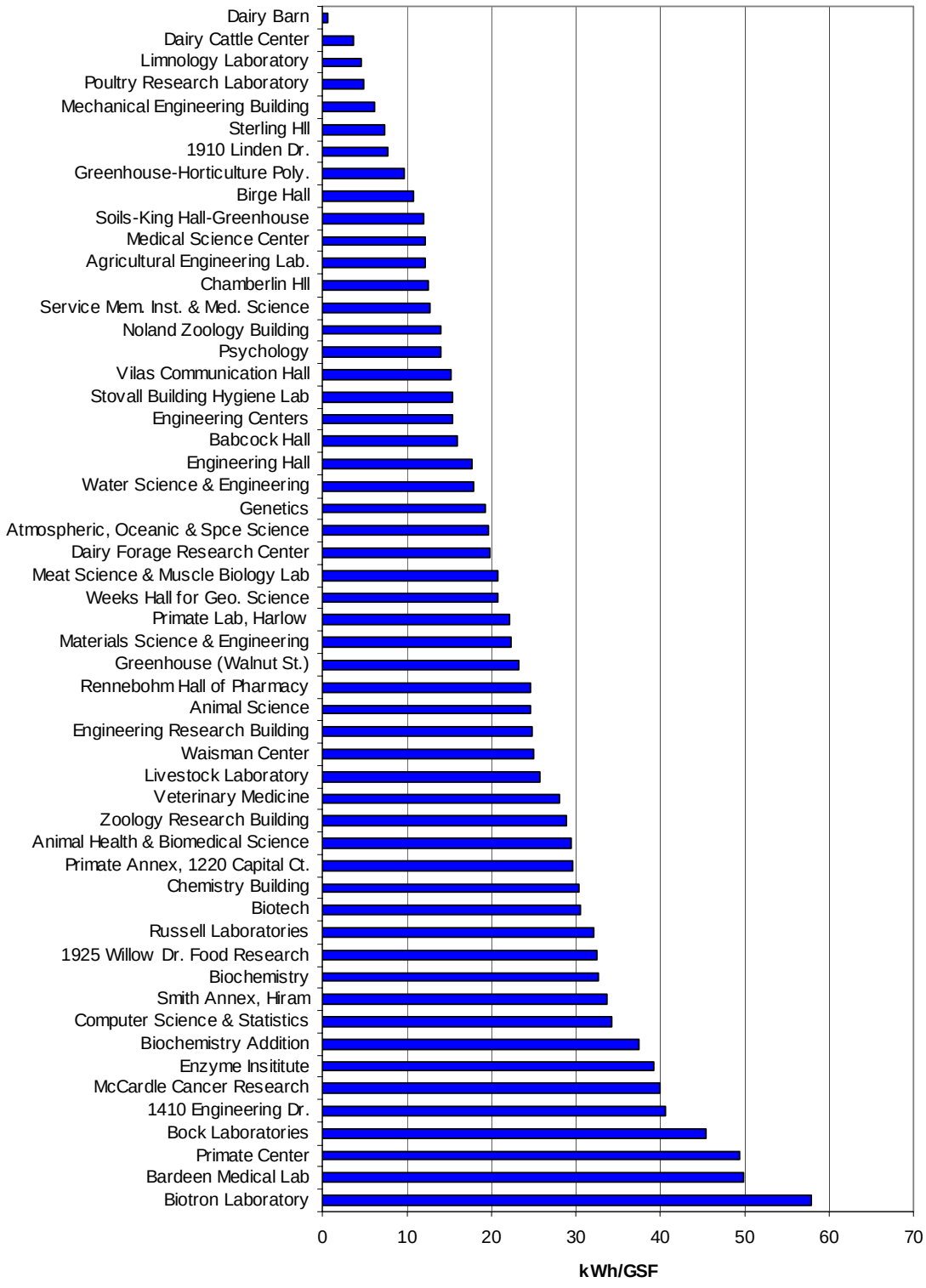

Figure 1.8: Electricity Usage for Each Campus Research Facility

As research facilities consume more campus energy than facilities, conservation measures in this sector resulting in a small percentage of energy savings translate into a large amount of energy. Techniques useful for monitoring energy usage in research facilities may be applicable, when simplified, to other types of buildings but the converse may not be valid. Thus, it is appropriate to begin an investigation of energy monitoring methodologies by focusing on research facilities.

1.5 Continuous Energy Monitoring

Continuously monitoring a building‘s energy consumption can dramatically reduce the amount of energy consumed. Reports in the literature show average consumption reductions of 15% to 20% (Herzog and Lavine, 1992, Gregerson, 1997, Dodds et al, 2000) with reductions considerably higher in some buildings (Claridge et al, 1994).

Energy monitoring programs may be instituted as part of a continuous commissioning process. Commissioning is generally a systematic review of building systems with the goal of verifying that the systems meet their design intent (ASHRAE, 1989) Commissioning is often completed before a new building is occupied, but the process can also be completed for existing buildings, it is then often termed *retrocommissioing*, or *continuous commissioning*.

Claridge et al, (2000) described a comprehensive, six stage, continuous commissioning process on the Texas A&M University campus. The stages are: (1) a survey of building occupants to identify comfort and air quality issues; (2) a determination of the baseline building energy consumption level; (3) a comprehensive building energy audit; (4) the commissioning of major equipment with a possible reset of control levels; (5) the

commissioning of the rest of the building systems; and (6) continuous monitoring of the building's energy consumption.

The reported results for 20 university buildings in the Texas A&M study included an average energy savings compared to baseline of 28% for chilled water and 55% for heating energy. However, the amount of energy savings varied widely: chilled water savings ranged from -13% to 82%, heating savings ranged from 2% to 89%, and electricity savings ranged from 0% to 21%. The cumulative reported monetary savings for these buildings was $4,147,000 over a period of 24 to 39 months, with a straight line payback of 1 to 2 years (Claridge et al., 2000). This program has been expanded to include 150 buildings and energy costs have been reduced by an average of 20%, without substantial building renovation or equipment upgrades (Claridge et al, 2004).

The benefits of continuous commissioning and other energy monitoring programs are greatest for large buildings, particularly for buildings with a substantial cooling load (Claridge et al, 2004). Research facilities and hospitals have also shown greater energy savings and shorter payback periods than other buildings (Dodds et al, 2000, Haasl and Sharp, 1999). Because these buildings use large amounts of energy, small improvements in efficiency may have a dramatic impact on energy savings and payback period.

1.6 Project Objectives

The primary objective of this research project is to develop a method for determining a baseline energy consumption level for large laboratory or research facilities with which the building's actual energy consumption level can be compared. Research facilities have uniquely tailored, often energy intensive, design requirements to protect occupant safety and

to protect research integrity. While estimates of baseline energy consumption levels have been detailed for standard office buildings, the energy requirements of research facilities vary so widely, that a laboratory's actual energy use should only be compared to its own designed energy consumption. This project investigates the detail of building modeling required for an estimate of baseline energy consumption.

As this project progressed, the benefits of systematically monitoring a building's energy consumption became evident and the focus of the project shifted slightly. Thus, a secondary objective was developed:

The second objective is to develop a series of simple energy monitoring techniques that could be used on any commercial building to identify energy intensive maintenance issues.

An additional requirement imposed on the energy monitoring and baselining techniques developed in this project is that they must be feasible to implement by the University of Wisconsin Physical Plant, given their time and labor power restrictions.

The building selected for the modeling component of this project is Rennebohm Hall, housing the department of Pharmacy at the University of Wisconsin – Madison. This building was selected because it is a new, well metered, state-of-the-art laboratory building. Building information from the Building Automation System (BAS) was collected over the span of one year in 10 minute intervals. These data were also used to develop the energy monitoring techniques.

Chapter 2: Rennebohm Hall

Rennebohm Hall houses the University of Wisconsin – Madison School of Pharmacy. It comprises 221,824 gross square feet of laboratory, classroom, office, and research laboratories that include live animal holding spaces. The building was designed by the architectural firms Perkins & Will of Chicago, Illinois and Potter Lawson of Madison, Wisconsin. Mechanical and electrical systems were engineered by Ring & DuChateau, Inc., and building controls were designed and installed by Johnson Controls, both of Milwaukee, Wisconsin. The Chicago and Wisconsin chapters of the American Institute of Architects (AIA) recognized Rennebohn Hall with honor awards for distinguished building design in 2002 and 2004, respectively.

Rennebohm Hall was selected for study for a number of reasons. First, the building has extensive metering equipment and is fully controllable through the campus Building Automation System (BAS). Second, it utilizes a number of energy efficient design features such as heat recovery, outside air economizers, and occupancy-sensor based lighting control. Third, because the building's electrical consumption per square foot is close to the campus mean for research facilities, it is representative of campus research buildings (see Figure 1.8).

Most campus buildings receive district steam and chilled water from one of three campus central utility plants. Rennebohm Hall requires steam for the Air Handling Unit (AHU) heating coils, for process loads such as cage washers and sterilizers, for humidification, and for hot water generation (domestic and hot water heating). Hot water is used both in terminal reheat coils to and for perimeter space heating. Baseboard radiators off-set heat loss to the environment and terminal reheat coils warm zone supply air zone

when air warmer than the 55°F AHU discharge temperature is required to maintain the room set point temperature. Terminal reheat coils are used for reheat year round as needed, since the amount of heating required for a zone is often more closely related to the building occupancy and internal gains to outside weather conditions. Chilled water is used to meet some equipment process loads, but is primarily required to meet space cooling loads through chilled water coils located in the AHUs.

There are 7 primary AHUs in Rennebohm Hall, serving 5 distinct zones (see

Table 2.1). AHUs 1, 2, 3, 6, and 7 were manufactured by Temtrol, Inc. Temtrol also provided the rooftop heat recovery modules (HRMs). AHUs 4 and 5 were manufactured by York. The supply fans for AHUs 1 through 7 and the return fans in AHUS 3 and 5 use variable frequency drives (VFDs) for capacity control. There are two additional small York AHUs for smoke control stair pressurization that are not considered in this project.

2.1 Building Ventilation Zones and Mechanical Systems

2.1.1 Vivarium

The *Vivarium* zone is primarily devoted to live animal holding areas, but also houses surgical procedure rooms, a cage washing area, and several other laboratories for a total of approximately 18,000 square feet (see Figure 2.1). AHUs 1 and 2 work in tandem in this zone and are designed to each continuously supply 18,000 cfm of outside air for a total of 36,000 cfm supplied to the zone. Tandem AHU operation is a safety feature to ensure continuous air supply to the zone in the case of AHU failure or planned maintenance. The zone does not use any recirculated air, so there are no return fans. It is designed as a constant

air volume zone (CAV). There are three rooftop laboratory exhaust fans that are designed for staged operation and are controlled with a bypass damper to maintain a constant static pressure in the exhaust duct.

The *Vivarium* uses a run-around loop for heat recovery. In the run-around loop, a glycol solution circulates to exchange energy with the zone exhaust air in the roof top heat recovery module (HRM1). The warmed (or cooled) glycol is then pumped through heat recovery coils in AHU1 and AHU2 and pre-conditions (cools or warms – depending on the season) the outside air. Each AHU glycol coil has a separately controlled bypass to maintain the air temperature leaving the coil at its set point of 55° F.

2.1.2 General Zone

The *General* zone contains approximately 78,500 square feet of office and classroom space including a student learning center, atrium, and auditorium. The zone spans the first two floors with additional atrium air space extending to the third floor (see Figure 2.1 through Figure 2.3 and Figure 2.10 through 2.12). AHU3 is a variable air volume (VAV) unit with a maximum supply air flow of 60,000 cfm. The unit is designed to maintain a constant 19,500 cfm of outside air that will mix with return air from the zone.

The *General* zone has undergone several program changes since its initial design. The student learning center was originally designated as library space but was reassigned following the construction of a new health sciences library complex. An elevated connecting passageway was constructed to connect the student learning center with the new library complex. And, a coffee shop and snack bar located in this zone has recently been closed.

2.1.3 Teaching Lab

The *Teaching Lab* zone consists of approximately 16,000 square feet of laboratory classroom space (see Figure 2.2 and Figure 2.11). It is served by AHU4 which is a constant volume 100% outside air unit with a nominal capacity of 15,000 cfm. There is no heat recovery for this zone.

2.1.4 Tower Offices

The *Tower Office* zone consists of 4 floors of office space, all located along the Northeast tower curtain wall (see Figure 2.4 and Figure 2.11). The 13,000 square foot zone is served by a VAV air handling unit having a maximum flow of 15,000 cfm (AHU5). The zone uses return air mixed with a constant 3,000 cfm of outside air. This zone is the only conditioned zone in the building with a glass curtain wall spanning the entire zone. Due to the orientation of the zone and the large unshaded glass area, the solar radiation gains for this zone are larger than for any other zone in the building.

2.1.5 Tower Labs

The *Tower Lab* zone consists of 4 floors, comprising approximately 65,000 square feet, of research laboratory space (see Figure 2.4 and Figure 2.10 through 2.12). This zone is supplied by AHU6 and AHU7 operating in tandem. Each unit is sized in the construction documents to continuously supply 65,000 cfm, for a total of 130,000 cfm to the zone. As in the Vivarium zone, this tandem AHU operation is designed for occupant safety – if one AHU fails or is taken offline for maintenance, the zone will continue to be partially ventilated. Each AHU has its own separate glycol run-around loop for heat recovery. Although the

supply fan in each AHU for the Tower Labs is VFD-equipped, both AHUs are designed as constant air volume (CAV) units. There are six staged rooftop exhaust fans serving the zone that are controlled in the same manner as the *Vivarium* exhaust fans.

2.1.6 *MER* and Heating Only Zones

Mechanical Equipment Rooms (*MER*) in the building are located on the 1st floor and the 3rd floor (see Figure 2.1 and Figure 2.3). These rooms are heating-only areas with continuous exhaust for space ventilation. The make-up air to the MERs is provided through air transferred from adjacent zones.

Table 2.1: Rennebohm Hall Ventilation Design Summary

Tag	Zone	Gross Area (ft^2)	Gross Volume (ft^3)	Max Occup	Max S.A. (cfm)	Min S.A. (cfm)	Min O.A. (cfm)	Tot ACH[4]	CAV/ VAV	Heat Recovery?
AHU1	Vivarium	17,910	286,560	1,795 [1]	18,000	18,000	18,000 [2]	7.5	CAV	Yes
AHU2	Vivarium				18,000	18,000	18,000 [2]		CAV	Yes
AHU3	General	78,568	1,265,455		60,000	24,000	19,500	2.8	VAV	No
AHU4	Teaching Labs	16,160	258,560		15,000	10,000	10,000 [2]	3.5	CAV	No
AHU5	Tower Offices	13,000	208,000	112	15,000	10,400	4,500 [3]	4.3	VAV	No
AHU6	Tower Labs	64,800	1,036,800	368	65,000	65,000	65,000 [2]	7.5	CAV	Yes
AHU7	Tower Labs				65,000	65,000	65,000 [2]		CAV	Yes

Notes:

[1] Occupancy for the 1st and 2nd floors combined, which includes 3 zones. The majority of the occupants are likely located in the General zone.

[2] 100% Outside Air

[3] 4,500 cfm is the design specification, however, at the time of this study the BAS was programmed to provide 3,000 cfm outside air.

[4] This ACH rate is based on the gross volume at the maximum SA cfm, including unvented areas receiving transfer air. The effective ACH may be significantly higher in some parts of the zone.

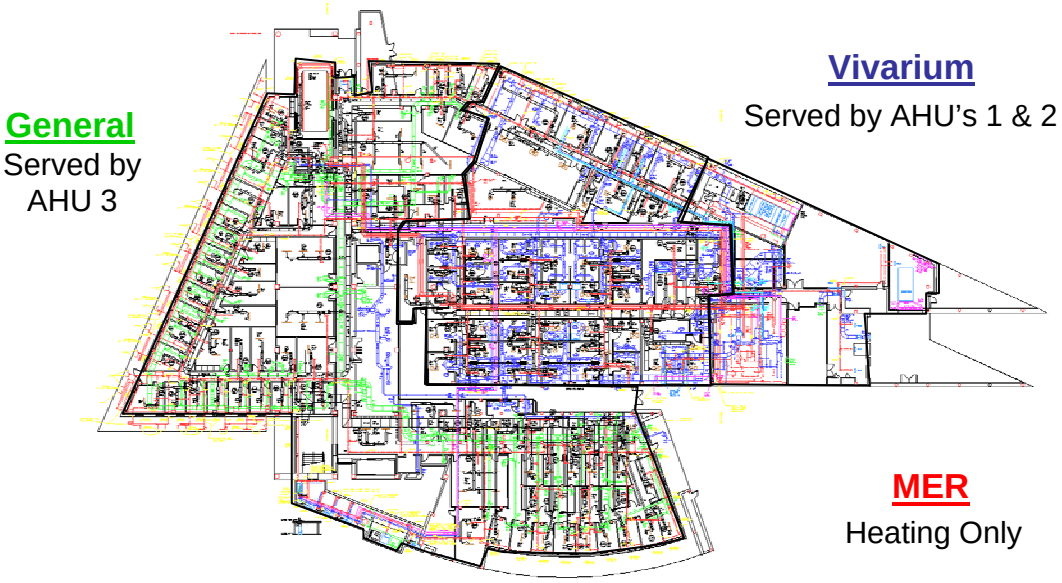

Figure 2.1: Rennebohm Hall, First Floor Zones

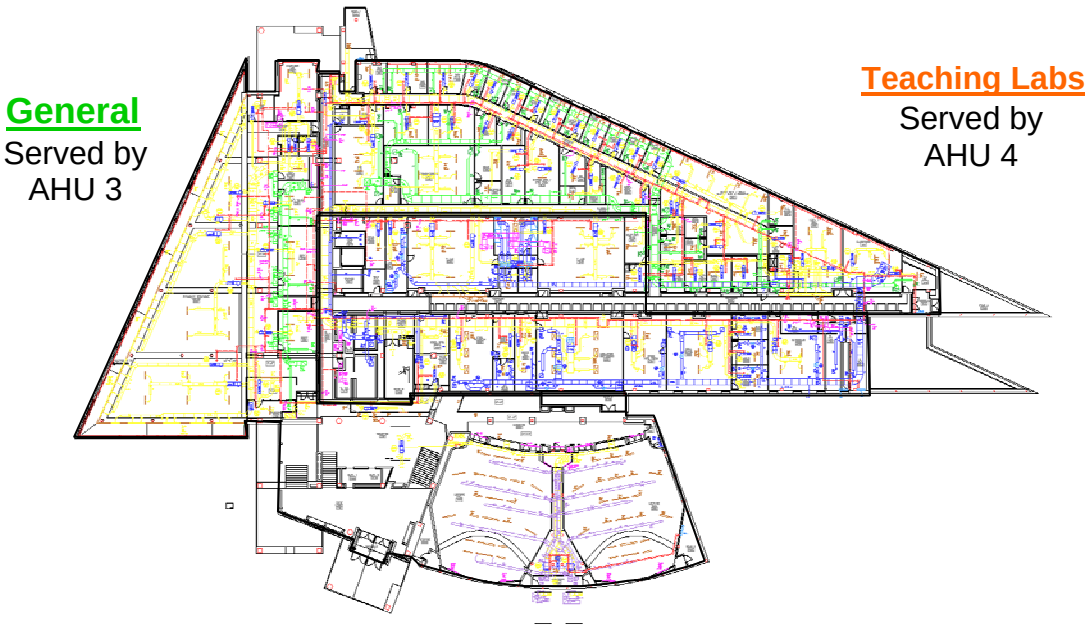

Figure 2.2: Rennebohm Hall, Second Floor Zones

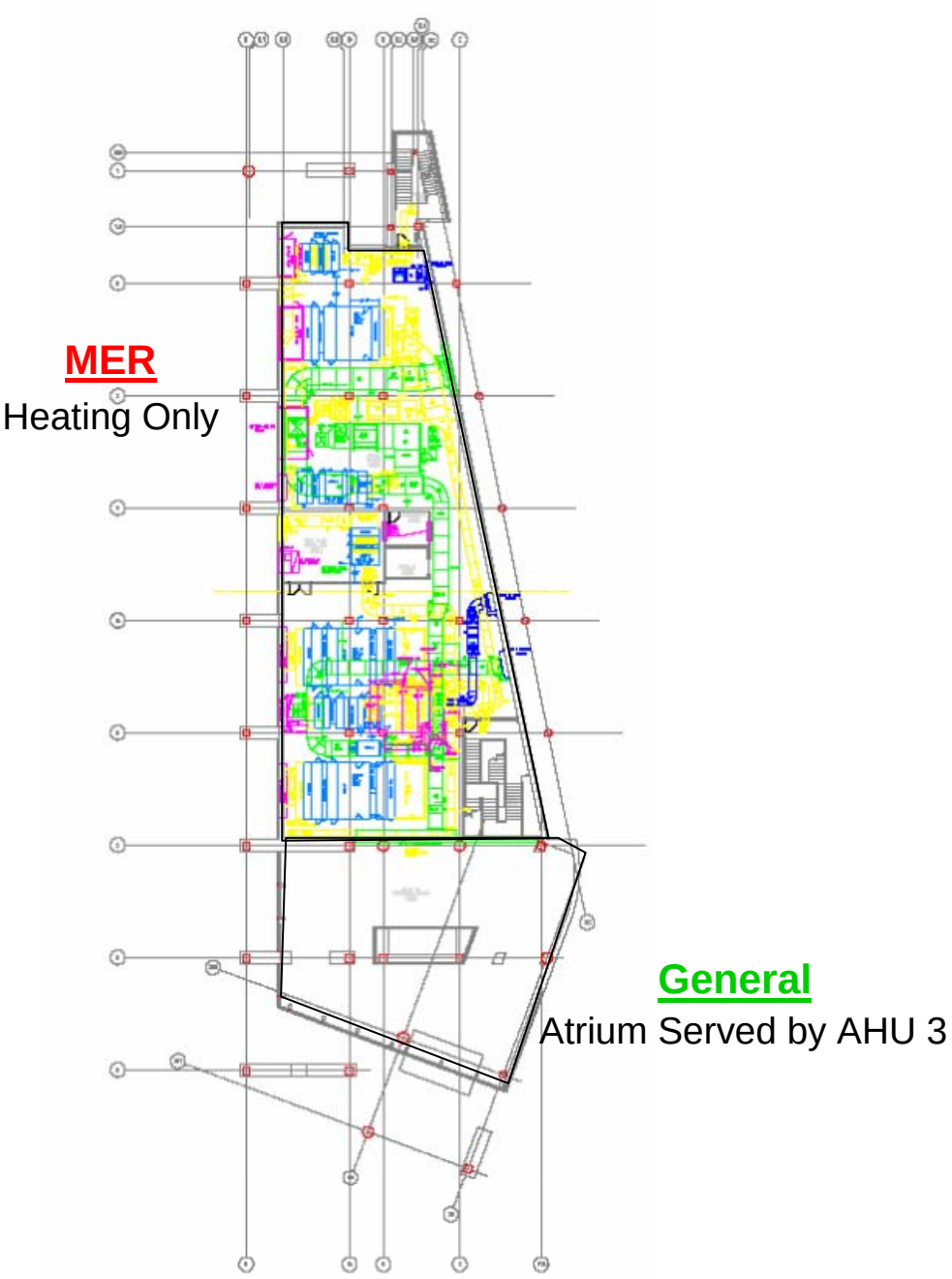

Figure 2.3: Rennebohm Hall, Third Floor

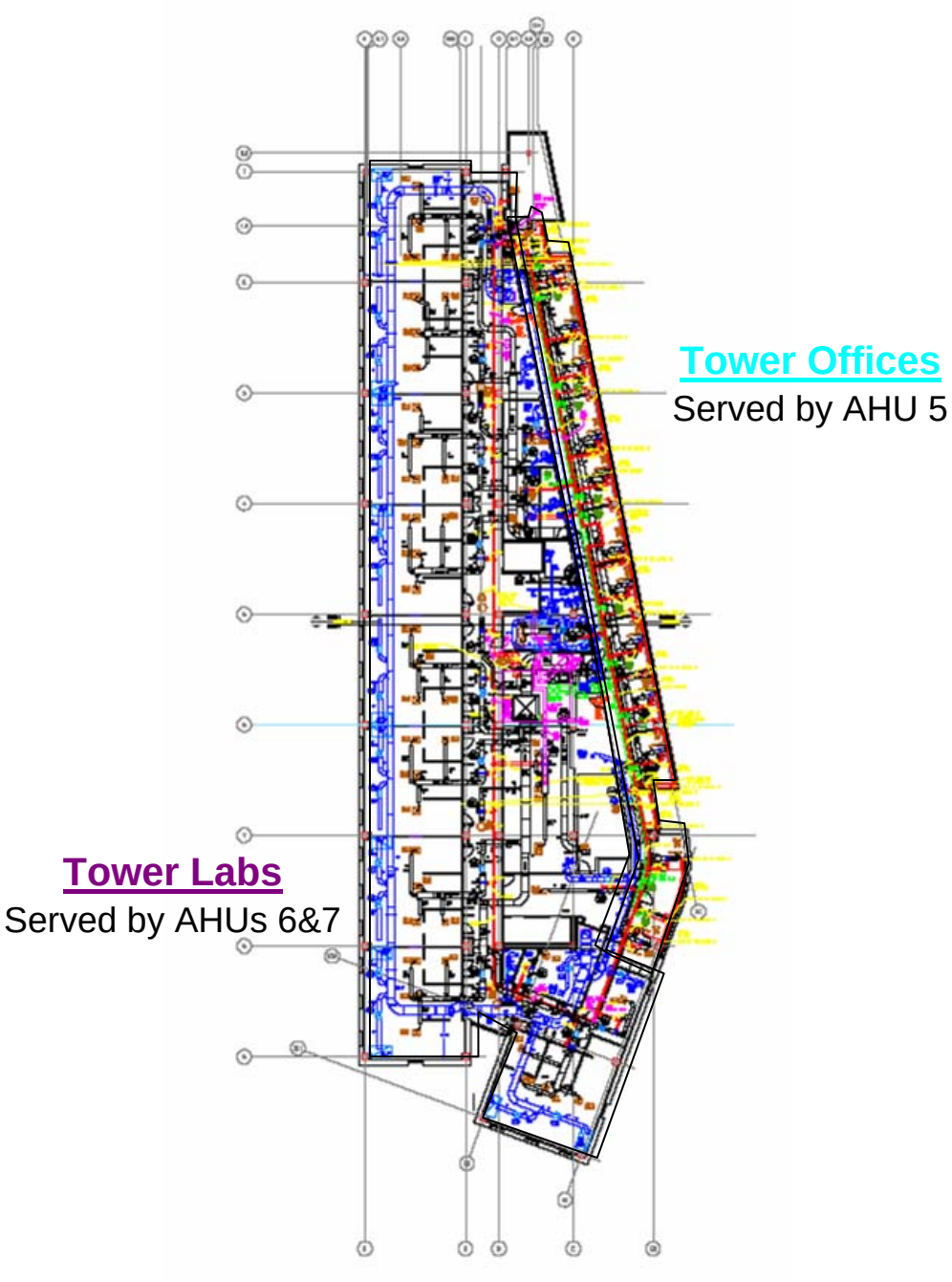

Figure 2.4: Rennebohm Hall, Floors 4 -7 Zones

2.2 Field Data Collection

The University of Wisconsin – Madison uses the Johnson Controls Metasys building automation system (BAS) to both monitor metered equipment on campus and to control building systems. The Metasys system is programmable and integrates HVAC, lighting, fire protection, and security systems.

Metasys is capable of logging data as a trend, point history, or totalization. Trend data can be collected in any time interval and for this project, most trend data were collected in 10 minute intervals. For some select data points, 5 minute or 1 minute data were collected when more data points were required for other Physical Plant monitoring projects. Because point history data primarily records changes in variable status, such as equipment on/off status, it is not generally collected at a set time interval. Totalization data include such variables as condensate flow that might be tracked and summed over a given time interval. Unless a specific data point is being monitored and archived, data points reside in the Metasys system for 48 hours before discarded (overwritten).

Data were archived and retrieved on a monthly basis. All temperature, pressure, valve position, and flow data for the seven primary AHUs in the building were logged. The actual data points selected for archival are detailed in Appendix I, Tables I.1 through I.6. The most salient data points are highlighted on the system schematics in Figure 2.5 through Figure 2.9. Each data point is located by its approximate position of collection and color coded by the BAS system designation in which it is archived.

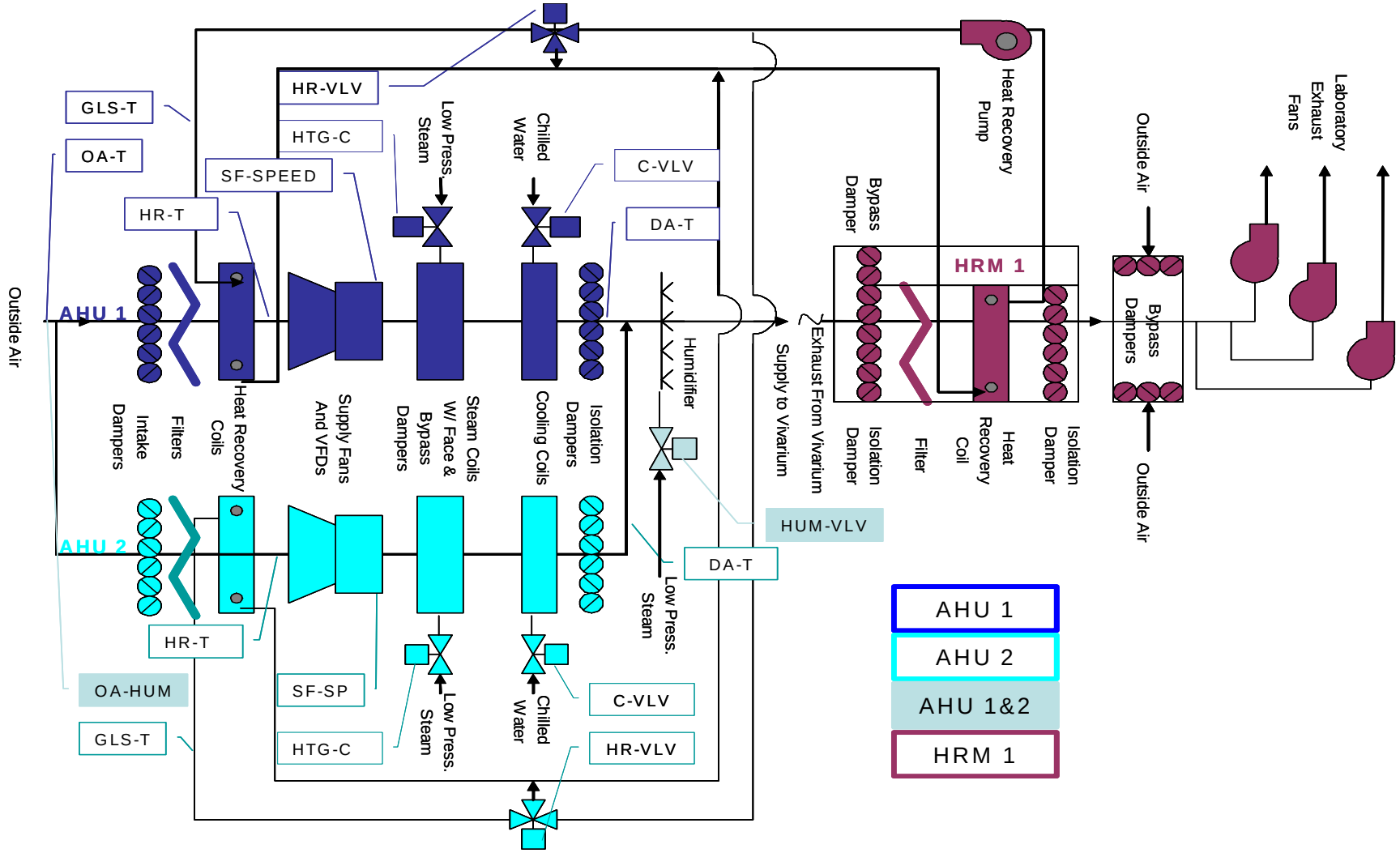

Figure 2.5: System Schematic For AHU 1, AHU 2, and HRM 1 with Data Collection Points, Vivarium Zone

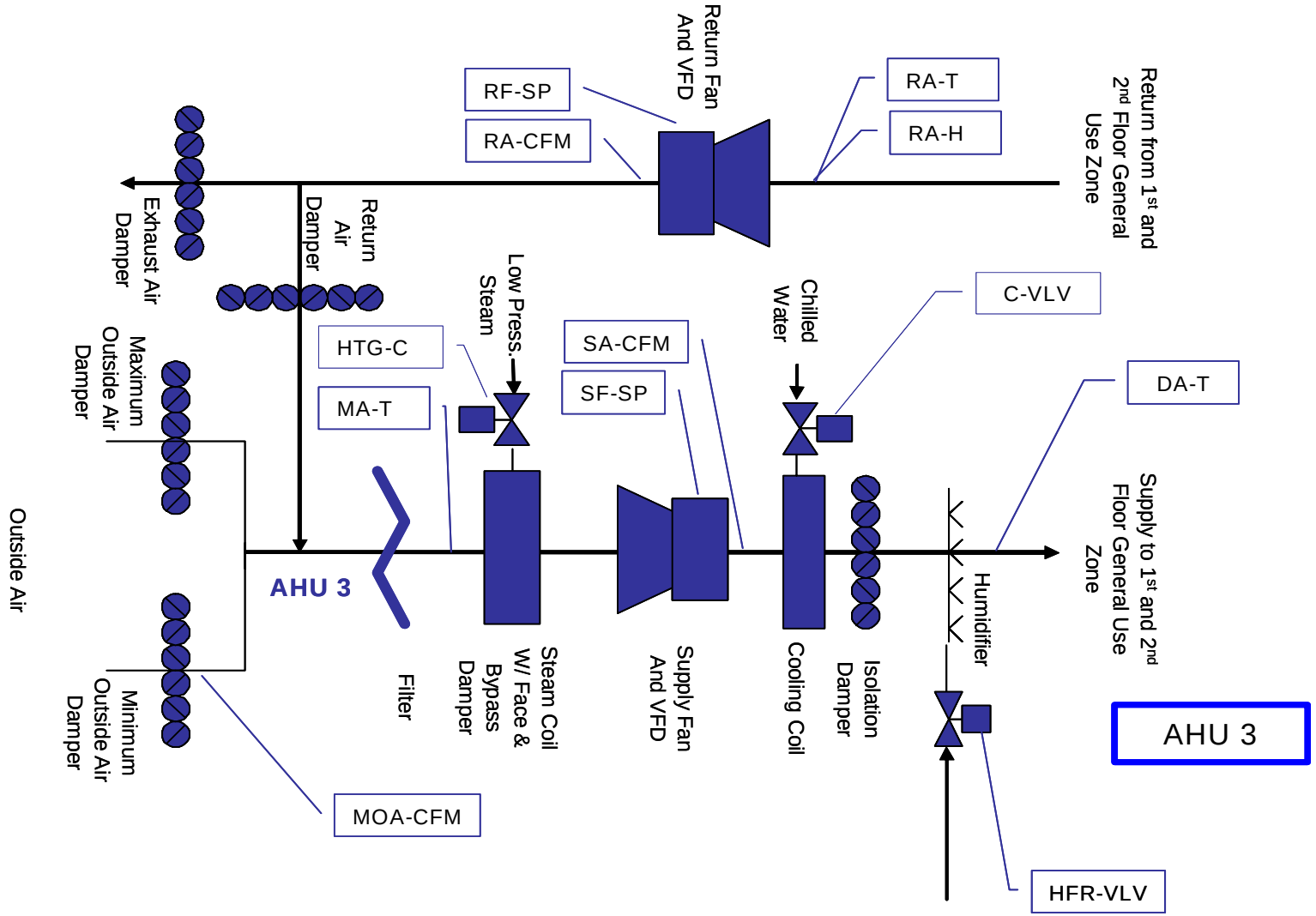

Figure 2.6: System Schematic for AHU 3 with Data Collection Points,, 1st and 2nd Floor General Zone

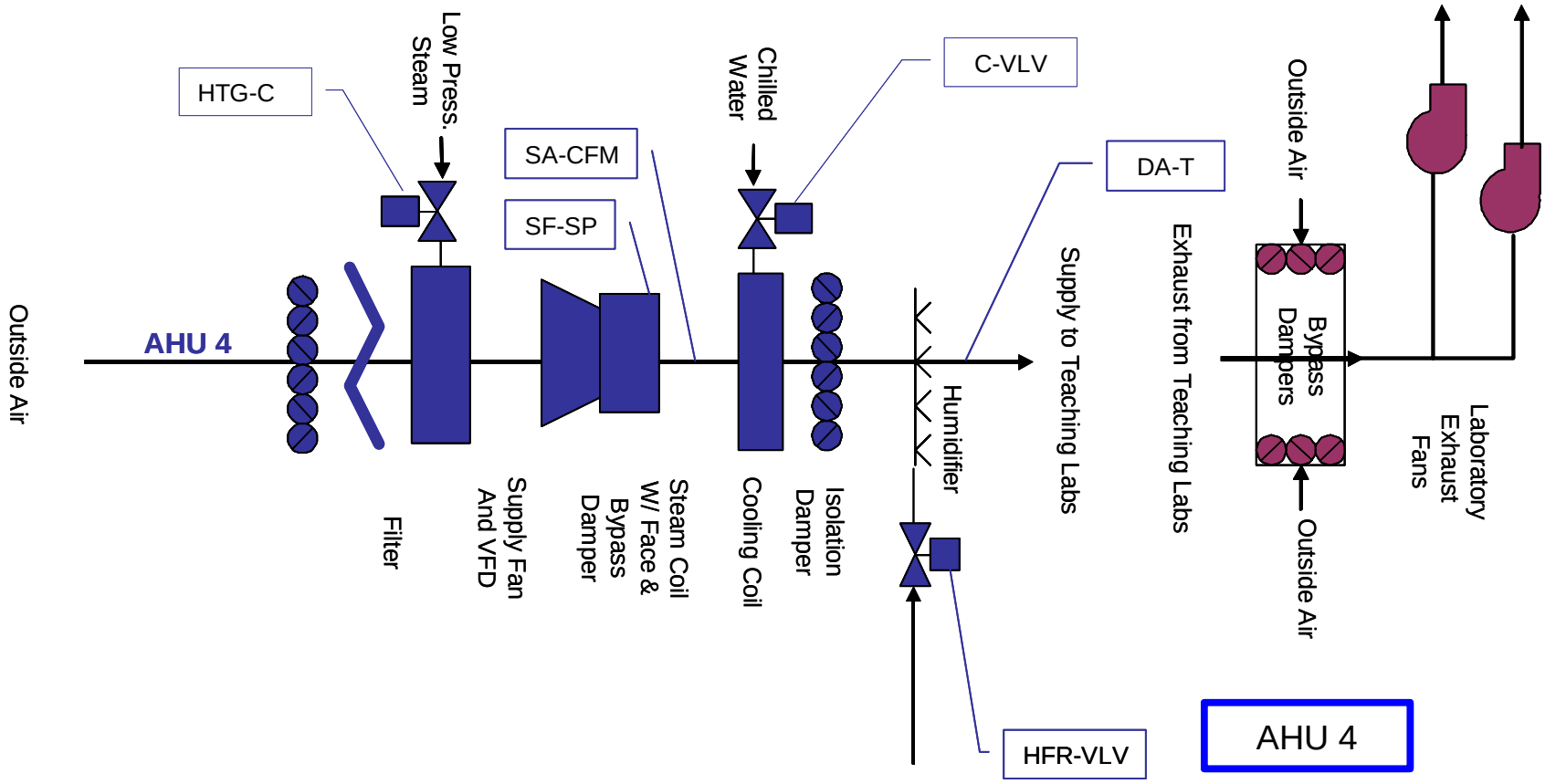

Figure 2.7: System Schematic for AHU 4 with Data Collection Points, Teaching Labs

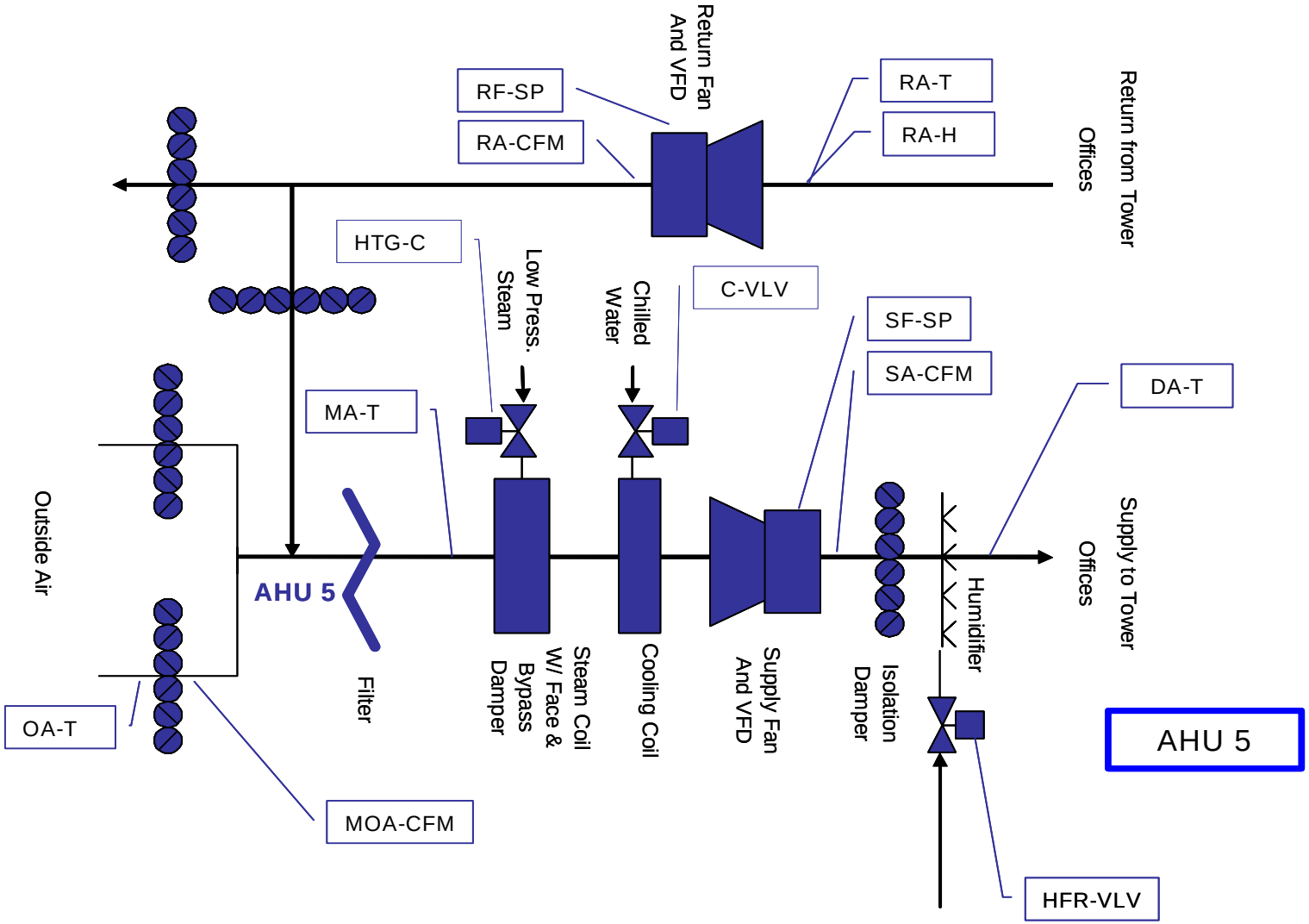

Figure 2.8 : System Schematic for AHU 5 with Data Point Location, Tower Offices

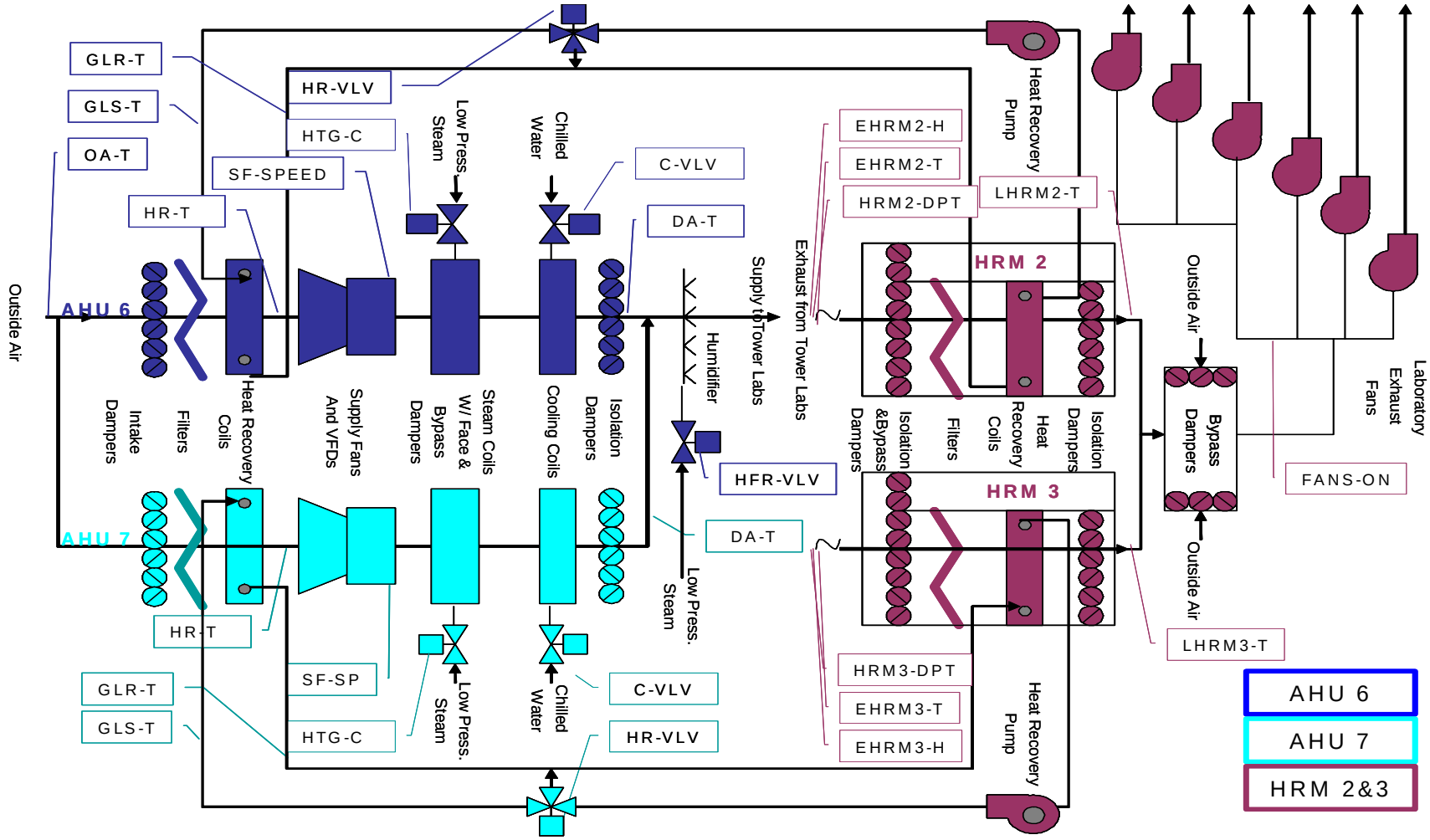

Figure 2.9: System Schematic for AHU 6, AHU 7, HRM 2, and HRM 3 with Data Collection Points, Tower Labs

Figure 2.10: Rennebohm Hall, West View, Showing Learning Center, Tower Laboratories, General 1st Floor Area, and Northern Staircase

Figure 2.11: Rennebohm Hall, East View Showing Tower Offices, Tower Laboratories, General, and Teaching Laboratory Areas

Figure 2.12: Rennebohm Hall, Southwest View Showing Atrium and Tower Laboratories

Chapter 3: TRNSYS Building Simulation

The Rennebohm Hall building simulation was created using TRNSYS 16. TRNSYS is a computer package used for simulation of transient systems. It has a modular structure, connecting individually programmed components in the TRNSYS environment. Each system component has a mathematical model, usually programmed in FORTRAN. These components are termed TRNSYS *Types*. Each Type has its own inputs and outputs, and its own program parameters. The source code for the TRNSYS kernel and the individual components is included with the TRNSYS package, allowing each component to be fully customized for individual projects.

3.1 TRNSYS Components Used in Rennebohm Hall Model

In addition to the standard components contained in the TRNSYS library there are supplemental libraries available, including a series of component libraries created by Thermal Energy Systems Specialists (TESS) (TESS, 2006). A combination of the standard TRNSYS components and components in the TESS libraries was used in the current project. A brief description, in order of type number, follows. For more detailed descriptions of these components, see the TRNSYS 16 Mathematical Reference (SEL, 2004).

While the TRNSYS Type 56 Building Component functions within the model as a typical component, its specification is quite different. Thus, the Type 56 model is discussed in section 3.2.1.

3.1.1 Type 5 – Counter-flow Heat Exchanger

The type 5 heat exchanger component takes as input the flow rates and temperatures of a cold stream and a hot stream as well as the overall heat exchange coefficient, UA. The heat exchanger effectiveness at each time step is calculated according to the following equation:

$$\varepsilon = \frac{1-\exp\left(-\frac{UA}{C_{\min}}\left(1-\frac{C_{\min}}{C_{\max}}\right)\right)}{1-\left(\frac{C_{\min}}{C_{\max}}\right)\exp\left(-\frac{UA}{C_{\min}}\left(1-\frac{C_{\min}}{C_{\max}}\right)\right)} \tag{3.1}$$

where C_{min} and C_{max} are the minimum and maximum capacitance rates (mass flow rate times specific heat) of the hot and cold streams. Using the calculated effectiveness, the total heat exchanged, Q_T, is then calculated by:

$$Q_T = \varepsilon C_{\min}\left(T_{h,i} - T_{c,i}\right) \tag{3.2}$$

where $T_{h,i}$ and $T_{c,i}$ are the hot and cold inlet temperatures, respectively. The outlet temperatures of the hot stream ($T_{h,o}$) and the cold stream ($T_{c,o}$) are calculated by

$$T_{h,o} = T_{h,i} - \varepsilon\left(\frac{C_{\min}}{C_h}\right)\left(T_{h,i} - T_{c,i}\right) \tag{3.3}$$

$$T_{c,o} = \varepsilon\left(\frac{C_{\min}}{C_c}\right)\left(T_{h,i} - T_{c,i}\right) + T_{c,i} \tag{3.4}$$

C_h is the capacitance rate of the hot stream, and C_c is the capacitance rate of the cold stream.

Table 3.1: Type 5 Parameters and Inputs

Parameters	Inputs
Flow mode (i.e. counter flow) Specific heat of hot side fluid Specific heat of cold side fluid	Hot side inlet temperature Hot side flow rate Cold side flow rate Overall heat transfer coefficient

(SEL, 2004, pg 5-100 through 5-103)

3.1.2 Type 11 – Bypass Valve – Type 11f

Type 11 has 7 different functional modes. In the current project, only mode 2 was used, the controlled flow diverter mode.

This type takes as inputs the temperature and flow rate of the fluid stream and a control variable. The flow is then split between two outlet streams as determined by the control variable. The outlet temperature of both streams is equal to the inlet temperature. The flow rate is divided according to the following relationships:

$$\dot{m}_1 = \dot{m}_i \left(1-\gamma\right) \tag{3.5}$$

$$\dot{m}_2 = \dot{m}_i \gamma \tag{3.6}$$

where $\dot{m}_1$ and $\dot{m}_2$ are the outlet flow rates, $\dot{m}_i$ is the inlet flow rate, and γ is the control variable that can vary between zero and one.

Table 3.2 Type 11f Parameters and Inputs

Parameters	Inputs
Flow mode (i.e., single inlet stream to two outlet streams)	Inlet temperature Inlet flow rate Control signal

3.1.3 Type 23 – PID Controller

Type 23 models a Proportional, Integral, and Derivative (PID) control device. The output of this component is a control signal calculated to maintain a controlled variable at a specified set point. (SEL, 2004 pg 5-23)

Table 3.3 Type 23 Parameters and Inputs

Parameters	Inputs
Mode (i.e. iterative or non-iterative) Number of iterations for iterative mode	Controlled variable set point Controlled variable On/off signal for controller Minimum control signal Maximum control signal Threshold for non-zero output Gain constant Integral time Derivative time

3.1.4 Type 31 – Pipes

The Type 31 component provides some capacitance for piping and duct simulation. It approximates the thermal behavior of fluid flow in a pipe by using discrete fluid segments. The mass of each fluid segment is calculated by multiplying the specified mass flow rate by one simulation time step. With the addition of each new fluid segment, the number (or fraction) of segments leaving the pipe is calculated so that an equivalent fluid mass leaves the component. The outlet temperature is the mass weighted average of the leaving segments. Energy losses are calculated for each segment in the pipe at each time step by multiplying the difference between the segment fluid temperature and the environment by the product of the segment surface area and the specified loss coefficient. A maximum of 25 segments is allowed, beyond that TRNSYS combines the two segments closest in temperature. The simulation begins with three fluid segments. (SEL, 2004, pg 5-191, 5-192)

Table 3.4 Type 31 Parameters and Inputs

Parameters	Inputs
Inside diameter Pipe length Loss coefficient Fluid density Fluid specific heat Initial fluid temperature	Inlet temperature Inlet flow rate Environment temperature

3.1.5 Type 33 Psychrometrics

This component calls the TRNSYS psychrometrics subroutine. The parameters determine the required inputs and the related outputs.

Table 3.5 Type 33 Parameters and Inputs

Parameters	Inputs
Psychrometrics mode (determines the inputs that will be supplied) Wet bulb mode Error mode	(Following inputs are for mode 2) Dry bulb temperature Percent relative humidity Pressure

3.1.6 Type 69 Effective Sky Temperature

Type 69 calculates an effective sky temperature for use in determining long wave radiative exchange with external building surfaces. The building model treats the sky as a black body, thus an effective temperature is calculated based on the ambient temperature, a calculated emittance of a clear sky, and a calculated cloudiness factor.

The emittance, ε, of the sky is calculated according to the following:

$$\varepsilon = 0.711 + 0.005T_{sat} + 7.3\times10^{-5}T_{sat}^{2} + 0.013\cos\left[2\pi\frac{time}{24}\right] + 12\times10^{-5}\left(p_{atm} - p_{o}\right) \qquad (3.7)$$

where T_{sat} is the ambient saturation temperature, p_{atm} is the ambient pressure, p_o is the pressure at sea level (for the current project, the height above sea level was assumed to be zero, so these pressures are equal), and time is the hour of the year.

There are two cloudiness factor modes. The cloudiness factor, *C*, can either be included as an input, or, as in the current project, it can be calculated using the diffuse solar radiation on a horizontal surface ($E_{diffuse}$) and the total radiation on a horizontal surface (E_{Total}):

$$C = \left(1.4286 \frac{E_{diffuse}}{E_{Total}} - 0.3 \right)^{0.5} \tag{3.8}$$

The nighttime cloudiness factor is taken as the average afternoon cloudiness factor. The effective sky temperature, T_{sky}, is then calculated as:

$$T_{sky} = T_{amb} \left(\varepsilon + 0.8(1-\varepsilon) C \right)^{0.25} \tag{3.9}$$

(SEL, 2004, pg 5-303 to 5-304)

Table 3.6 Type 69 Parameters and Inputs

Parameters	Inputs
mode for cloudiness factor height above sea level	Ambient temperature Dew point at ambient conditions Beam radiation on the horizontal Diffuse radiation on the horizontal

3.1.7 Type 114 Pump

In TRNSYS type 114, the pump's rated power, flow rate, the fluid specific heat, and the fraction of the motor losses that enter the fluid stream as heat are set as parameters. The motor loss fraction ($f_{motorloss}$) is set to 1 if the motor is in the fluid stream, and zero if it is external to the fluid stream. Type 114 also requires inputs of fluid inlet temperature, overall

pump efficiency, and motor efficiency. The overall pump efficiency ($\eta_{overall}$) and the motor efficiency (η_{motor}) are used to calculate the pumping efficiency:

$$\eta_{pumping} = \frac{\eta_{overall}}{\eta_{motor}} \tag{3.10}$$

The shaft power consumed by the pump is calculated with the rated power ($\dot{P}_{rated}$) and the motor efficiency:

$$\dot{P}_{shaft} = \dot{P}_{rated}\eta_{motor} \tag{3.11}$$

The energy transferred to the fluid is then:

$$\dot{Q}_{fluid} = \dot{P}_{shaft}\left(1-\eta_{pumping}\right)+\left(\dot{P}_{rated}-\dot{P}_{shaft}\right)f_{motorloss} \tag{3.12}$$

and the outlet fluid temperature is calculated as:

$$T_{out} = T_{in} + \frac{\dot{Q}_{fluid}}{\dot{m}c_p} \tag{3.13}$$

where $\dot{m}$ is the rated fluid mass flow rate and c_p is the fluid specific heat. The outlet mass flow rate is the same as the rated flow rate as this is a single speed component.

The energy transferred to the surroundings, $\dot{Q}_{ambient}$, is calculated with the relationship:

$$\dot{Q}_{ambient} = \left(1- f_{motorloss}\right)\left(\dot{P}_{rated}-\dot{P}_{shaft}\right) \tag{3.14}$$

(SEL, 2004, pg 5-199, 5-200)

Table 3.7 Type 114 Parameters and Inputs

Parameters	Inputs
Rated flow rate Fluid specific heat Rated power Motor heat loss fraction	Inlet fluid temperature Inlet fluid flow rate Control signal Overall pump efficiency Motor efficiency

3.1.8 Type 647 Diverting Valve

Type 647 is a diverting valve, found in the TESS library that can accommodate up to 100 branches. It uses the relationship:

$$\dot{m}_i = \dot{m}_{in} f_i \tag{3.15}$$

where $\dot{m}_{in}$ is the mass flow from the pump, f_i is the fraction of the flow to the i^{th} branch, and $\dot{m}_i$ is the mass flow into the i^{th} branch.

Table 3.8 Type 647 Parameters and Inputs

Parameters	Inputs
Number of outlet ports	Inlet temperature Inlet flow rate Fraction of flow to each outlet

3.1.9 Type 648 Air Return Plenum

This TESS component mixes up to 100 inlet air flows, the number of flows desired is set in the component parameters, to determine exiting air properties. It takes as inputs the inlet air temperature, humidity level, pressure, and flow rate for each air stream as well as the air side pressure drop for the component. The outlet air flow rate ($\dot{m}_{out}$) is the sum of all the inlet ($\dot{m}_i$) flows. The outlet air pressure is set to the minimum pressure of the inlet streams, minus the airside pressure drop.

The TRNSYS Psychrometrics routine is called to determine the saturated humidity ratio, enthalpy, and relative humidity of each inlet stream from the corresponding pressure, temperature and either relative humidity or humidity ratio input. If the stream humidity levels are higher than saturation, the values are reset to a saturated level for the given temperature. The outlet humidity ratio is determined by:

$$\omega_{out} = \frac{\sum_{i=1}^{nports} \dot{m}_i \omega_i}{\dot{m}_{out}} \tag{3.16}$$

and the outlet enthalpy (h_{out}) is calculated using the stream enthalpies (h_i) returned from the psychrometrics routine:

$$h_{out} = \frac{\sum_{i=1}^{nports} \dot{m}_i h_i}{\dot{m}_{out}} \tag{3.17}$$

The psychrometrics routine is called again to calculate the exit temperature and relative humidity from the calculated humidity ratio and enthalpy. If ω_{out} proves to be greater than the saturation level, for the outlet temperature, the saturation level for the outlet temperature is returned instead. The condensate flow rate is then calculated as:

$$\dot{m}_{cond} = \dot{m}_{out} \left(\omega_{out} - \omega_{sat} \right) \tag{3.18}$$

where ω_{sat} is the saturated outlet humidity ratio returned by the psychrometrics routine.

Table 3.9 Type 648 Parameters and Inputs

Parameters	Inputs
Humidity mode Number of inlet ports	Inlet air temperature for each port Inlet air relative humidity for each port Inlet air flow rate for each port Inlet air pressure for each port

3.1.10 Type 649 Mixing Valve

The type 649 mixing valve functions like Type 648, but without the humidity calculations. It mixes up to 100 inlet streams and calculates the temperature and flow rate of the resulting outlet stream. (See section 3.1.9).

Table 3.10 Type 649 Parameters and Inputs

Parameters	Inputs
Number of inlets	Temperature at each inlet Flow rate at each inlet

3.1.11 Type 662 (111) Supply Fans

The TRNSYS type 662 variable air volume (VAV) fan from the TESS library is identical to the type 111 component in the standard library. This fan component requires the rated air flow rate, rated power, motor efficiency, motor heat loss fraction, number of power coefficients and their values to be set as parameters. The motor heat loss fraction can be set between zero and 1, with a value of 1 representing a motor located in the air stream with all motor losses resulting in heat addition to the air. The fan also requires inputs of inlet air temperature, inlet air humidity (relative humidity was used in this case), inlet air pressure, the air-side pressure increase and a control signal – a ratio of the operating mass flow rate to the design mass flow rate.

The fan speed (N) is related to the volumetric flow rate ($\dot{V}$) by the following fan law:

$$\dot{V}_1 = \dot{V}_2 \left(\frac{D_1}{D_2} \right)^3 \left(\frac{N_1}{N_2} \right) \tag{3.19}$$

(ASHRAE, 2000)

Thus for each individual fan of size D, the volumetric flow rate varies linearly with fan speed. And, the ratio of operating volumetric flow rate to volumetric rated flow rate is equivalent to the ratio of operating fan speed to rated fan speed. Since the air density can be assumed to be constant for this application, this also means that the ratio of operating mass flow rate to rated mass flow rate (γ) is equal to the fan speed ratio and to the volumetric flow ratio. The operating mass flow ($\dot{m}_{air}$) is then simply

$$\dot{m}_{air} = \dot{m}_{rated} \gamma \tag{3.20}$$

The following fan law can be used to relate the fan operating power to its rated power:

$$\dot{P}_1 = \dot{P}_2 \left(\frac{D_2}{D_1} \right)^4 \left(\frac{\dot{V}_1}{\dot{V}_2} \right)^2 \left(\frac{\rho_1}{\rho_2} \right) \tag{3.21}$$

(ASHRAE, 2000)

For an individual fan the size (D) is constant, and for an HVAC application it can be assumed that the air density (ρ) remains constant. Thus the operating power changes from its rated power by the cube of the fan speed ratio or fan flow ratio. In the TRNSYS type 662 component, the power used by the fan is calculated according to the following equation:

$$\dot{P} = \dot{P}_{rated} \left(a_0 + a_1 \gamma + a_2 \gamma^2 + a_3 \gamma^3 + a_4 \gamma^4 + \ldots \right) \tag{3.22}$$

where the a_n are the power coefficients and γ is the fan control signal (mass flow rate ratio). In order to replicate the fan power law, the number of power coefficients set in the fan parameters was 4, with $a_0 = a_1 = a_2 = 0$ and $a_3 = 1$.

The air-side pressure increase input required for the component is calculated in an equation external to the fan component. The equation is based on the fan law:

$$p_1 = p_2\left(\frac{D_1}{D_2}\right)^2\left(\frac{N_1}{N_2}\right)^2\left(\frac{\rho_1}{\rho_2}\right) \tag{3.23}$$

(ASHRAE, 2000)

with p equal to either the total pressure or the static pressure developed by the fan. For a fan of size D, with the density assumed to be constant, the pressure developed at any speed can then be calculated as:

$$p = p_{rated}\gamma^2 \tag{3.24}$$

Using the calculated power ($\dot{P}$), the motor efficiency (η), and the motor heat loss fraction (f), the type 662 fan calculates the energy transferred to the air stream as

$$\dot{Q}_{air} = (\eta + (1-\eta)f)\dot{P} \tag{3.25}$$

With f = 1, $\dot{Q}_{air} = \dot{P}$. The fan component then calculates the enthalpy (h) of the exiting air stream as:

$$h_{air,out} = h_{air,in} + \frac{\dot{Q}_{air}}{\dot{m}_{air}} \tag{3.26}$$

The exiting air temperature is then calculated based on the exiting enthalpy and specified pressure increase.

(SEL, 2004 pg 5-195 through 5-196)

Table 3.11 Type 662 Parameters and Inputs

Parameters	Inputs
Humidity mode	Inlet air temperature
Rated flow rate	Inlet air relative humidity
Rated power	Air flow rate
Motor efficiency	Inlet air pressure
Motor heat loss	Control signal
Number of power coefficients	Air side pressure increase
Power coefficient values	

3.1.12 Type 684 Air Side Economizer

An air side economizer is used to reduce the amount of cooling needed in an air distribution system by controlling the amount of outside air in the system. Type 684 can be operated in temperature, enthalpy, or humidity mode. In temperature mode, if the outside air temperature is greater than the zone temperature set point, the economizer will bring in the minimum amount of outside air. When the outside air temperature is between the zone set point and the cooling coil discharge value, the maximum outside air is brought in by the economizer. If the outside air temperature is lower than the cooling coil set point, the economizer will modulate the amount of outside air brought in. Enthalpy or humidity mode operation follows the same decision procedure, but the comparison is made based on enthalpy or humidity rather than temperature. See (TESS, 2004) for more details regarding the calculation of the appropriate outside air fraction.

Once the appropriate outside air fraction has been determined, the Type 684 component calculates the energy from the outside air stream ($\dot{Q}_{out}$) based on the mass flow of the supply air ($\dot{m}_{SA}$) and the enthalpies of the return air and mixed air (h_{return} and h_{mix}):

$$\dot{Q}_{out} = \dot{m}_{SA}\left(h_{return} - h_{mix}\right) \tag{3.27}$$

The energy saved by the economizer ($\dot{Q}_{saved}$) is also calculated using the fraction of outside air brought in by the economizer (f_{OA}), the minimum outside air fraction (f_{min}), and the enthalpy of the outside air (h_{OA}):

$$\dot{Q}_{saved} = \left(f_{OA} - f_{\min} \right) \dot{m}_{SA} \left(h_{return} - h_{OA} \right) \quad (3.28)$$

Table 3.12 Type 684 Parameters and Inputs

Parameters	Inputs
Humidity mode (relative humidity or absolute humidity ratio as an input) Economizer mode (temperature, enthalpy, or humidity mode)	Ambient outside air temperature Ambient air humidity Ambient air pressure Zone air temperature Zone air humidity Zone air pressure Supply air flow rate Minimum outside air fraction Outside air damper pressure drop Exhaust air damper pressure drop On/Off control signal Zone set point temperature Cooling coil set point temperature

3.1.13 Type 752 Cooling Coil

The type 752 cooling coil is contained in the TESS library. This cooling coil model, as with the heating coil type 754, assumes an unlimited cooling capacity and allows three different control strategies: outlet air temperature control, outlet air humidity control, or control of both outlet air temperature and humidity by means of reheat. In the current project, control was based on outlet air temperature only.

The component requires inputs of the inlet air conditions (temperature, pressure, mass flow rate, and humidity), the airside pressure drop across the coil, an on/off control signal, and the outlet air temperature setpoint. In addition, the component requires the input of an air bypass fraction (f_{bypass}). The coil bypasses the cooling coil with the specified fraction of

the air flow rate and mixes it with the remaining air coming off the coil. This bypass approach is used primarily to mimic the complexities of latent transfer from a wet coil (Mitchell & Braun, 2006).

The outlet air pressure is calculated, as with the heating coil type 754 according to:

$$P_{out} = P_{in} - \Delta P \tag{3.29}$$

Type 752 calls the TRNSYS Psychrometrics routine to calculate the humidity ratio from the air relative humidity at inlet. The then component uses an iterative process to determine the temperature of the air leaving the coil. It starts with the inlet conditions as a first guess, then iterates the outlet air temperature until the mixed temperature reaches the outlet setpoint, or 100 iterations are completed. With the temperature of the air leaving the coil known, the leaving mixed air properties are calculated according to the following relationships:

$$h_{air,out} = f_{bypass} h_{air,in} + (1 - f_{bypass}) h_{air,coil} \tag{3.30}$$

$$\omega_{air,out} = f_{bypass} \omega_{air,in} + (1 - f_{bypass}) \omega_{air,coil} \tag{3.31}$$

where $h_{air,out}$, $h_{air,in}$, and $h_{air,coil}$ are the enthalpies of the outlet mixed air, the inlet air, and the air leaving the coil, respectively, and $\omega_{air,out}$, $\omega_{air,in}$, and $\omega_{air,coil}$ are the humidity ratios of the mixed air, inlet air, and air leaving the coil, respectively. The humidity ratio of the air leaving the coil is assumed to be the smaller of the coil inlet condition or a saturated level. The mass flow of condensate ($\dot{m}_{cond}$) is calculated using the total air mass flow rate($\dot{m}_{air}$) and humidity ratios as

$$\dot{m}_{cond} = \dot{m}_{air} (\omega_{air,in} - \omega_{air,out}) \tag{3.32}$$

When the coil is commanded off using the control command, or if the bypass fraction is set to 1, the outlet dry bulb temperature is assumed to be the same as the inlet condition.

However, the outlet air pressure is still calculated according to the same pressure relationship above, and a call is made to the psychrometrics routine with the new pressure to identify any condensation that may occur due to the pressure change (TESS, 2004b).

Table 3.13 Type 684 Parameters and Inputs

Parameters	Inputs
Control mode Humidity mode	Air inlet temperature Air humidity Air flow rate Air pressure Air side pressure Coil bypass fraction On/Off control signal Outlet air temperature set point Outlet air humidity set point

3.1.14 Type 754 Heating Coil

This heating coil component, contained in the TRNSYS TESS library, assumes an unlimited heating capacity and will also provide humidification if desired. It allows three control strategies – control of outlet air temperature, outlet humidity, or a combination of both temperature and humidity. In the current project the humidity control options were not used.

The component requires inputs of inlet air temperature, humidity (relative or humidity ratio) pressure, and mass flow rate, as well as the air-side pressure drop across the coil, an outlet temperature setpoint, and a relative humidity setpoint. In addition, there is an on/off command input for the component. When there is no air flow through the coil or the coil is commanded off, the outlet pressure is calculated with

$$P_{out} = P_{in} - \Delta P \tag{3.33}$$

where ΔP is the pressure drop across the coil and P_{in} and P_{out} are the inlet and outlet air pressures. The remaining outlet air properties are set to their corresponding inlet values.

When there is air flow across the coil and the coil is commanded on, the outlet air pressure is calculated as above. If the inlet dry bulb temperature is higher than the setpoint, the latent energy, $\dot{Q}_{latent}$, is then calculated as:

$$\dot{Q}_{latent} = \dot{m}_{air}(\omega_{out} - \omega_{in}) \tag{3.34}$$

where $\dot{m}_{air}$ is the mass flow rate of air across the coil and ω_{out} and ω_{in} are the outlet and inlet humidity ratios. While the humidification option was not used in the current project, it is still possible for the latent energy to be non-zero when the air is at saturation conditions.

When the inlet temperature is lower than setpoint, the outlet air temperature is increased to the desired level, the air properties are calculated, and the sensible heat is determined using the outlet and inlet enthalpies (h_{out} and h_{in}) as:

$$\dot{Q}_{sensible} = \dot{m}_{air}(h_{out} - h_{in}) \tag{3.35}$$

When the sensible heat addition is non-zero and the component is set for temperature control only, the latent energy is set to zero since condensation will not occur with a sensible addition (TESS, 2004c).

Table 3.14 Type 754 Parameters and Inputs

Parameters	Inputs
Control mode Humidity mode	Inlet air temperature Inlet air relative humidity Air flow rate Inlet air pressure Control signal Air side pressure increase

3.2 Rennebohm Hall Model

3.2.1 Type 56 Building Model

The building model was created using the TRNBuild program packaged with TRNSYS 16.

Eight wall types were created for this building: exterior brick, concrete partition, gypsum partition, wall stud, roof, ground floor, louver, and spandrel (see Table 3.15).

Table 3.15 Type 56 Wall Types

TRNSYS Tag	Type	U Value Btu/ft^2-R [W/m^2-K]	Layers	Thickness inch [m]
PHR_BRICK_EXT	Exterior Brick	.078 [.444]	Wall Board	2.18 [.055]
			Cement Mortar	8 [.203]
			Polystyrene	2 [.051]
			Air Gap	--
			Face Brick	3.63 [.092]
CONCPARTITION	Concrete Partition	.483 [2.745]	Cement Mortar	.4 [.010]
			Air Gap	--
			Cement Mortar	.4 [.010]
GYPSPARTITION	Gypsum Partition	.425 [2.411]	Gypsum Resistance	--
			Air Gap	--
			Gypsum Resistance	--
METALSTUD	Wall Stud	.925 [5.252]	Cement Mortar	.4 [.010]
			Metal Stud	3.63 [.092]
			Cement Mortar	.4 [.010]
ROOF	Roof	.039 [.224]	Steel	1.75 [.044]
			Polystyrene	4 [.102]
			Rubber	1 [.025]
			Roof Deck	.5 [.013]
GROUNDFLOOR	Ground Floor	.495 [2.809]	Concrete Slab	6.5 [.165]
			Granite	5.5 [.140]
LOUVER	Louver	.144 [.818]	Polystyrene	1.5 [.038]
			Steel	.75 [.019]
SPANDREL	Glass Spandrel	.098 [.555]	Wall Board	.63 [.016]
			Air Gap	--
			Polystyrene	2 [.051]
			Glass	.25 [.006]

The partition types (concrete and gypsum) were used to define interior walls between zones. To account for the metal studs within the walls, a fraction of the wall was defined as metal stud, and the rest was defined as either a concrete or gypsum partition without studs. The metal stud fraction was determined from the wall sections in the architectural drawings. No walls were defined within each zone assuming no internal temperature gradients and a low capacitance. Air gaps are not assigned a thickness in TRNSYS because they provide negligible capacitance. Similarly, the gypsum layers in the gypsum partition are not assigned a thickness as the capacitance of these partitions is considered negligible. All wall layers are assigned a total heat transfer resistance value. Because internal walls are not defined explicitly, the total capacitance assigned to each zone is increased from the TRNSYS 16 default of $1.2 \cdot volume$ to $10 \cdot volume$, a value still within a standard rule-of-thumb range for zone capacitance, but designed to capture some of the capacitance of the internal zone structures.

Two window types were created, each using the same type of glass; one for the curtain wall with no frame area, and one for the smaller 1.2 m x 1.2 m (4 ft x 4 ft) windows with an aluminum pane. The building construction documents specified that the curtainwall glazing should have an external glass panel equivalent to Viracon VA 1-35 #2, an air gap of ½ inch, and an internal clear float glass panel. Data on this glazing was requested from the manufacturer and a new glazing type was created for TRNSYS 16 using the Lawrence Berkeley National Labs Window 5.2a software (LBNL, 2005). The glazing data are summarized in Table 3.16.

Table 3.16 Glazing Data

Viracon Reflective Insulating Glazing	
Transmittance	
Visible Light	34%
Solar Energy	24%
Ultra-Violet (300 to 380 nanometer)	15%
Reflectance	
Visible Light-Exterior	12%
Visible Light-Interior	31%
Solar Energy	10%
ASHRAE U-Value	
Summer Daytime	0.46 Btu/(hr-ft^2-°F)
Winter Nighttime	0.45 Btu/(hr-ft^2-°F)
European U-Value	2.6
Shading Coefficient	0.42
Relative Heat Gain	91 Btu/(hr-ft^2)
Solar Factor	0.36
LSG	0.93

Wall and window dimensions were measured from the Rennebohm Hall architectural drawings. Only external walls and partitions separating zones were modeled. The floor to floor height taken from the building elevation drawings was used to compute zone volumes.

Heating types were created for all zones in the building component with the exception of the MER heating only zones with large internal gains and very few ventilation or transmission losses. The heating types were created to allow unlimited heating power. Type 56 receives ventilation from the air handler models at 55 °F. The gains and losses for the zone are calculated, then the heating type computes the heating energy required to bring the zone temperature to its set point. This simulates the hot water used in terminal reheat coils and the perimeter radiant heating. The zone set point for the 100% outside air zones is a

constant 72 °F, however, for the VAV zones with return air the zone temperature set point is variable – this control will be discussed further in section 3.2.3.

Internal gains due to sources such as lighting, equipment, people, and animals were estimated and scheduled in Type 56. Details of the gains scheduled will be discussed in Section 3.2.4.

3.2.2 Heat Recovery

The two heat recovery systems in the building use the same components, but differ in their piping loops. There is only one heat recovery module (HRM1) serving the Vivarium – shown in Figure 3.1 as the Type 5b heat exchanger. This component receives air at a flow rate received from the Type 648 air plenum that provides ventilation to the zone. The air temperature across HRM1 is provided by the Vivarium zone temperature from the building component. On the glycol side, the flow rate is input directly from the Type 31 pipe, but the glycol flow rate for the entire loop is determined by the Type 114 pump. Neither of the flow rates in the HRM1 vary significantly when the heat recovery system is operating and so the heat exchanger UA is entered as a constant value. After the pump, the flow is equally divided into two streams by a Type 647 diverting valve. The two streams then each enter a separately controlled bypass valve, modeled as Type 11. The bypass valves are controlled by Type 23 PID controllers that have the temperature of the air exiting the heat recovery supply coils (also Type 5 heat exchangers) as the controlled variables. As the glycol flow through the supply coils in the air handlers is variable, the effective UA of the supply coils is adjusted based on the bypass command from the PID. More discussion of the UA determination for

the heat recovery coils can be found in Section 4.2. After passing through the supply coils, the two glycol streams are mixed in a Type 649 mixing valve.

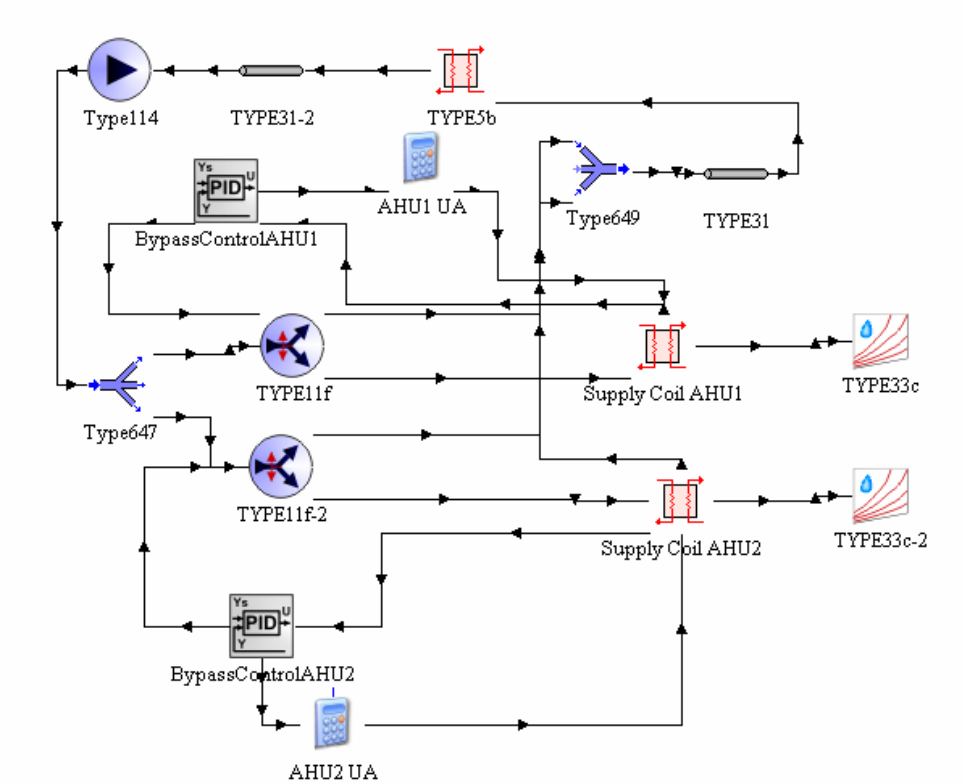

Figure 3.1 Vivarium Heat Recovery Model

The air flow rates for the heat recovery supply coils in AHU1 and AHU2 are determined by the supply fans, and the outside air temperatures are determined by the weather data. The exiting air is passed from the supply coil to a Type 33 psychrometrics calculator, and air properties are calculated based on the temperature of the air leaving the coil and the humidity from the weather data. These are properties are passed to the supply fans.

The heat recovery system for the Tower Labs zone functions in much the same way, but there are two separate HRMs (HRM2 and HRM3). Figure 3.2 shows the heat recovery system for AHU6. The system is identical for AHU7.

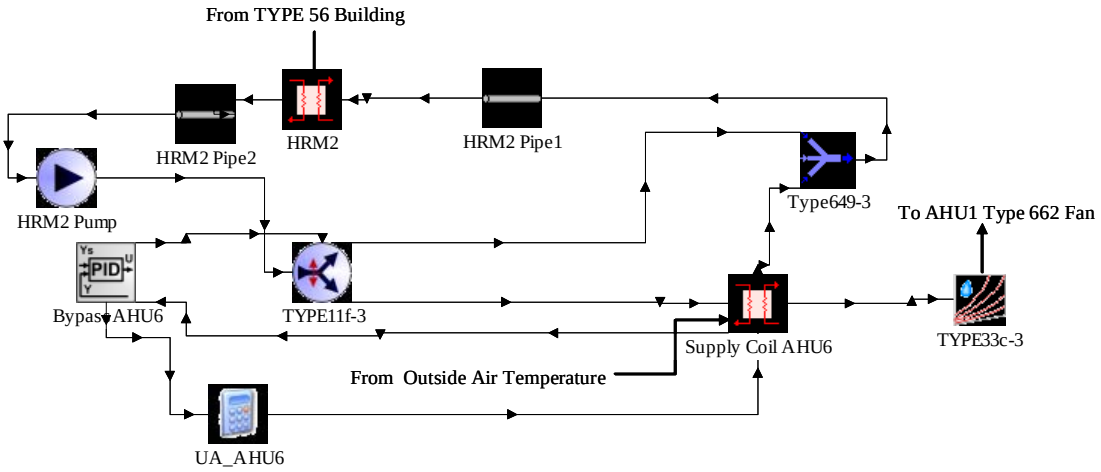

Figure 3.2 AHU6 Heat Recovery - Tower Lab Zone

3.2.3 Air Handler Models

Figure 3.3 shows the components used in the AHU7 model. The same model components are used in AHU1, AHU2, AHU4 and AHU6. For the zones with two AHUs operating in tandem, air is mixed using a Type 648 air plenum (as shown in Figure 3.3) and the combined air flow is passed to the building component. AHU4 operates individually and so an air plenum is not required for the Teaching Lab zone.

While most of the 100% outside air systems are designed as CAV, building data indicates that they generally are not running at their design fan speeds. Thus, each fan has a formula providing a control signal to the fan component to scale the air flow from its rated flow.

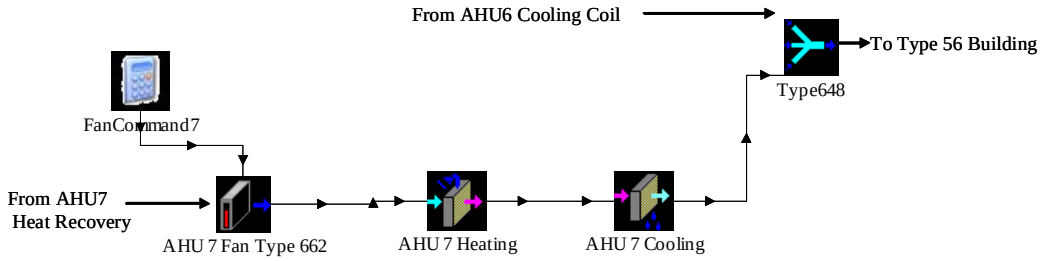

Figure 3.3 AHU7 Air Handler Model

AHU3 and AHU5 are VAV systems using return air and are modeled using the same components. The model used for AHU5 is shown in Figure 3.4. The economizer adjusts the amount of outside air based on the zone set point, cooling coil set point, and outside air temperature as described in Section 3.1.12. The VAV zones in this building are designed to receive a minimum volumetric outside airflow, rather than a constant minimum outside air fraction. Thus, a formula calculates the minimum outside air fraction based on the minimum air flow rate required and the fan airflow at each time step. The VAV fans for AHU3 and AHU5 are each controlled by a Type 23 PID controller that has the zone air temperature as its controlled variable. The controller has a negative gain constant, so when the zone temperature falls below the set point of 72°F, the fan speed will decrease, until its minimum speed at which time the hot water heating should increase the zone temperature.

As the hot water reheat coils should only be activated in heating mode and only when the air flow is at a minimum, the Type 56 zone temperatures for the General Zone and the Tower Offices Zone are taken calculated according to the following formula:

$$T_{goal}\left(EQL\left(Fan_{Control}, Fan_{Min}\right)+LT\left(Fan_{Control}, Fan_{Min}\right)\right) \tag{3.36}$$

where T_{goal} is the desired zone temperature (72°F in this case), $Fan_{Control}$ is the control signal from the PID controller, and Fan_{min} is the minimum control signal. Thus, when the fan control signal is less than or equal to the minimum fan setting, the quantity within the

parentheses will be 1, and the zone temperature will be set at the desired temperature so that the reheat and perimeter heating will turn on in the zone. When the fan signal is greater than its minimum setting, the unit should be in cooling mode and the quantity within the parentheses in equation (3.36) will be zero, making the zone temperature set point artificially low. This prevents the hot water heating from activating in cooling mode.

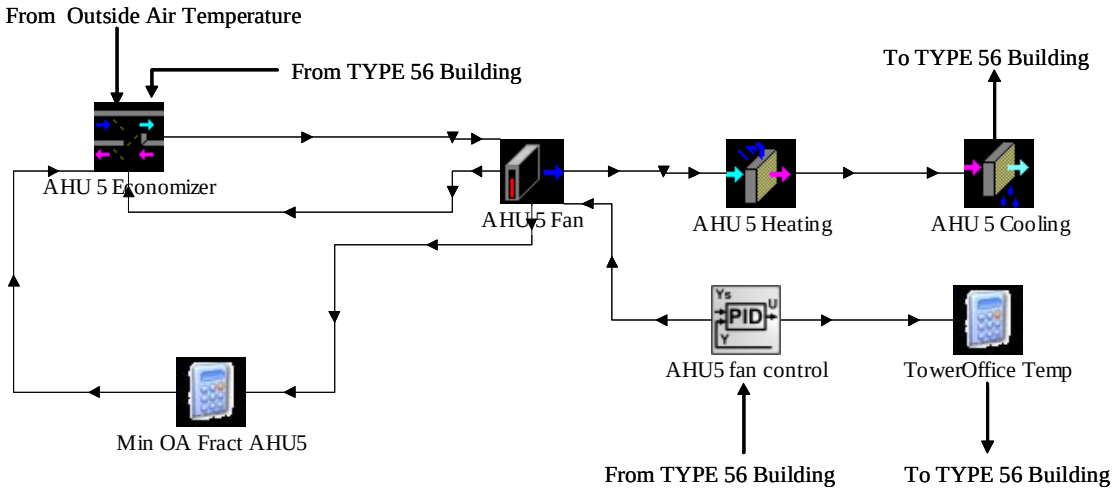

Figure 3.4 AHU5 Air Handler Model

3.2.4 Internal Gains

The internal gains specified for most zones were standard rule-of-thumb values: 1.5 W/ft^2 for lighting, 230 W of office equipment per person, and an occupancy diversity stepped over the workday with a maximum of 80% of the design maximum zone occupancy during weekday office hours, a maximum of 30% of the design zone occupancy on Saturdays, and a maximum of 30% of the zone occupancy on Sundays. The minimum occupancy diversity scheduled at any time was 10%. The design zone occupancy values were taken from the

architectural construction documents and are listed in Table 2.1. Additional gains of 1 W/ft^2 were included in laboratory zones to account for laboratory equipment. No internal gains were included in the heating only MER or North Stairway zones.

Chapter 4: Model Calibration

Calibration of a building simulation with measured data can establish the validity of the simulation. The calibration process involves setting simulation variables and parameters to reflect the actual functionality of the building with the goal of replicating collected building data. If the results of the building simulation reflect the behavior of the measured building data, then the model can be used to predict the behavior of building systems under new operating conditions and possibly the behavior of buildings of similar design.

A number of adjustments to the model were made during the calibration process In the calibration process for the Rennebohm Hall building simulation.. Simulated air flow rates were matched with measured rates. The behavior of the heat recovery coils and heat recovery glycol flow rates were adjusted. The sensible and latent heat removed by the chilled water coils were compared to estimates of heat removal made from the measured temperature and humidity levels. The simulated steam energy was compared to the measured steam flow, and the building internal gains were approximated. In some cases, complete calibration data were not available, and in those cases, rule of thumb approximations were used.

4.1 Air Flow Rate Calibration

Inspection of the building automation system (BAS) data revealed that the building fans were often not operating at their design speeds. Review of the Test and Balance Report completed at the end of construction revealed that all but two of the units in the building had been balanced at their maximum design supply flow rates (Balco, 2001). The two that were

assigned new design flow levels were AHU6 and AHU7, serving the Tower Labs zone. It was discovered during balancing, that the sum of the flow rates in all the terminal units served by AHU6 and AHU7 differed slightly from original design flow of 65,000 cfm each. Thus, they were balanced to match the sum of the terminal unit flow rates resulting in AHU6 delivering 55,700 cfm and AHU7 delivering 58,200 cfm at their maximum variable frequency drive (VFD) commands.

The exact reasons for the observed differences from design air volume flow rates were not clear. It is possible that the new flow rates were the result of building or control faults. But it is also possible that there were changes in zone air flow requirements due to changes in building occupancy, space utilization, or for occupant comfort. As the supplied air flow rates have a large impact on building energy usage, the TRNSYS model fan speeds were adjusted to mimic the actual BAS fan speeds for model calibration.

AHUs 1 and 2 serving the Vivarium zone, AHU 4 serving the Teaching Lab zone, and AHUs 6, and 7 serving the Tower Labs zone are all100% outside air, constant air volume (CAV) units. In these zones, most, if not all, of the terminal units are set with a fixed valve position yielding a fixed zone air flow. The supply fans serving these zones are fitted with VFDs and small variations in air flow rate are to be expected due to pressure variations in the zone or due to a limited number of variable flow terminal units located in some of the zones. However, the fans are designed to supply flow a constant air flow to these zones. As air flows in the building CAV systems are not measured directly, the actual volumetric flow rates were approximated by assuming a scaling with fan VFD speed from the design flow rate using the fan laws. The results of this calculation for each CAV unit are presented in

Figure 4.1 through Figure 4.5. The color changes in the lines in the Figures indicate a new month of the year.

For AHUs 1, 2, and 4, the BAS fan VFD speeds reveal little daily variation in fan speed, but there seemed to be distinct changes in speed over the course of the year. In the interest of simplicity, a step function was used to approximate these changes in fan speed, rather than using the actual BAS data file as an input to the model. The use of a formula input instead of data input makes it simpler to adjust the model for investigation of the effects of fan speed on building performance. Summaries of the fan speed steps used in TRNSYS are presented in Table 4.1 through Table 4.3. The control signal was provided to the fan PID controller as a variable input, and was calculated as actual flow divided by design flow.

Table 4.1 TRNSYS Fan Control Stepping Function for AHU1

AHU1 (Design Flow18000 cfm)		
Hour of Year Range	Flow [cfm]	Control Signal
0-300	12000	.667
300-2580	10790	.599
2580-3055	11730	.652
3055-3740	12210	.678
3740-5510	17060	.948
5510-6660	16210	.901
6660-8160	15790	.877
8160-8760	15180	.843

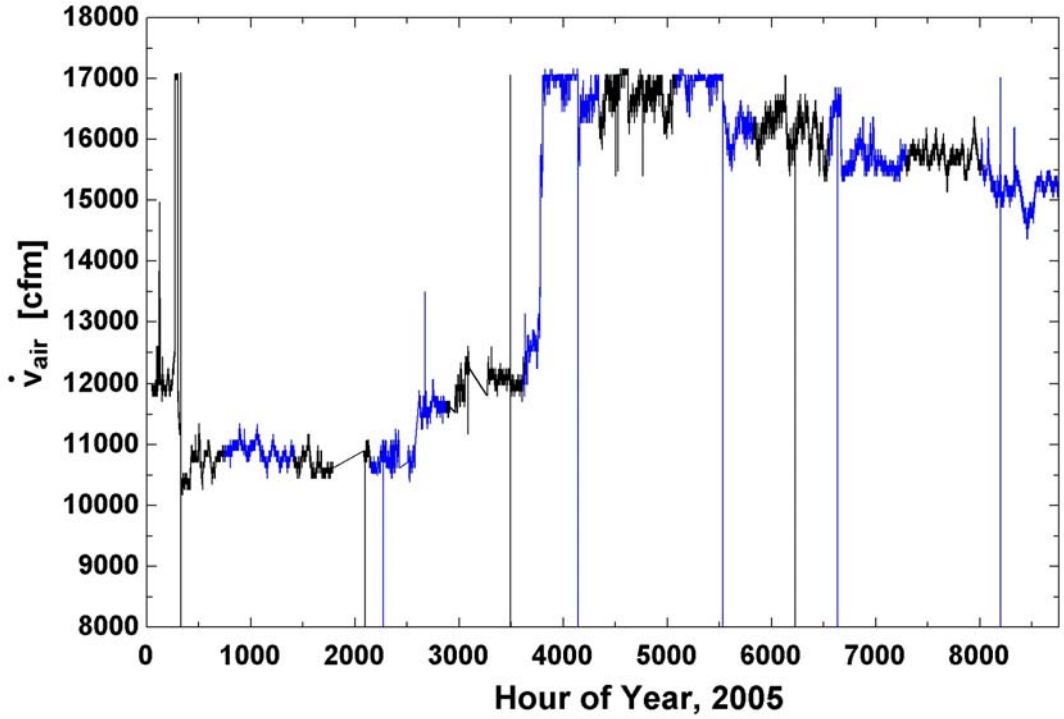

Figure 4.1 AHU1 Air Flow Rate as Calculated from BAS VFD Data.

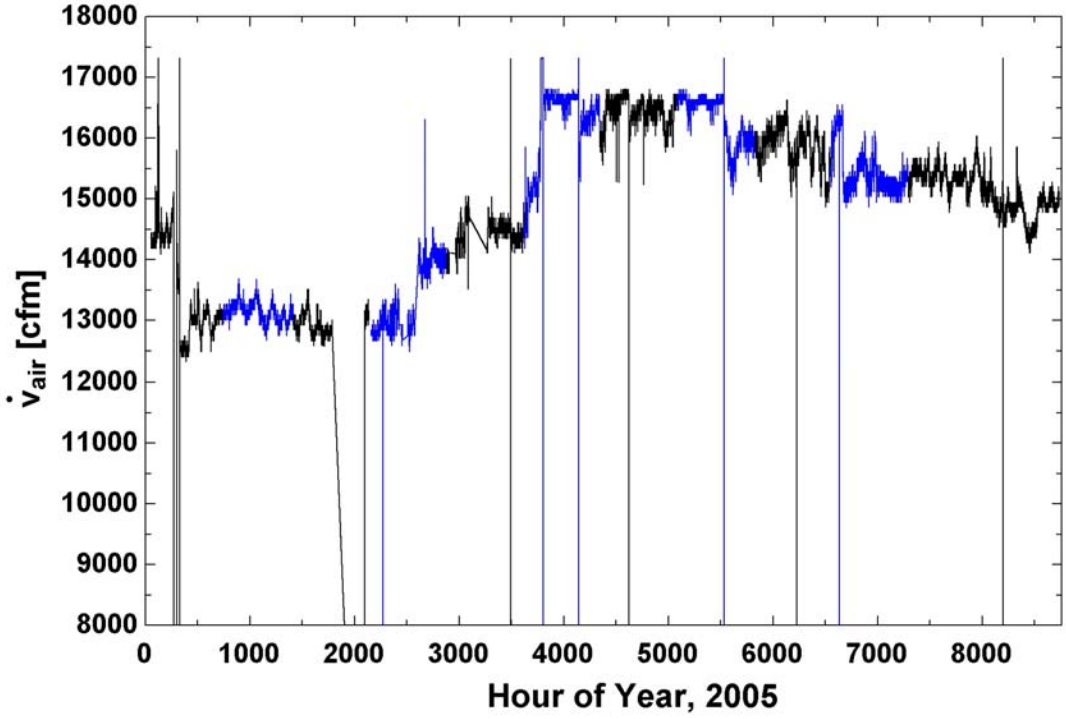

Figure 4.2 AHU2 Flow Rate as Calculated from BAS VFD Data.

Table 4.2 TRNSYS Fan Control Stepping Function for AHU2

AHU2 (Design Flow18000 cfm)		
Hour of Year Range	Flow [cfm]	Control Signal
0-300	14485	.805
300-2600	13120	.729
2600-2970	14030	.779
2970-3640	14455	.803
3640-5530	16600	.923
5530-6680	15880	.882
6680-8760	15300	.850

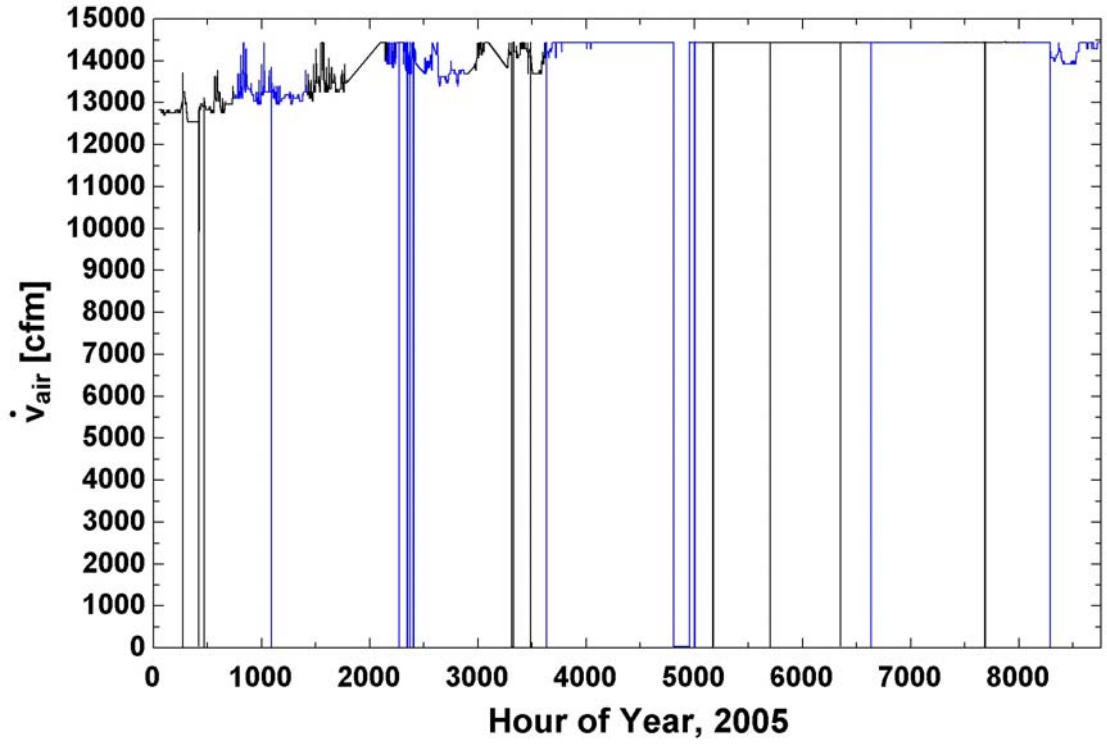

Figure 4.3 AHU4 Flow Rate as Calculated from BAS VFD Data.

Table 4.3 TRNSYS Fan Control Stepping Function for AHU4

AHU4 (Design Flow15000 cfm)		
Hour of Year Range	Flow [cfm]	Control Signal
0-1925	13500	.900
1925-8670	14500	.967

The daily changes in fan speed for AHU6 and AHU7 were greater than those of the other CAV units. But, there was not a clear step pattern over the year as with the other units so an average fan speed over the year was used to determine a constant control signal for these units. For AHU6, the control signal in the simulation was fixed at 0.748 of the maximum. With the new design flow rate of 52,600, this control value yields an operating flow rate of 41,660 cfm. For AHU7 with a new design flow rate of 58,200 cfm, the operating air flow rate for AHU7 was fixed at 44,870 cfm using the corresponding control signal of 0.771.

AHU3 and AHU5 are variable air volume (VAV) units equipped with return air recirculation. Consequently, the volumetric air flow rate calibration process is different for these units. When the zones served by these AHUs are in cooling mode, the fan speed depends indirectly on the building zone temperature. The fan speed is controlled to maintain a constant duct static pressure and the terminal units in the zone are controlled based on zone temperature. If the zone is too cold, the terminal units modulate closed until their minimum setting. If more heating is needed, they then initialize the hot water reheat coil. If the zone is too hot, the reheat coil modulates shut and then the air valve modulates open to supply more cool air. A duct static pressure sensor will speed up the supply fan when static pressure decreases (terminal units demanding more air) and slow down the supply fan when static pressure increases (terminal units demanding less air).

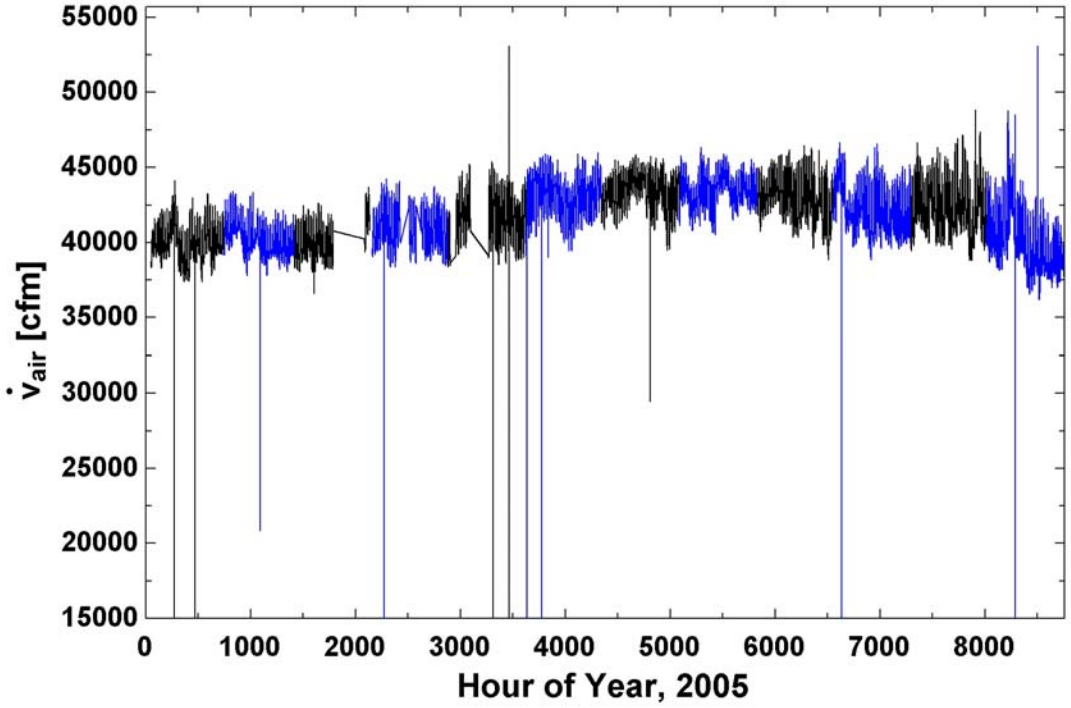

Figure 4.4 AHU6 Flow Rate as Calculated from BAS VFD Data.

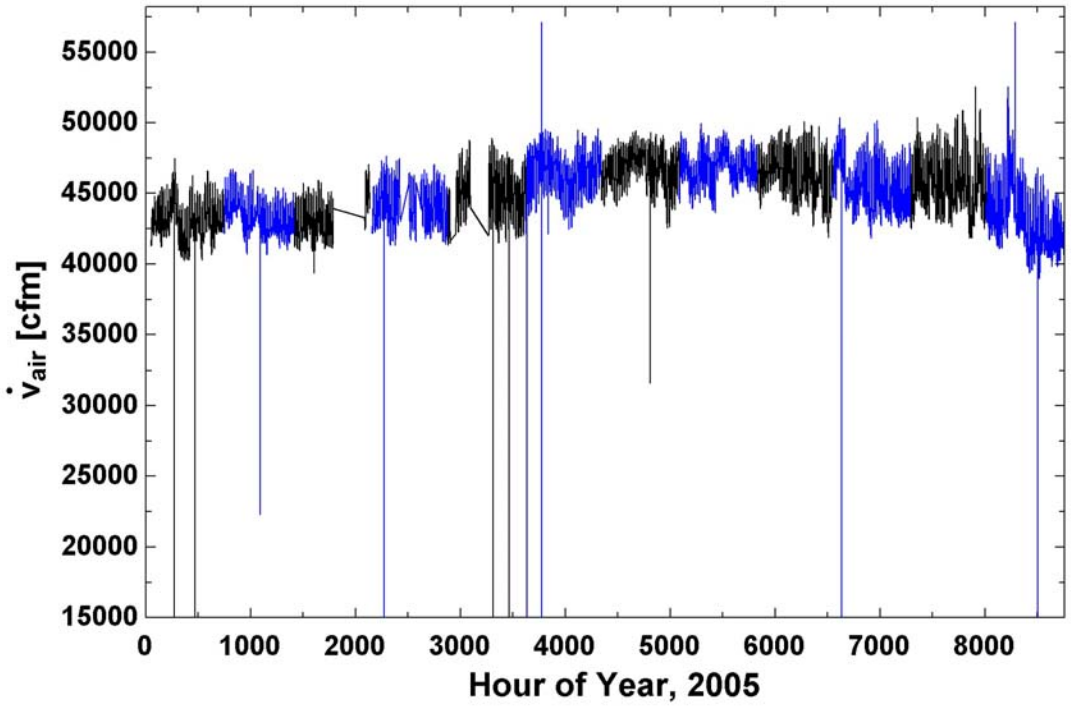

Figure 4.5 AHU7 Flow Rate as Calculated from BAS VFD Data

When the zones served by AHU3 and AHU5 require heating, the supply fans should, theoretically, revert to their minimum settings. However, the BAS data indicated that these units never actually ran at their design minimum settings of 24,000 cfm for AHU4 and 10,000 cfm for AHU5. There are a number of possible explanations for this behavior. It could be due to faulty terminal VAV boxes that don't revert to their minimum settings, to simultaneous heating and cooling modes in different parts of the zone, or to some combination of these issues. Simultaneous heating and cooling modes in the zone normally does not indicate a fault, but rather occurs in response to different loading within the zone.

Flow measuring stations are located at the supply fan, at the return fan, and at the minimum outside air damper for AHU3 and AHU5. However, the measured flow rates and flow rates calculated using the fan VFD data and design flow rates were not always internally consistent. The supply and return flows for AHU3 and AHU5 are presented in Figure 4.6 and Figure 4.7, respectively. As shown in Figure 4.6, AHU3 exhibited faults resulting in unreliable flow measurement and unstable fan speed for the first two thirds of the year. However, the supply airflow, as calculated from the VFD command for both AHU3 and AHU5 (the dark blue line in the Figures), appears to provide a good approximation to the actual supply air flow. Building faults will be discussed further in Chapter 6.

As these systems consistently operate at flow rates above their design minimum rates, the minimum fan speeds on the supply fan controller components in the model were increased to reflect the minimum flows observed based on data collected by the BAS system.

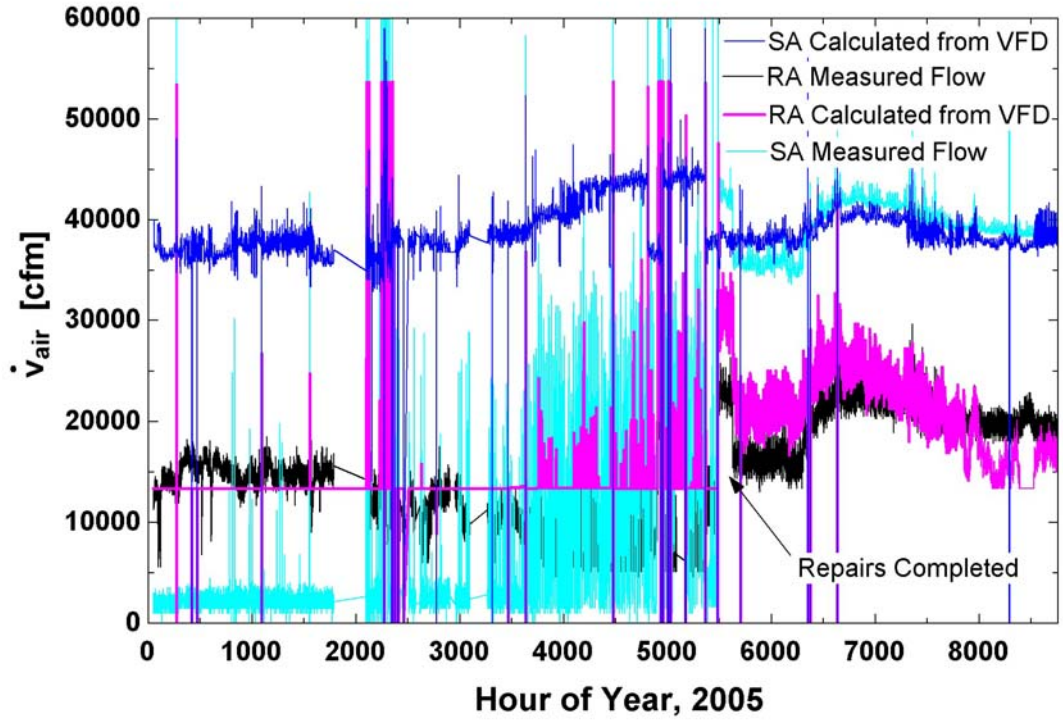

Figure 4.6 AHU3 Supply and Return Air Flows, as Measured and as Calculated from BAS VFD Data

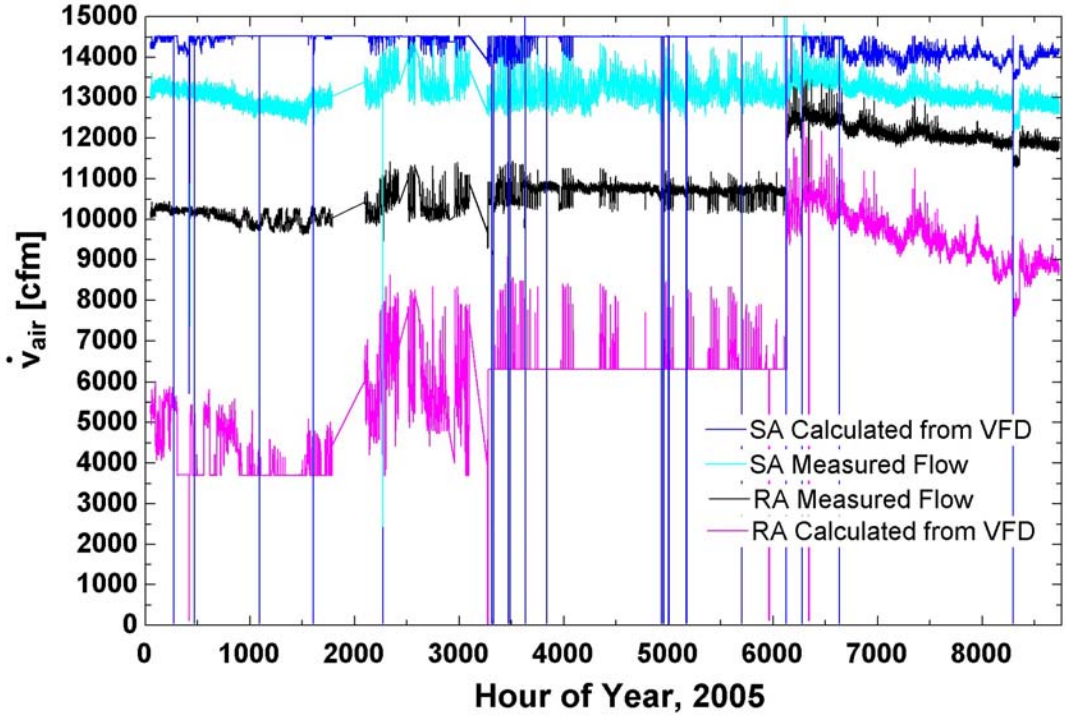

Figure 4.7 AHU5 Supply and Return Air Flows, as Measured, and as Calculated from BAS VFD Data

As seen in Figure 4.7, the measured and calculated flow rates for the AHU5 return fan appear to have a constant offset. In this case, the measured return air flow appears to be more accurate than the VFD calculated value. This was verified through examination of the mixed air temperatures in the unit. The mixed air temperature can be calculated using the outside air temperature (T_{OA}), the return air temperature (T_{RA}), and the return, outside air, and total supply air flow rates ($\dot{V}_{RA}, \dot{V}_{OA}, \dot{V}_{SA}$, respectively):

$$T_{MA} = T_{OA}\frac{\dot{V}_{OA}}{\dot{V}_{SA}} + T_{RA}\frac{\dot{V}_{RA}}{\dot{V}_{SA}} \tag{4.1}$$

The mixed air temperature using the measured flow rates matched the measured mixed air temperature much better than the same calculation using the flow rates calculated from VFD data. This indicates that there may have been a change in the return fan specifications. However, as the TRNSYS simulation does not model the return fans but instead utilizes the supply fan and an outside air fraction to calculate the return air fraction, this deviation from design is not important to the calibration.

4.2 Heat Recovery System

The TRNSYS Type 5 heat exchanger models require the overall heat transfer coefficients (UA) as inputs. As only limited manufacturer's data were available for the heat recovery coils, the effective UA was estimated from the BAS data. All UA calculations were performed with data from February, 2005. This month was selected for the completeness of the data, and for the range of outdoor air temperatures that occurred causing the heat recovery system to modulate through its range of operation.

For AHU6 and AHU7, data were available for the supply (T_{GS}) and return (T_{GR}) glycol solution temperatures, the outside air temperature (T_{OA}), and the air temperature after the heat recovery coil (T_{HR}). The log mean temperature difference can be calculated by:

$$\Delta T_{lm} = \frac{\left(T_{GS} - T_{HR}\right) - \left(T_{GR} - T_{OA}\right)}{\ln\left(\frac{T_{GS} - T_{HR}}{T_{GR} - T_{OA}}\right)} \tag{4.2}$$

Since the mass flow rate of air ($\dot{m}_{air}$) can be calculated from the fan VFD data, the heat transfer rate is calculated with an air side energy balance as follows :

$$\dot{q} = \dot{m}_{air} c_{p,air} \left(T_{HR} - T_{OA}\right) \tag{4.3}$$

Then, UA can be calculated based on:

$$\dot{q} = \left(UA\right) \Delta T_{lm} \tag{4.4}$$

While valve position data were available for the heat recovery coil bypass valve, the mass flow rate of glycol solution does not change linearly with valve position. Thus, a flow fraction F_{Flow} was calculated as:

$$\dot{q} = \dot{m}_{EG,Design} F_{Flow} c_{p,EG} \left(T_{GS} - T_{GR}\right) \tag{4.5}$$

where $\dot{m}_{EG,Design}$ is the flow rate of ethylene glycol solution provided by the coil manufacturer's data. Figure 4.8 plots the calculated glycol flow fraction versus the measured valve position.

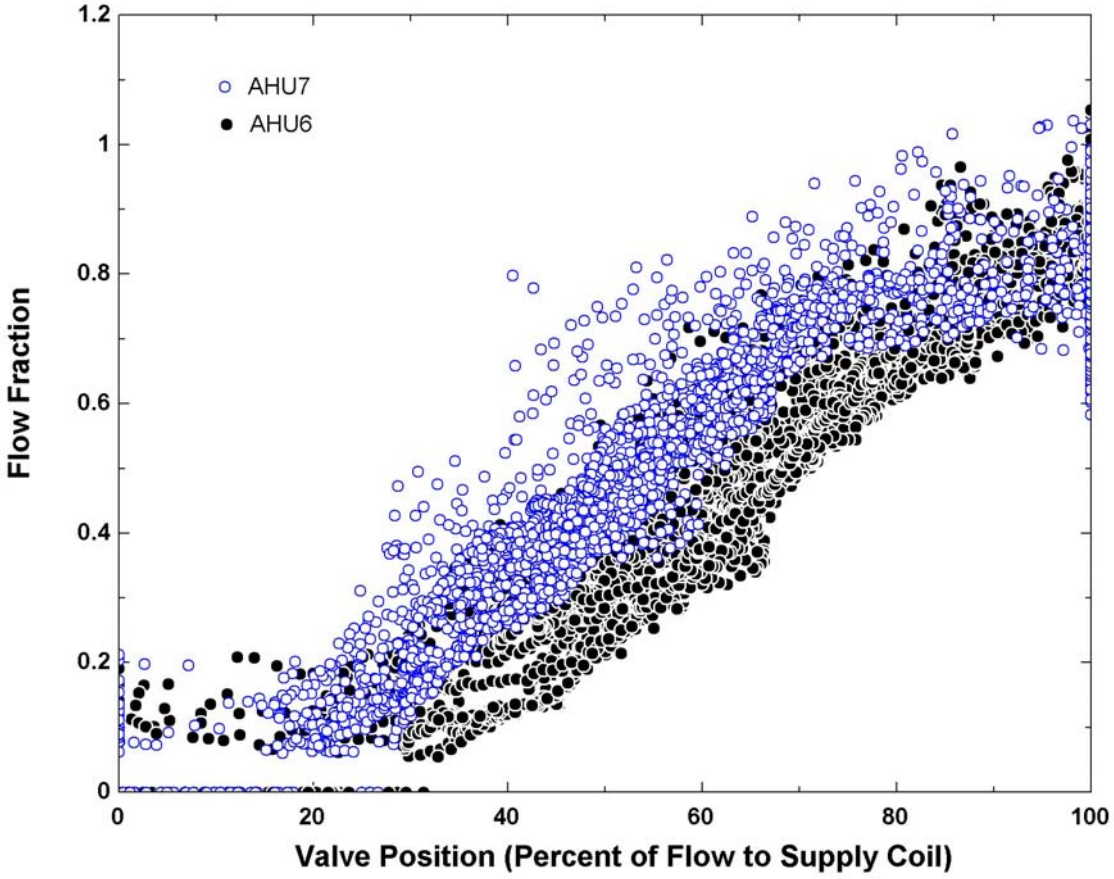

Figure 4.8 Calculated Glycol Mass Flow Fraction vs. Valve Position

At the design flow levels for AHU6 and AHU7 (118 gpm) from the pump manufacturer's data and the construction documents, F_{Flow} was often greater than unity. When the design ethylene glycol mass flow rate, $\dot{m}_{EG,Design}$, was replaced with 1.6 times the published design flow rate, F_{Flow} was much closer to unity when the bypass valve was commanded 100% open (100% of flow through the supply coil). Inspection of the manufacturer's pump curves revealed that only a 5 to 10% change in pump head would result in mass flow rate variation of this magnitude. Thus, the maximum flow rate of the heat recovery pumps for these two systems was increased to 1.6 times the design flow rate.

The overall heat transfer coefficient includes the thermal resistance due to convection in the glycol solution, conduction through the coil, and convection in the air stream. As demonstrated in section 4.1, the air flow varies over the course of the year, but the scale of this variation is not likely to significantly affect the convection coefficient on the air side. The air flow varies by only a few thousand cfm, generally resulting in a variation of no more than ±15%. The bypass valve on the glycol side, however, modulates from full flow to no flow in heating mode and this does have a substantial effect on the overall heat transfer coefficient.

For turbulent flow through a smooth, straight pipe, the Dittus-Boelter equation relates the Nusselt number (Nu_D) to the Reynolds number (Re_D) and the Prandtl number (Pr) according to the following:

$$Nu_D = 0.023 \mathrm{Re}_D^{4/5} \mathrm{Pr}^n \tag{4.6}$$

where n = 0.4 for heating and 0.3 for cooling (Incropera & DeWitt, 2002). Re_D is the only parameter on the right side of the Dittus-Boelter equation dependent on flow velocity, it was expected that the heat transfer coefficient for the glycol, and thus the UA, might vary as a function of the glycol mass flow rate raised to the 4/5 power. The UA was then calculated according to:

$$UA = UA_{FullFlow} F_{Flow}^{0.8} \tag{4.7}$$

Where $UA_{FullFlow}$ is the UA calculated from the data when the bypass valve is closed and 100% of the glycol solution is flowing through the supply heat recovery coil, and F_{Flow} is the calculated fraction of glycol flow. While this provided a reasonable fit with the data, a better fit was obtained with:

$$UA = UA_{FullFlow} F_{Flow}^{0.5} \quad (4.8)$$

These results are presented in Figure 4.9 and Figure 4.10.

There are possible physical explanations for the better fit of equation (4.8). The Dittus-Boelter correlation is valid for fully-developed turbulent flow in a smooth, circular pipe. However, elbows in the coil may result in a small percentage of the flow that is not fully developed, while the coil is made of copper which should be relatively smooth, the coil is mechanically expanded into the aluminum fin collars which may add roughness, and there may be some fouling in the tubing. Each of these factors would lessen the dependence of the UA on Reynolds number.

The glycol return temperatures were not collected for AHU1 and AHU2, so the bypass valve position is used to calculate flow rate. The glycol return temperature is then calculated from an energy balance on the glycol side of the heat recovery unit. This method produced unreliable results at low flow rates due to the non-linearity of mass flow with valve position. Thus, the UA for the AHU1 and AHU2 heat recovery supply coils were calculated at full flow condition, and it was assumed that the same relationship between UA and mass flow rate determined for AHU6 and AHU7 was applicable to these systems as well.

The simulated heat recovery results tracked the calculated values from the BAS data fairly well. Results for AHU6 and AHU7 are shown in Figure 4.11 and Figure 4.12. An equipment fault occurred in the AHU6 heat recovery system during November and December that will be discussed further in Chapter 6. Simulated and measured heat recovered for a typical winter month (January) and a typical summer month (July) for AHU6 are also presented in Figure 4.13 and Figure 4.14.

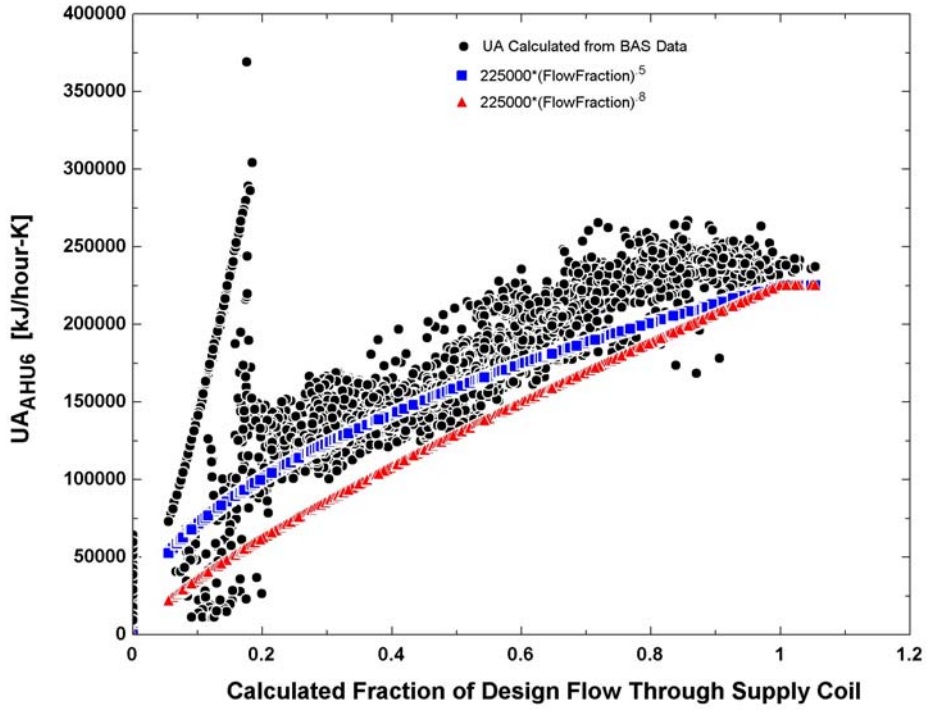

Figure 4.9 AHU6 Heat Recovery Coil UA from BAS Data

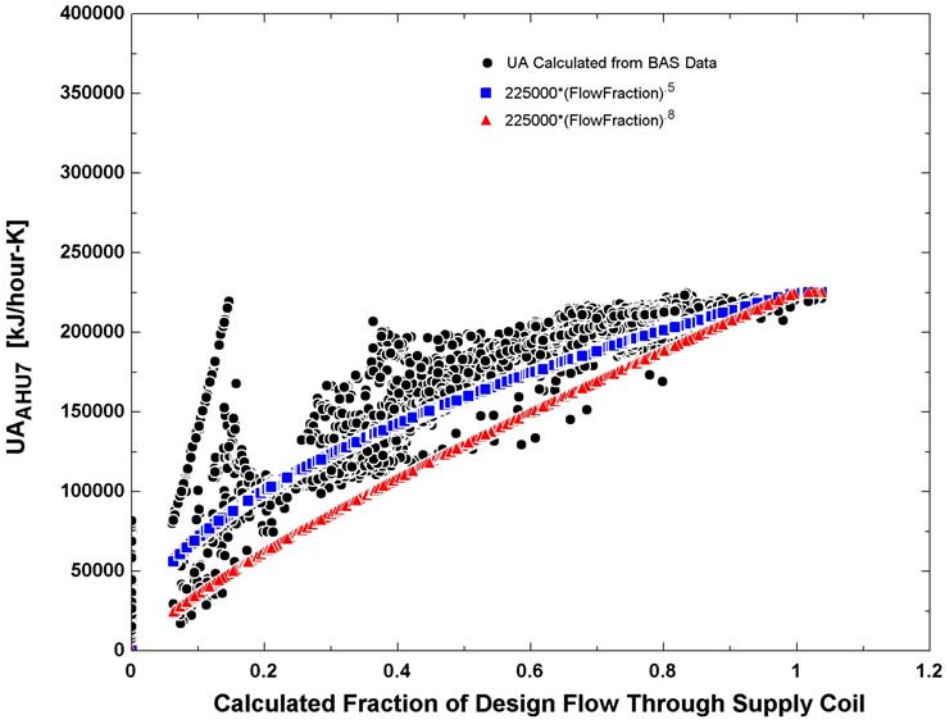

Figure 4.10 AHU7 Heat Recovery Coil UA from BAS Data

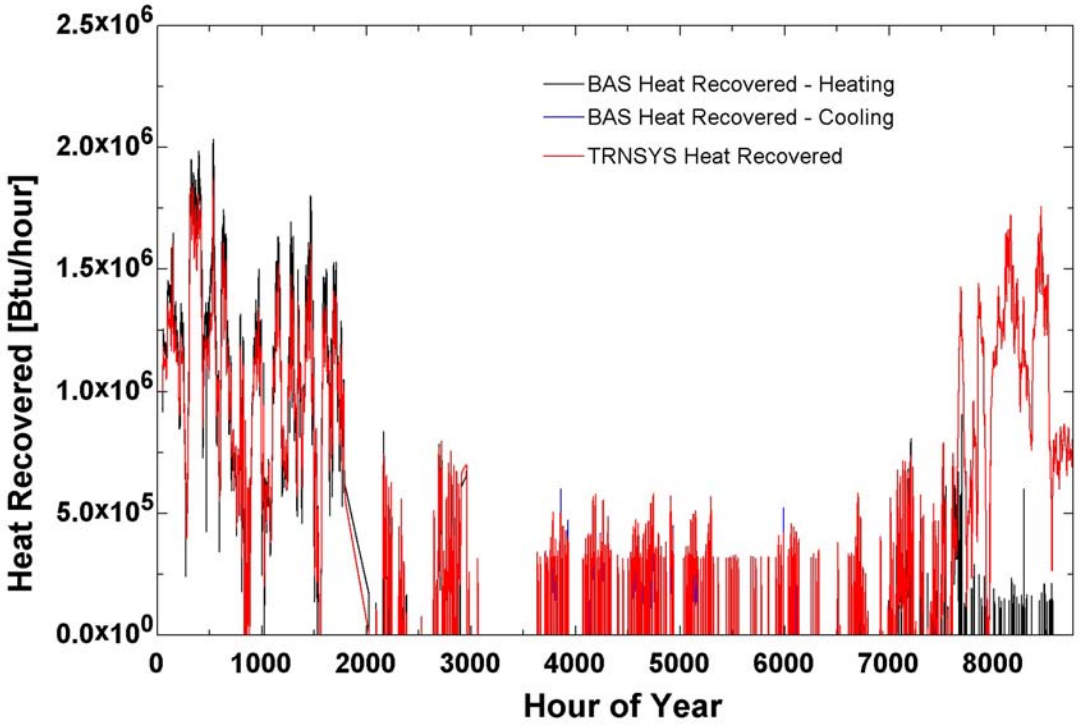

Figure 4.11 AHU6 Simulated and Measured Heat Recovered

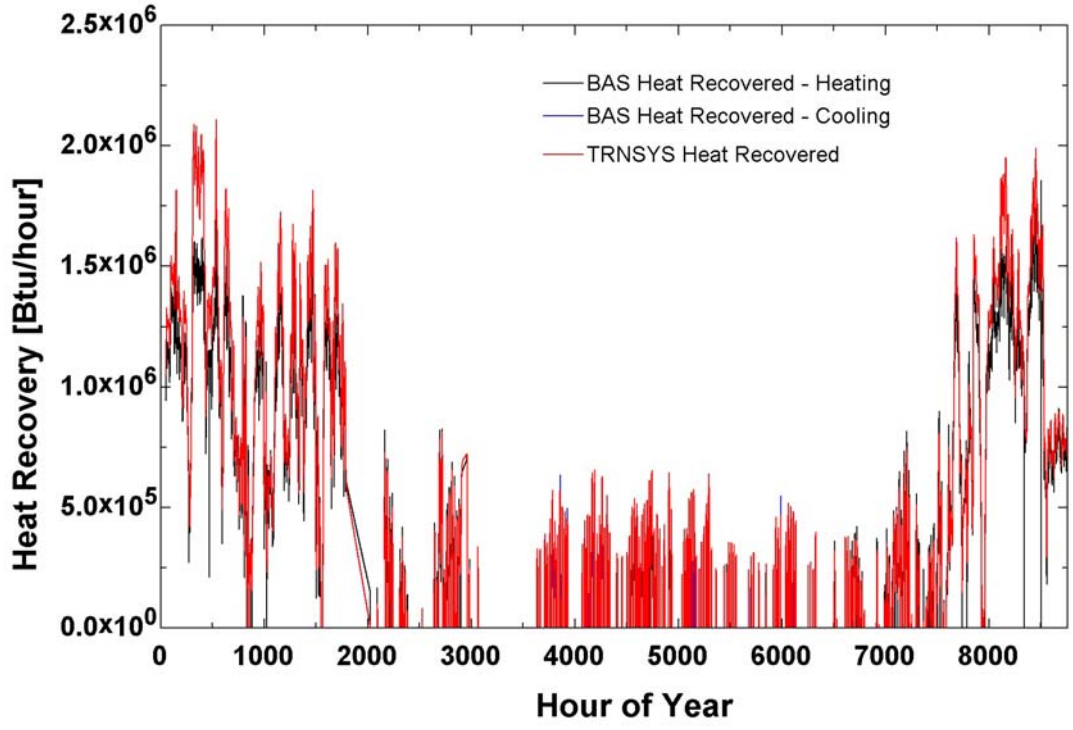

Figure 4.12 AHU7 Simulated and Measured Heat Recovered

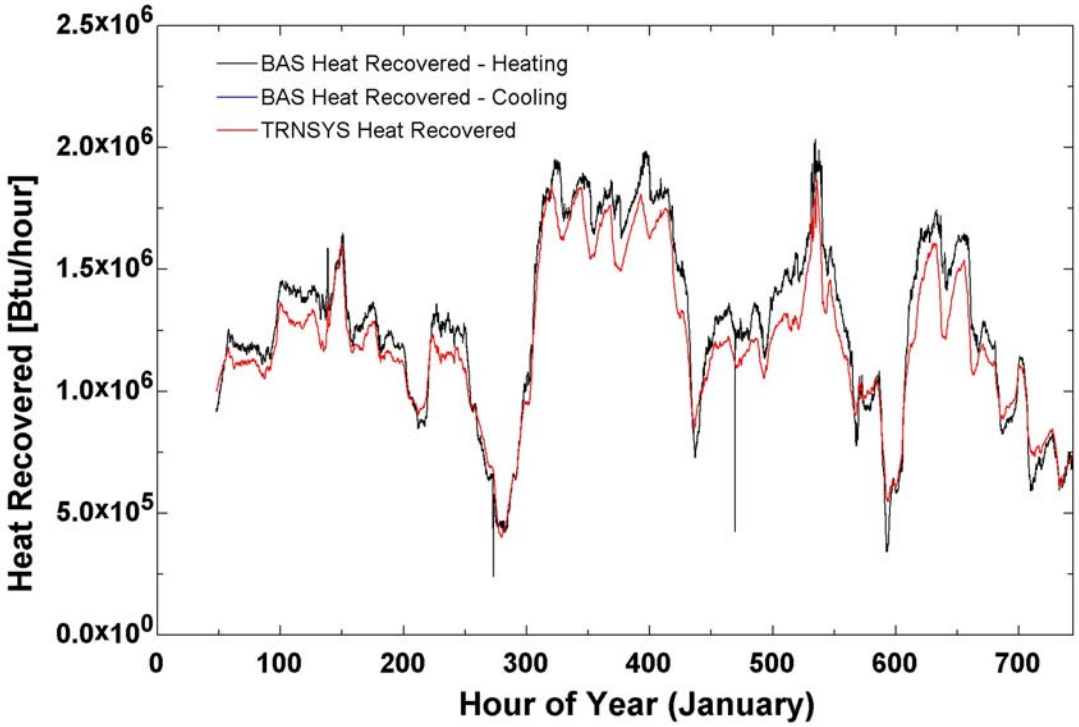

Figure 4.13 AHU6 January Simulated and Measured Heat Recovered

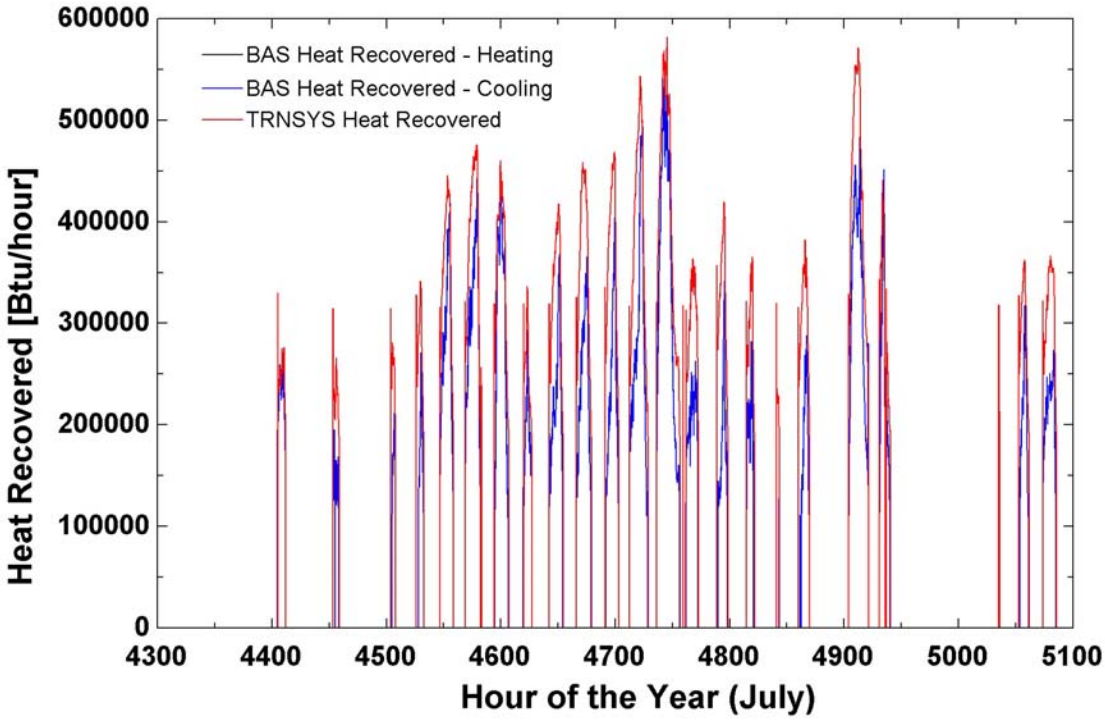

Figure 4.14 AHU6 July Simulated and Measured Heat Recovered

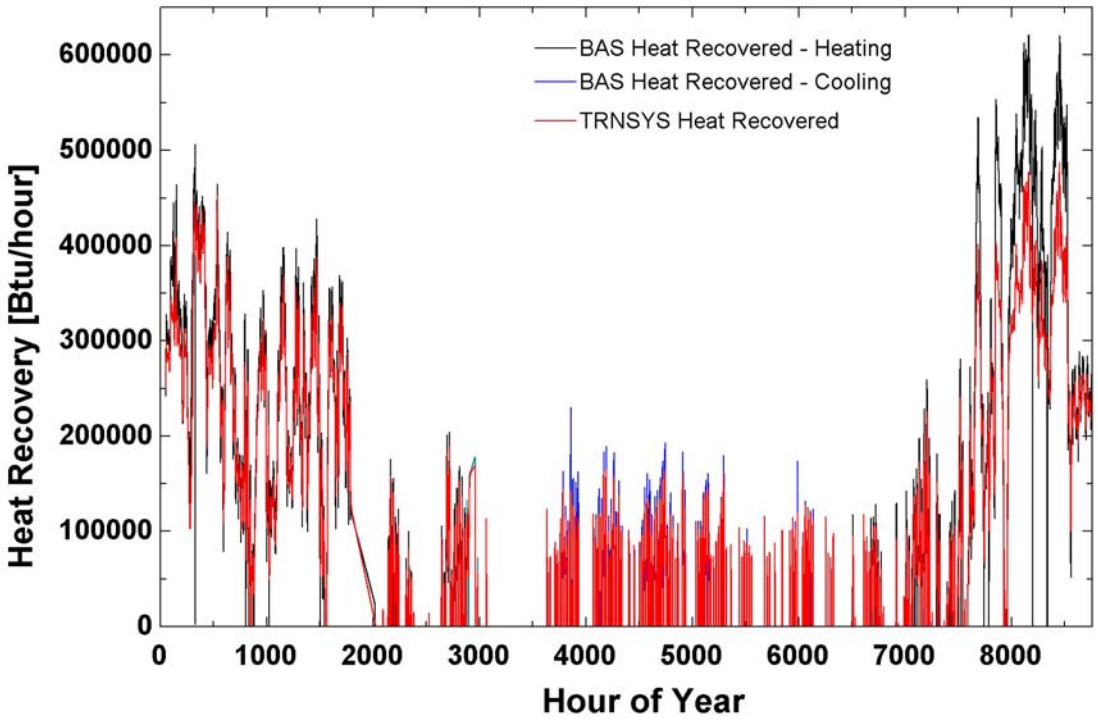

Figure 4.15 AHU1 Simulated and Measured Heat Recovered

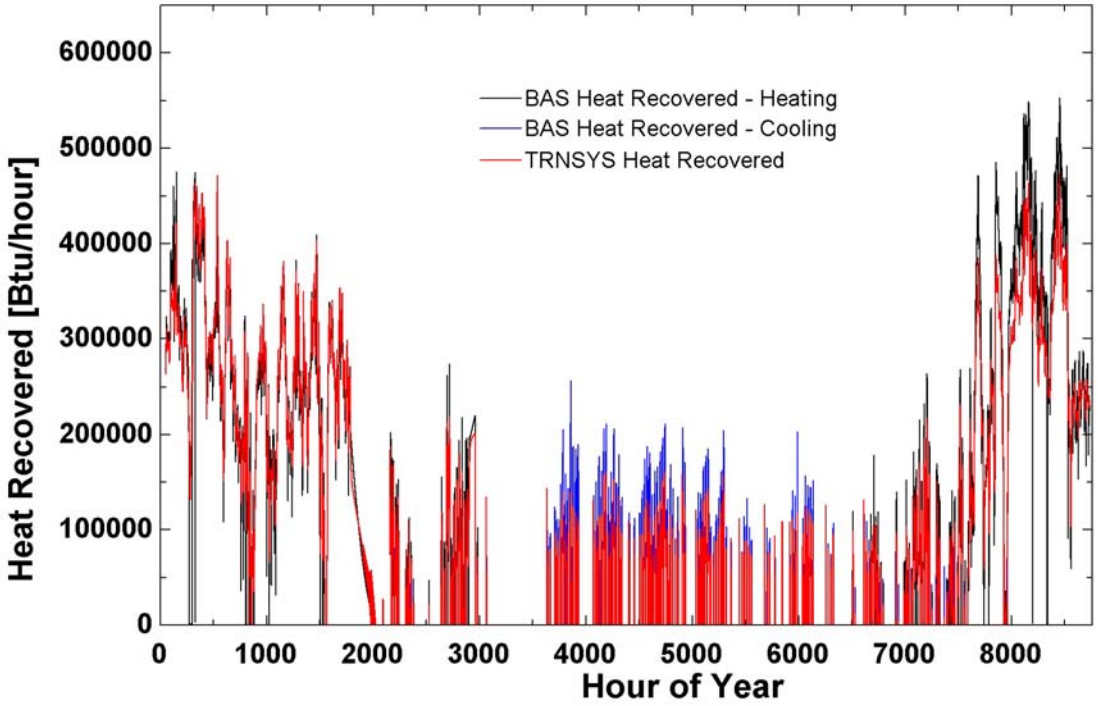

Figure 4.16 AHU2 Simulated and Measured Heat Recovered

The TRNSYS simulation tended to underestimate the heat recovered for AHU1 and AHU2 as shown in Figure 4.15 and Figure 4.16. However the simulated and measured total heat recovered for the building as presented in Table 4.4 are within 6%.

Table 4.4 Measured and Simulated Heat Recovered Totals

	Measured Btu	Simulated Btu	% Difference[1]
AHU1	9.8899 E08	8.7445 E08	11.6%
AHU2	9.8355 E08	9.2792 E08	5.7%
AHU6 12 month[2]	2.0292 E09	3.1074 E09	-53.1%
AHU6 10 month[3]	1.9596 E09	2.0424 E09	-4.2%
AHU7	2.9922 E09	3.4658 E09	-15.7%
Total[3]	**6.9243 E09**	**7.3076 E09**	**-5.5%**

[1]Percent difference calculated as $\frac{Measured - Simulated}{Measured}$

[2]The AHU6 heat recovery system failed during the months of November and December

[3]Excluding November and December data

[4]Excluding AHU6 November and December data

4.3 Chilled Water

The building chilled water flow rate is measured by the BAS as well as the chilled water supply temperature. However, according to the building control system drawings, the chilled water return temperature is measured only after the process load, and not for the chilled water return from the building mechanical equipment, see Figure 4.17. This missing temperature measurement means that it is not possible to estimate the actual cooling load of the building.

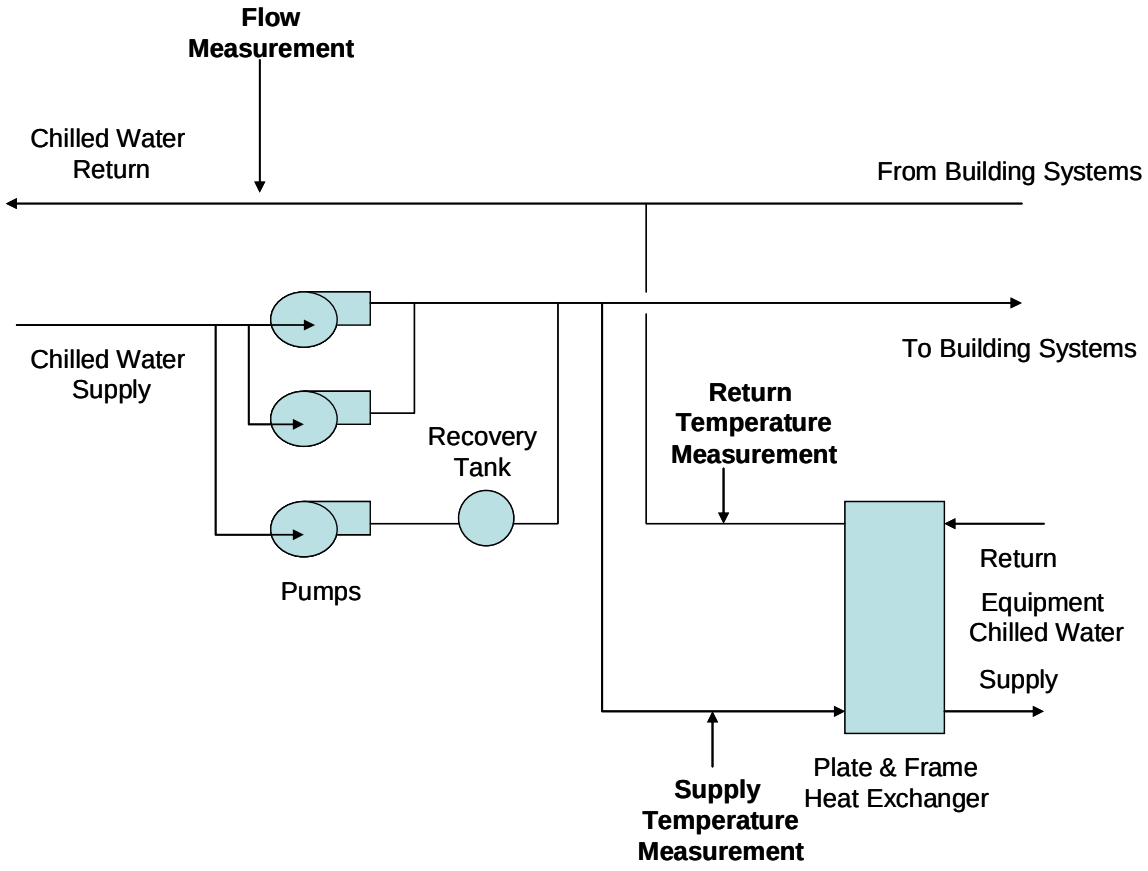

Figure 4.17 Building Chilled Water System Schematic

Very few data were collected at the zone level, but return air relative humidity data were available for AHU3 and AHU5. These data were used to validate the bypass fraction

that is required as input for the TRNSYS chilled water coil models (see Section 3.1.13), and the internal latent gains for the building. The bypass fraction provides an estimate for the fraction of air that doesn't contact the cooling coil, and it affects the humidity ratio of the air leaving the cooling coil. The latent gains for the building zones depend on the zone occupancy. The building maximum occupant capacity was taken from the architectural drawings for each zone. However, it would be unusual for the building to be fully occupied at any given time. So, diversity factors are applied to approximate the fraction of the maximum occupancy in the building.

The TRNSYS zone relative humidity estimates were compared with the measured return air data at 3 different internal latent gain settings and two different coil bypass fractions. Results for a representative summer week (the first week in August) are presented in Figure 4.18. The effect of increasing the bypass fraction in the TRNSYS component is to decrease the relative humidity of the air leaving the coil. The coil is controlled to maintain a constant outlet temperature. Since the bypass fraction is merged with the remainder of the air stream at the coil inlet air temperature and humidity level, the fraction of the air that passes through the coil will be colder with a higher bypass fraction. If the air is cooled further, more dehumidification is possible.

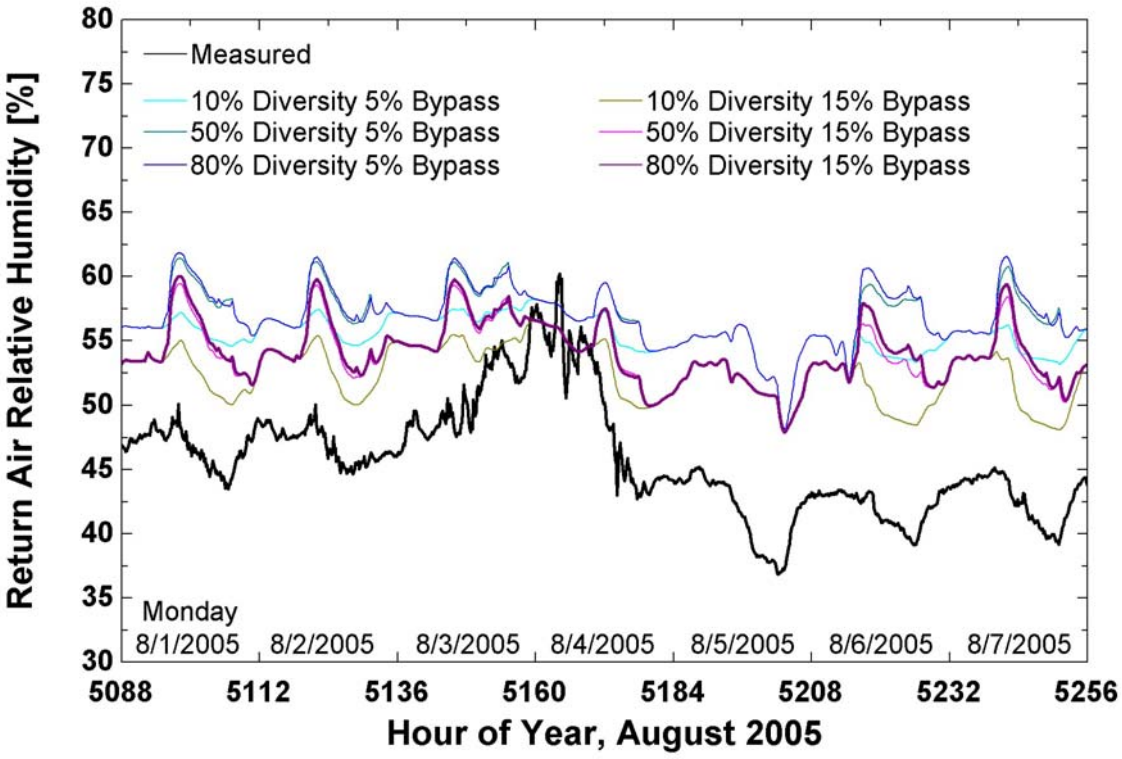

Figure 4.18 AHU3 Zone Relative Humidity Calibration

In general, use of the 15% bypass resulted in zone humidity estimates closer to the measured values than lower bypass fractions, although the simulated results still did not match the measured humidity levels exactly. Fifteen percent is still within an acceptable range of air that could pass through a cooling coil unaffected, but assuming a higher fraction would require stronger justification. Thus, a 15% bypass fraction was selected.

The loading diversity factors were step functions with the maximum (during work week business hours) set at 10%, 50% or 80% of the building occupancy. There was very little difference between the 50% and 80% diversity approximations, and the 10% diversity factor is a rather extreme value to select without other loading validation data. Without more information to justify otherwise, the 80% diversity level selected for the TRNSYS model.

The 15% bypass setting for the cooling coil appears to provide a closer approximation to the measured data in the Tower Office zone served by AHU5, as shown in Figure 4.19. However, these results may be misleading as the zone temperature was not well maintained by the TRNSYS model for this zone.

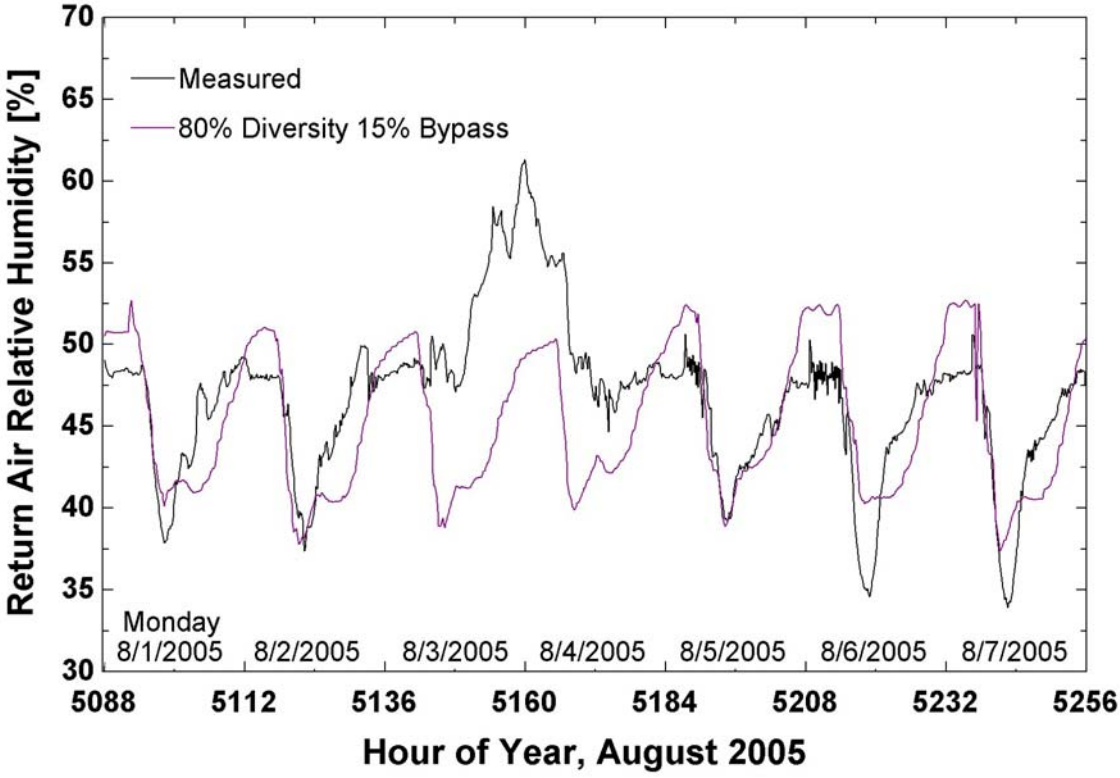

Figure 4.19 AHU5 Zone Relative Humidity Calibration

Without an estimate of the whole building cooling energy usage, it is not possible to compare measured chilled water usage for the whole building to simulated chilled water usage. Instead, an energy balance across the chilled water coil was performed for each AHU. As the relative humidity of the supply air was not collected, it was assumed that the supply air would leave the chilled water coil at a maximum of 90% relative humidity. In general, the TRNSYS model estimates are close to 10% higher than the estimates based on measured temperatures as shown in Table 4.5.

Table 4.5 Comparison of BAS Cooling Estimate and TRNSYS Cooling Estimate

AHU	Cooling Estimate BAS Data (Btu)	Cooling Estimate TRNSYS (Btu)	Percent Difference[1]
AHU1	1.950 E09	2.096 E09	-7.5%
AHU2	1.736 E09	2.009 E09	-15.8%
AHU3	4.241 E09	4.312 E09	-1.7%
AHU4	1.664 E09	1.930 E09	-16.0%
AHU5	1.350 E09	1.459 E09	-8.1%
AHU6	4.898 E09	5.323 E09	-9.3%
AHU7	5.212 E09	5.741 E09	-10.1%
Total	**2.105 E10**	**2.287 E10**	**-8.6%**

[1]Percent difference calculated as $\frac{BAS - TRNSYS}{BAS}$

Most of the difference between the two cooling energy estimates is due to differences in the amount of dehumidification of the air stream, and without a measured supply air relative humidity it is unclear which estimate is more accurate. In addition, the measured building supply air temperatures and zone temperatures are not constant as they are for most of the TRNSYS zones. Figure 4.20 presents a comparison of the two cooling estimates for AHU1 over the entire year and the measured discharge air temperature. Figure 4.21 presents the same data for just the month of July, 2005. It is apparent from the figures that the simulated and the measured values follow the same trends. So, while it is likely that there is some offset between the simulated relative humidity and cooling energy and the actual values, relative changes in these variables under different simulated conditions may prove reasonably accurate.

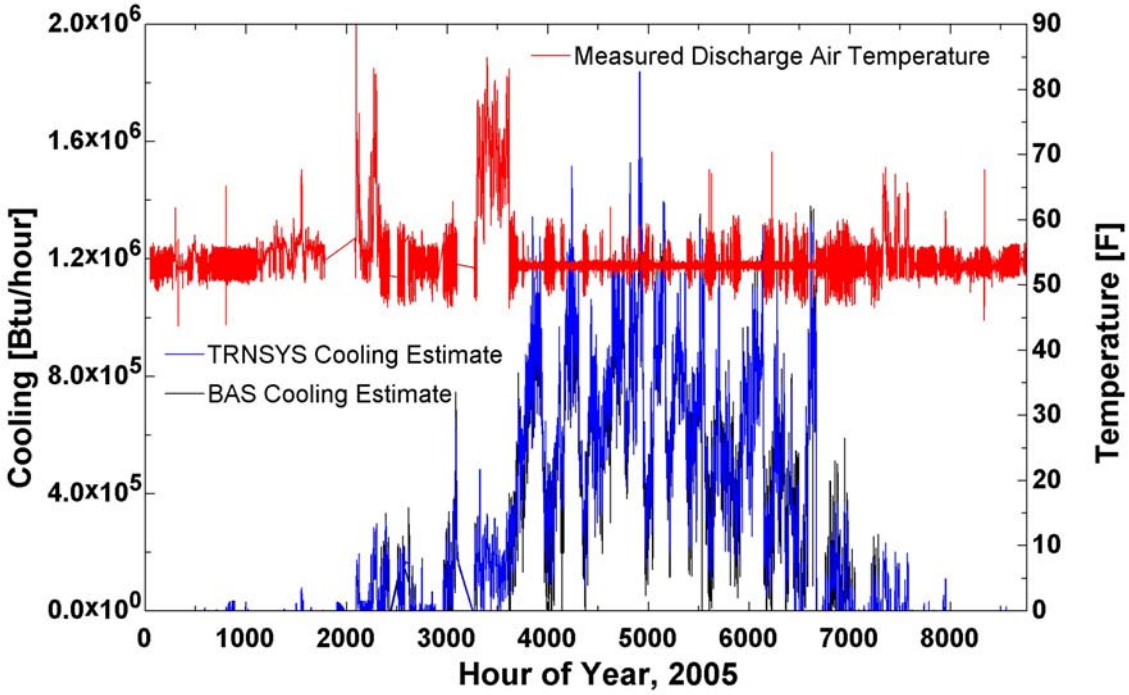

Figure 4.20 Comparison of Cooling Energy Estimates for AHU1

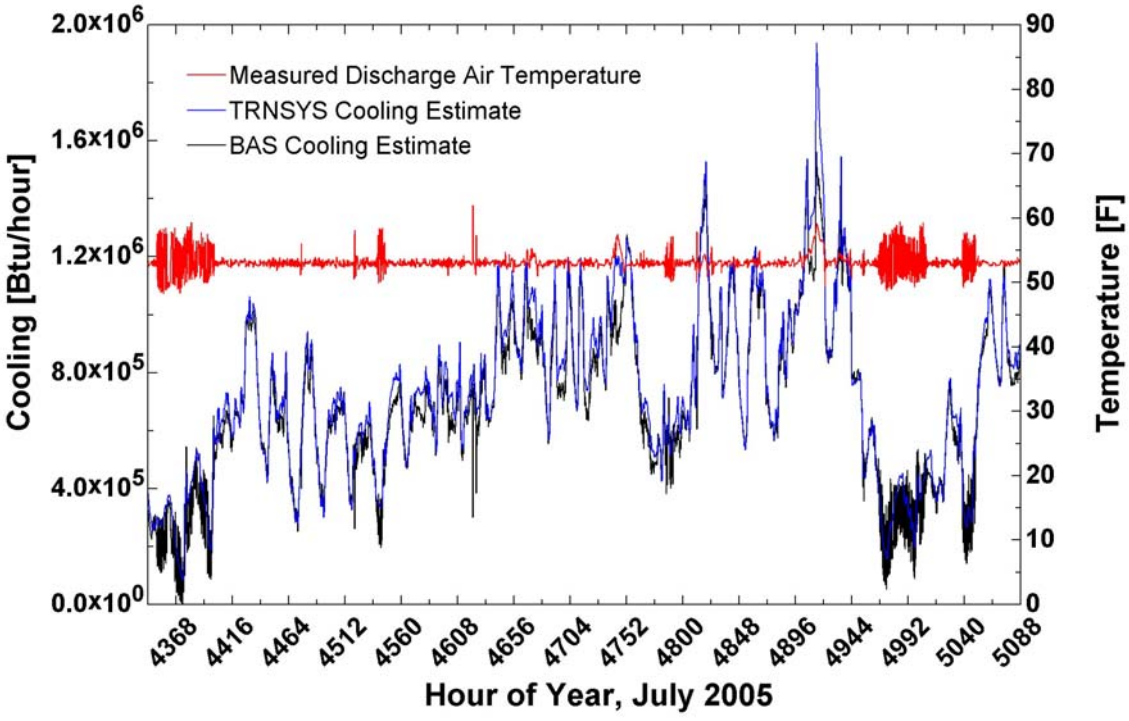

Figure 4.21 Comparison of Cooling Energy Estimates for AHU1, July 2005

4.4 Steam and Hot Water

The building does have a meter installed to measure the total steam flow supplied to the building; however, the actual steam usage for the building is difficult to verify for a number of reasons. The meter installed to measure steam condensate from the building was non-functional for the entire year of data collection, and condensate temperatures are not collected. There is no separate metering for process loads within the building (cage washers and autoclaves, for example) and space heating loads. In addition, a portion of the steam supplied is used for humidification; thereby, complicating a water mass balance.

The steam flow as measured from the building total steam supply meter is shown in Figure 4.22. The reported steam flow data never drop below 12,000 lb_m/hour. Although there are process steam loads throughout the year, it is reasonable to expect the total steam usage during the summertime to be low, even while serving reheat loads. It appears that the total building steam supply flow meter requires other independent data to validate its accuracy.

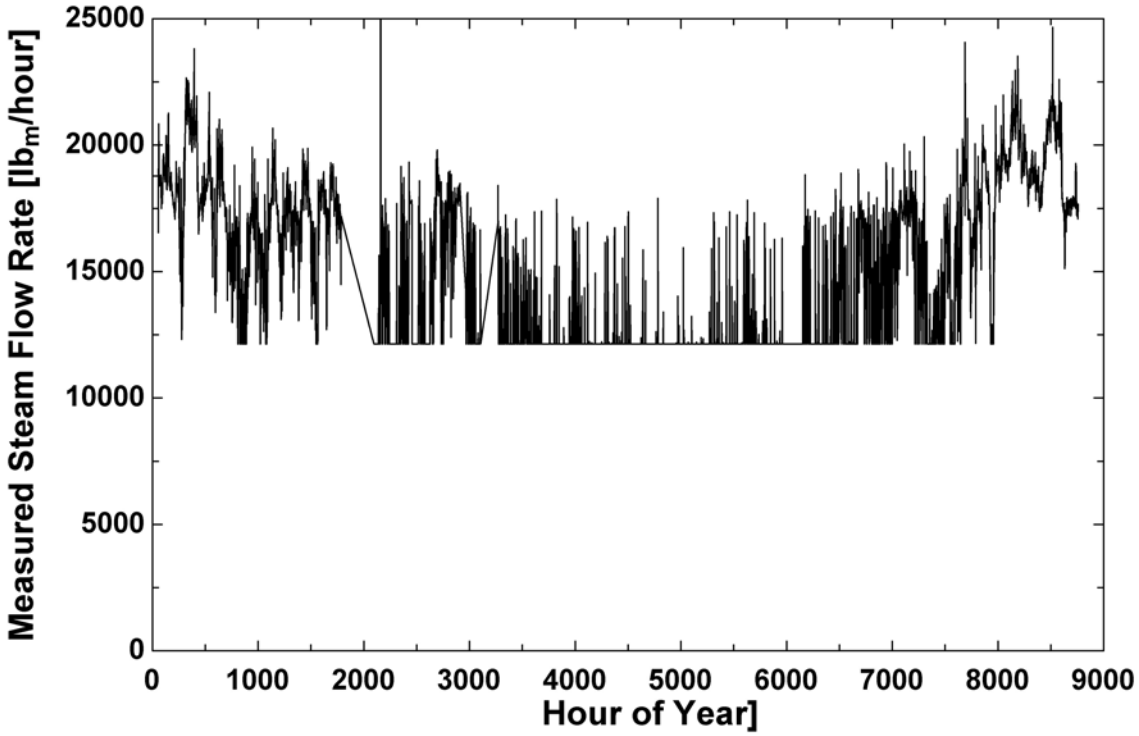

Figure 4.22 Measured Whole Building Steam Flow Rate

The TRNSYS simulation calculates the steam power requirement of each AHU and the heating requirements of each zone. These zone heating requirements represent the building perimeter heating and terminal reheat loads. The simulated steam flow rate is calculated from the steam power assuming a saturated steam inlet condition, the measured steam inlet temperature, and an assumed condensate temperature of 180°F. The resulting flow rate appears to be offset from the measured amount by approximately 10,000 lb_m/hour. Figure 4.23 shows the simulated flow rate, the measured flow rate, and the measured flow rate with a constant 10,000 lb_m/hour reduction. In general, the building reheat load is likely to be relatively constant over the course of the year, while steam heat at the AHU level and perimeter heating are generally only required during the winter months. This behavior is reflected in the TRNSYS steam usage results.

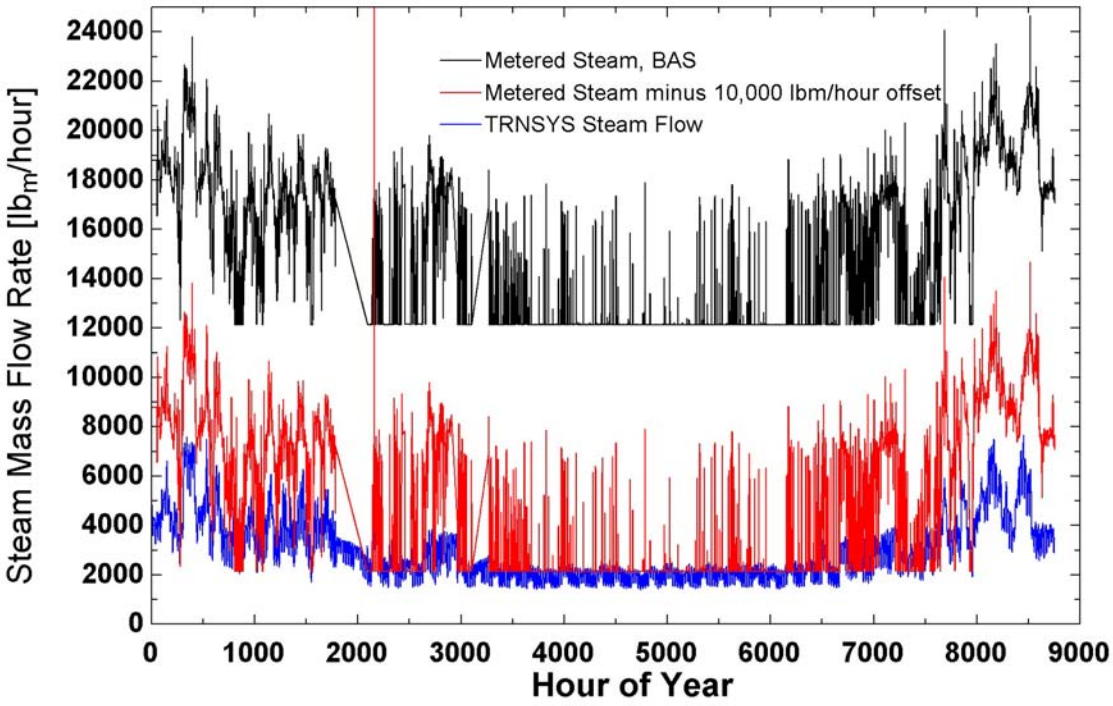

Figure 4.23 Measured and Simulated Steam Flow Rates

The same steam flows are plotted for a single winter month (February) in Figure 4.24. There is a reduction in steam flow rate on the weekends which is to be expected as many of the process loads are not required on the weekends, and the building occupancy is lower. The measured flow rate with the 10,000 lb_m/hour offset is actually very close to the measured amount on the weekends. This observation provides more credibility to the idea that the steam meter is reading a constant offset. While little is known about the magnitude of the steam process load, the difference between the TRNSYS simulated amount and the offset measurement is generally in the range of 5,000 lb_m/hour. This difference is within a range of believable process load flow rates.

The source of the possible steam flow meter offset is unknown. It is possible that a multiplier for the meter is incorrect. However, there are a number of other unknowns such as

the process load, the condensate temperature, the domestic water flow and the internal building gains that could account for a portion of the measurement and simulation discrepancy.

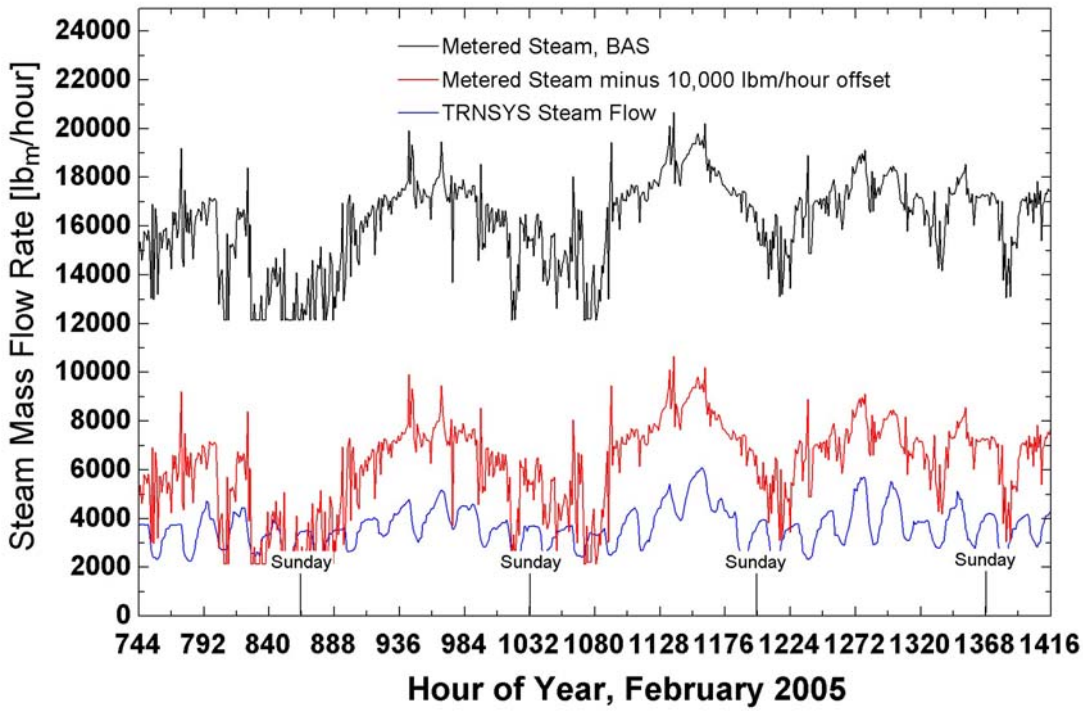

Figure 4.24 February Measured and Simulated Steam Flow Rates

4.5 Calibration Conclusions

The TRNSYS simulation appears to reflect the actual behavior of the building. It is not possible to ascertain the exact cooling load or heating loads of the building from the measured data. However, the overall pattern of response for both the cooling and heating loads are similar between the TRNSYS model and the data that is available. Thus, it is reasonable to use this building simulation to examine the relative effects of changes in building control or design.

Chapter 5: Simulation Results

The model calibration process presented in Chapter 4 provides verification that the simulation is a reasonable representation of the actual building systems. Since the Rennebohm Hall building simulation appears to reflect the actual building function, the model can be used to estimate the system effects of changing selected parameters. The building simulation can be particularly useful for comparing design or retrofit options and for evaluating potential control changes. This chapter presents TRNSYS simulation results that investigate the effects of alternative building control strategies. Each simulation is compared to a baseline of the calibrated model described in Chapter 4.

5.1 AHU3 and AHU5 Minimum Airflow Rates at Design Levels

It became apparent during the building model calibration process that more than one supply fan was not operating at its design speed. In particular, it was shown that AHU3 and AHU5, the two zones utilizing return air, consistently supply more air than their design minimum flow rates (see Figure 4.6 and Figure 4.7). Increased supply air delivery leads to increased fan electric energy demand and the potential for increased reheat, steam, and chilled water usage. The energy impact associated with lowering the supply air flow rates in these zones is quantified in this chapter.

The TRNSYS fan control was adjusted to allow the fans to operate at the minimum flow rates scheduled in the construction documents, 24,000 cfm for AHU3, and 10,000 cfm for AHU5. The minimum outside air requirements for each zone were not changed as it was

assumed that these ventilation levels were fixed to meet indoor air quality standards and code requirements.

The supply air flow rates are affected by the zone loads with the new minimum settings.. The zone loads are approximate, and the control strategy for the simulation of the variable air volume (VAV) terminal units is also an approximation (see Section 3.2.3). Thus, it is the change in the simulated variables, all other assumptions held constant, that will be evaluated.

The air flows predicted in the baseline simulation and the design minimum flow simulation are presented in Figure 5.1 and Figure 5.2. The maximum possible flow rate for AHU3 is 60,000 cfm. The AHU3 supply fan has ample capacity to meet a higher zone load as illustrated in Figure 5.1. There is a reduction in the required air flow at the assumed loading and with the simulated control strategy. A similar, though smaller, change can be seen for the simulated AHU5 supply air flows in Figure 5.2. However, unlike AHU3, AHU5 often operates close to its maximum flow. This observation indicates that this unit may not be able to provide adequate cooling for the zone, particularly if the cooling load is higher than that assumed in these simulations.

The entire zone level heat addition is lumped together in the TRNYS simulation. The heat addition includes reheat from the hot water coils in the terminal units as well as perimeter baseboard heating. As expected, at constant zone temperature conditions, when the supply air flow rate is decreased, the additional thermal energy that must be added at the zone level also decreases. This trend is evident during the entire year, as seen in Figure 5.3 and Figure 5.4. The cooling requirements from the chilled water coils in the AHUs decreased with the decreased flow rate for each AHU, as shown in Figure 5.5 and Figure 5.6.

The fan power requirements decrease with the decrease in flow rate, as shown in Figure 5.7 and Figure 5.8. Because there is a greater change in flow rate for AHU3 than AHU5, there is also a greater impact on the energy usage for the zone served by AHU3. These results are summarized in Table 5.1.

Table 5.1 Simulated Energy Usage and Savings at Baseline and at Design Minimum Supply Air Flow

		Baseline Energy for 2005 [Btu]	Design Minimum Energy for 2005 [Btu]	Energy Savings [Btu]	Percent Savings[1]
AHU3	Zone Level Heat	4.310 E09	2.339E09	1.971 E09	45.7%
	Steam Coil	6.110 E08	1.506 E09	-8.947 E08	-146.4%
	Chilled Water	4.053 E09	2.870 E09	1.183 E09	29.2%
	Fan Power	5.173 E08	1.502 E08	3.671 E08	71.0%
	Total	**9.492 E09**	**6.865 E09**	**2.627 E09**	**27.7%**
AHU5	Zone Level Heat	9.115 E08	6.106 E08	3.008 E08	33.0%
	Steam Coil	0	3.999 E06	-3.999 E06	--
	Chilled Water	1.419 E09	1.167 E09	2.520 E08	17.8%
	Fan Power	2.557 E08	1.370 E08	1.186 E08	46.6%
	Total	**2.586 E09**	**1.919 E09**	**6.674 E08**	**25.8%**

[1]Percent Savings calculated as $\frac{Baseline - DesignMinimum}{Baseline}$

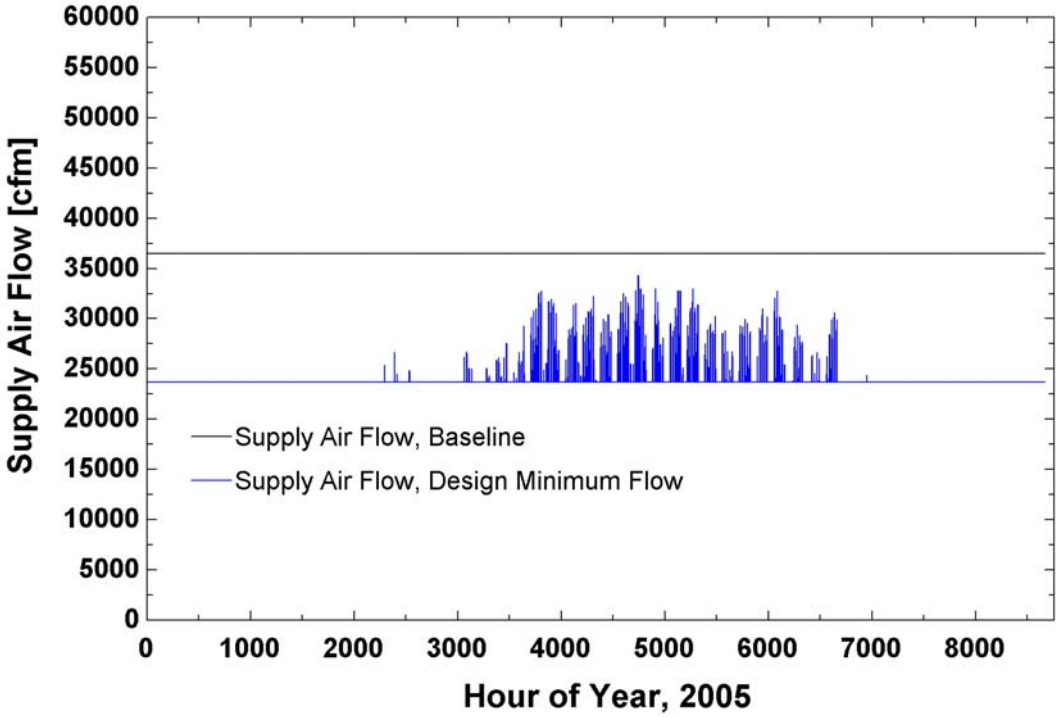

Figure 5.1 AHU3 Baseline and Design Minimum Supply Air Flow Rates

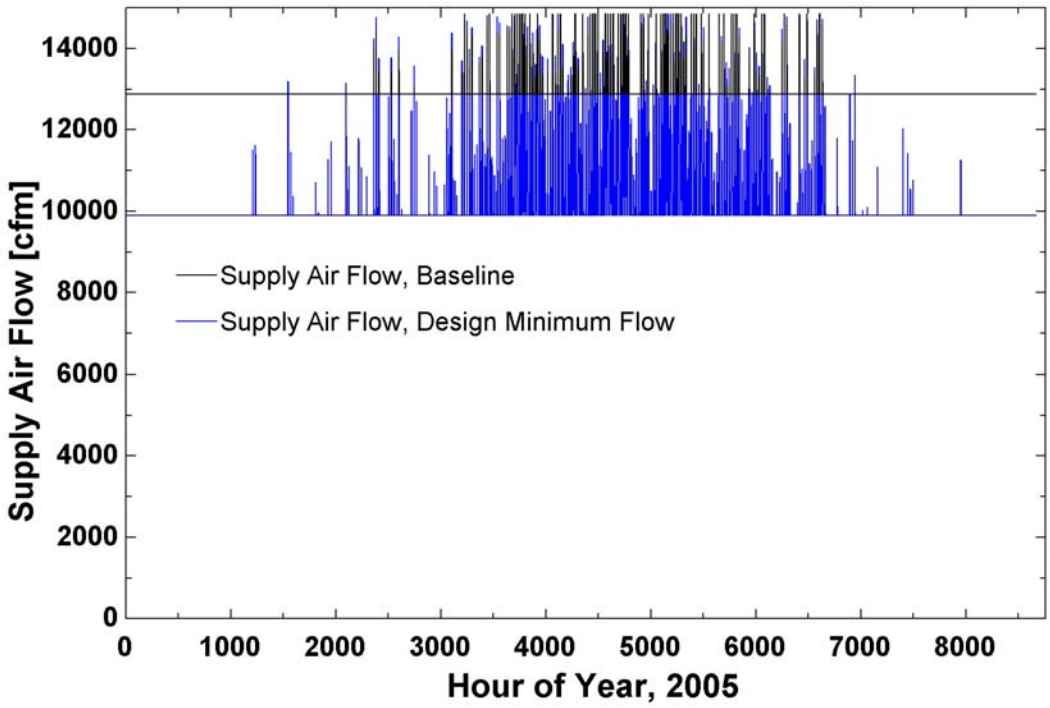

Figure 5.2 AHU5 Baseline and Design Minimum Supply Air Flow Rates

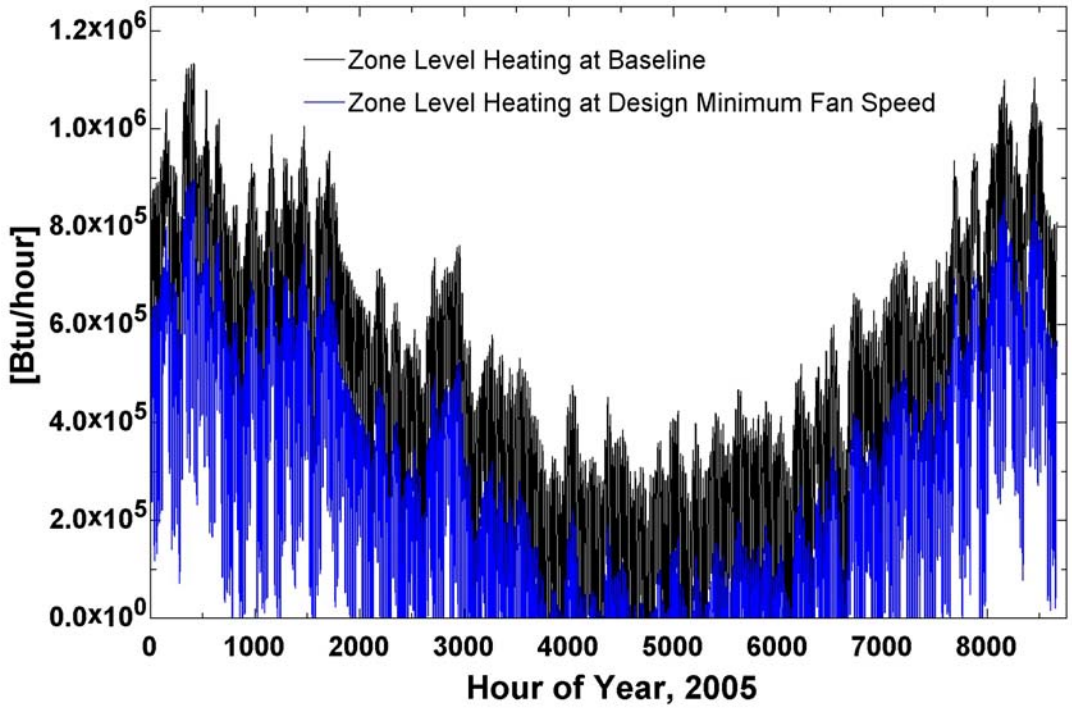

Figure 5.3 Zone Level Heating Comparison at Baseline and Design Minimum Flow Rates for General Zone, AHU3

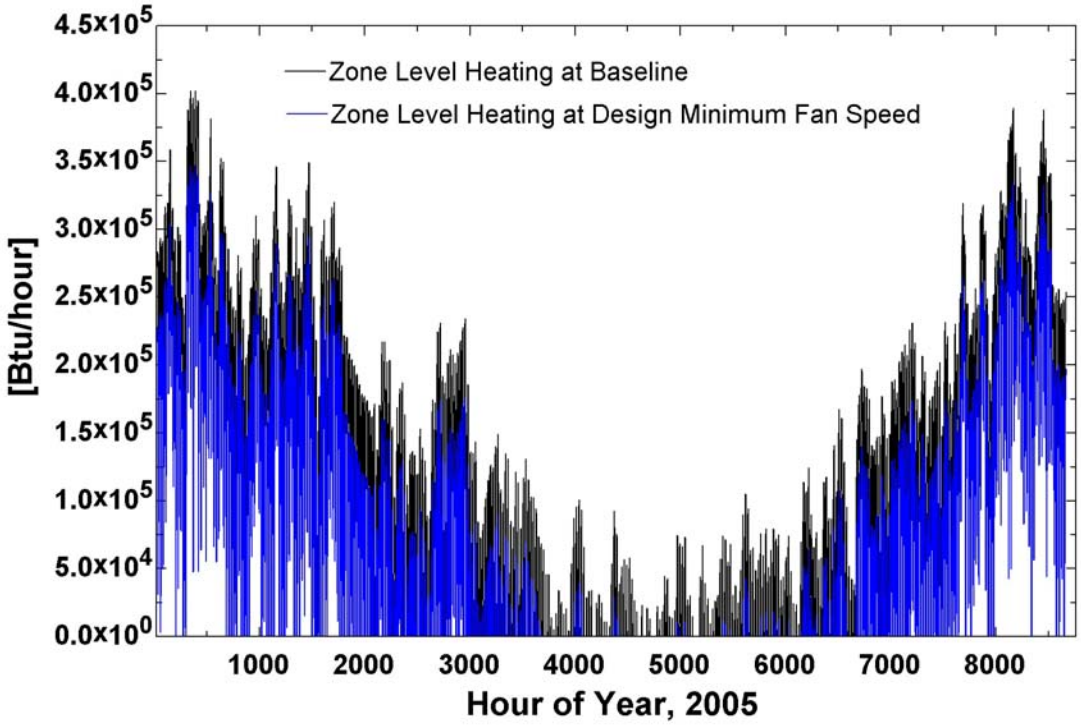

Figure 5.4 Zone Level Heating Comparison at Baseline and Design Minimum Flow Rates for Tower Offices Zone, AHU5

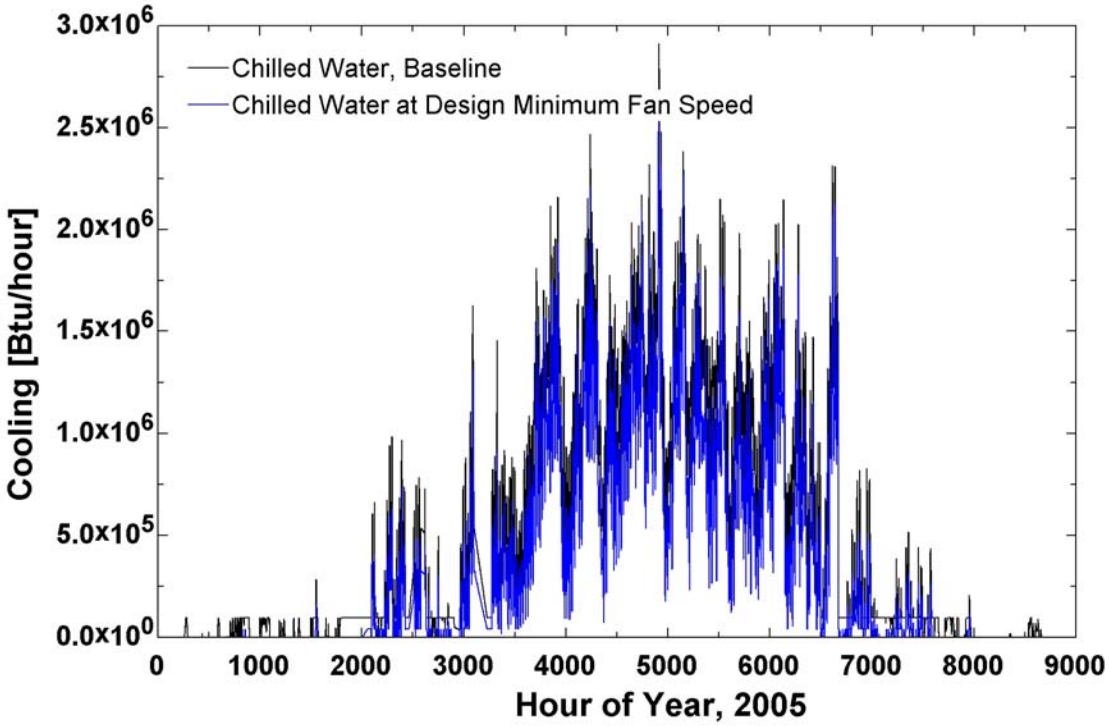

Figure 5.5 AHU3 Chilled Water Comparison at Baseline and at Design Minimum Air Flow Rates

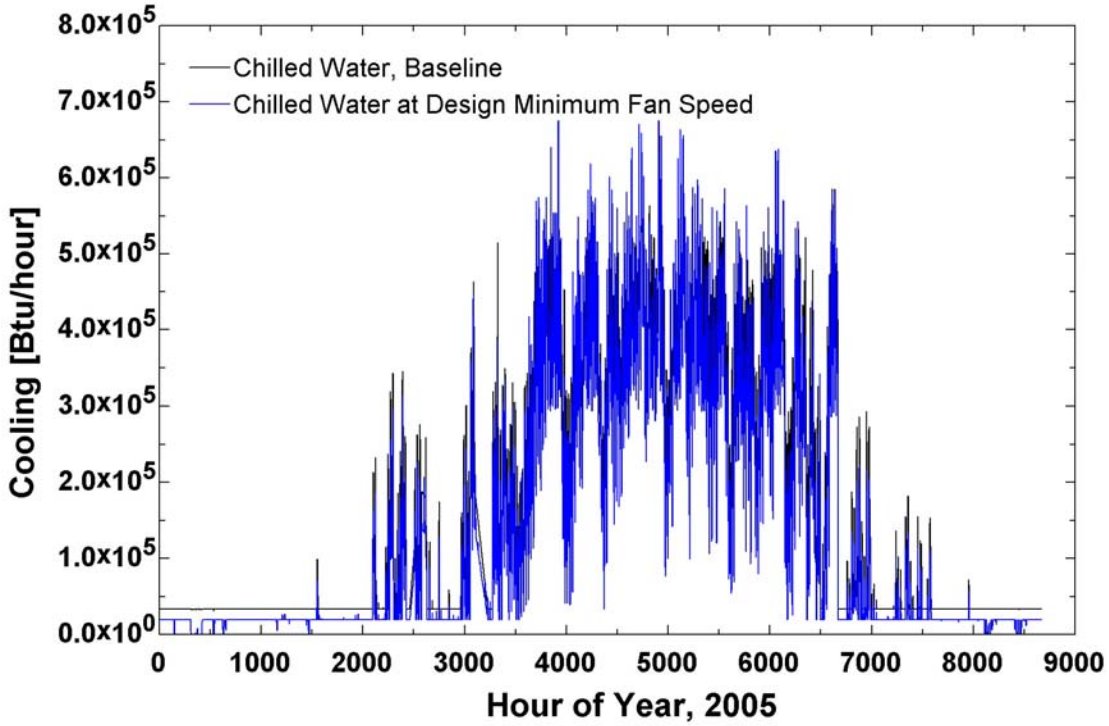

Figure 5.6 AHU5 Chilled Water Comparison at Baseline and at Design Minimum Air Flow Rates

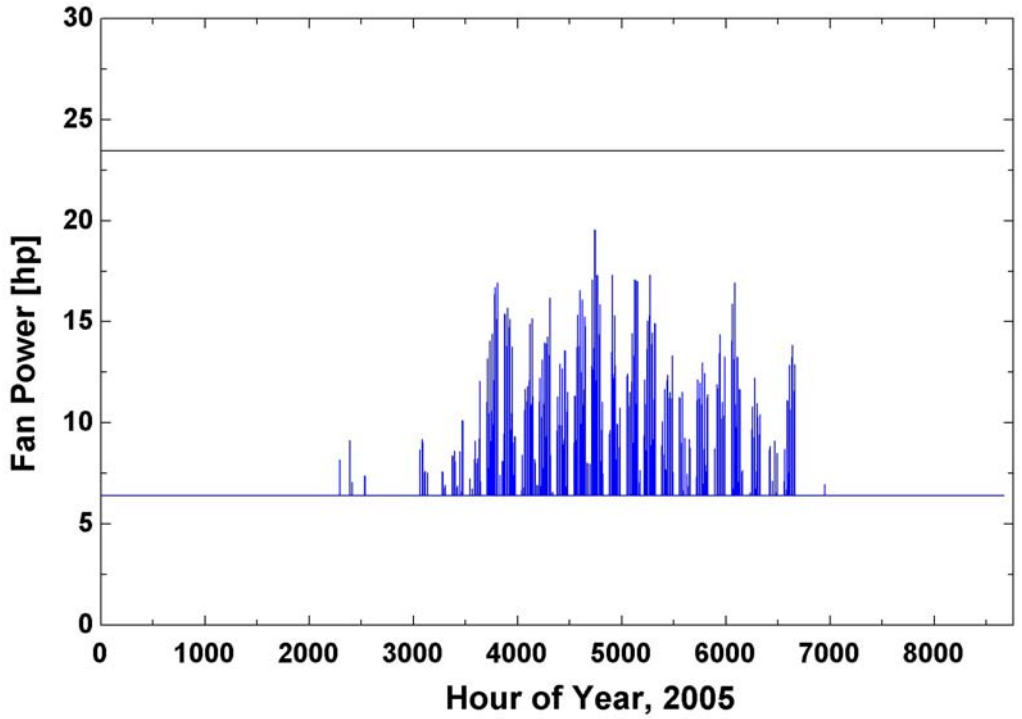

Figure 5.7 AHU3 Fan Power Comparison at Baseline and at Design Minimum Air Flow

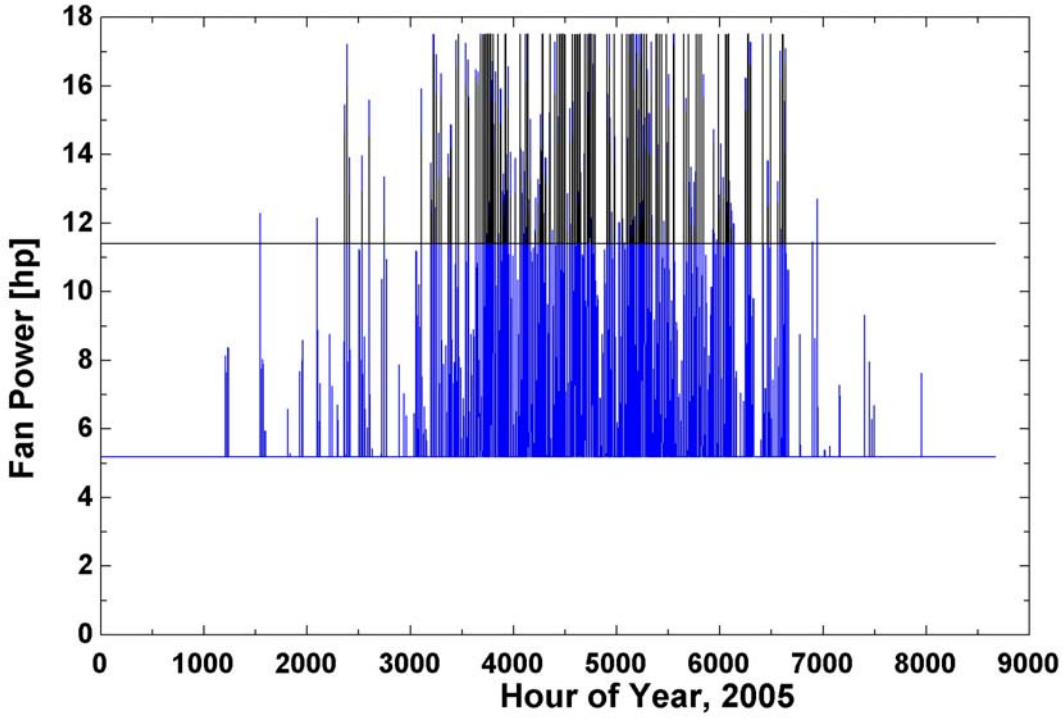

Figure 5.8 AHU5 Fan Power Comparison at Baseline and at Design Minimum Air Flow

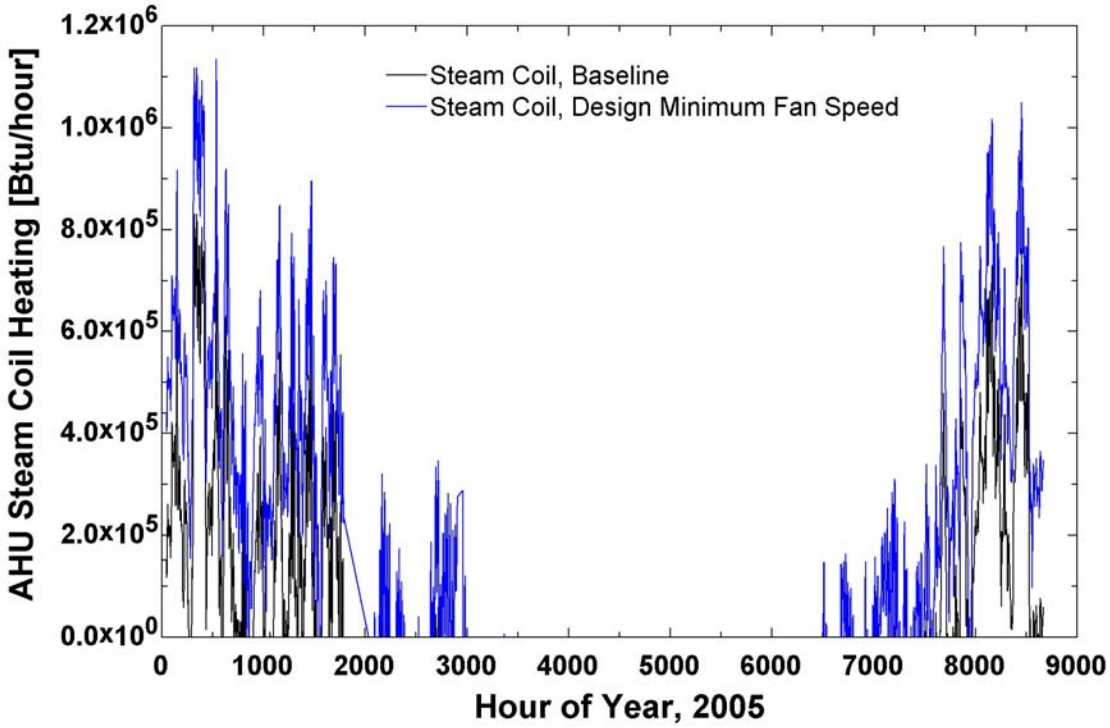

Figure 5.9 AHU3 Steam Coil Energy Comparison at Baseline and at Design Minimum Air Flow

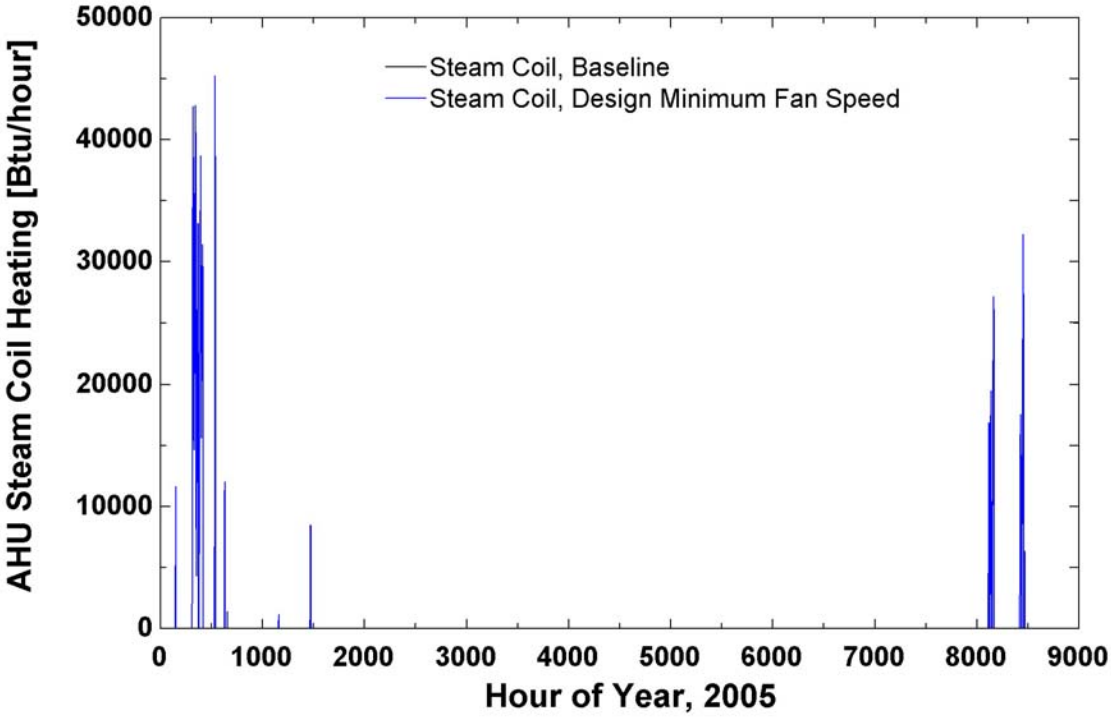

Figure 5.10 AHU5 Steam Coil Energy Comparison at Baseline and at Design Minimum Air Flow

Unlike the other energy flows, more steam energy is required for the AHU heating coils at reduced flow rates than at the baseline flow rate. This behavior is illustrated in Figure 5.9 and Figure 5.10. Because the volumetric flow of outside air remains constant between the two simulated conditions, only the return air flow rate is affected by the change in total supply flow rate. In the design minimum supply flow condition, there is less return air to condition the stream of outside air resulting in higher steam consumption at the AHU level..

The differences (baseline condition – design minimum condition) for each of these energy flows are plotted in Figure 5.11 and Figure 5.12. In Figure 5.12, the difference in cooling energy occasionally is negative, indicating a higher chilled water requirement at the lower air flow settings. However, integrated over a year, there is a net savings in chilled water demand. This behavior is related to the slow response of the proportional fan control AHU5 fan in the TRNSYS model. A different VAV control strategy would likely remove this behavior. See section 5.2 for more information regarding temperature control in this zone.

For both AHU3 and AHU5, reducing the minimum supply air flow rate by 35% and 23%, respectively, results in a net energy savings in excess of 25%. In both cases, the increase in steam heating required is offset by the reduction in zone level heating, chilled water requirements, and fan power. However, depending on the cause of the high baseline flow rates, this change may not be as simple as adjusting fan control set points. If the high flow rate is caused by faulty terminal unit air valves that are not properly modulating to a lower flow rates, then making this adjustment may require replacement of terminal unit valve

actuators. If that is the case, the simulation results presented here could be used to balance the amount of potential energy savings with the estimated cost of repair.

It is possible that the increased flow rate is simply due to uneven zone loading. The building was modeled assuming a constant internal gain throughout each zone. However, typically some rooms within a zone have greater loads than others. An internal room with large gains may have a high cooling load during the entire year, while rooms with large windows and low gains may have more seasonal loading changes. If uneven zone loading is the cause of the higher supply flow rate, then it is not possible to reduce the flow rate to the design minimum without sacrificing occupant comfort in some rooms.

5.2 Increase in AHU Discharge Air Temperature

Based on the significant amount of zone level heating required during the year (terminal reheat and radiant perimeter baseboard heating), it may be possible to increase the discharge air temperature above the current set point of 55°F. A simulation was run with a discharge air temperature of 60°F to determine the potential savings resulting from the higher discharge air temperature for constant air volume (CAV) zones and for zones that can meet loads without increasing air flow rates.

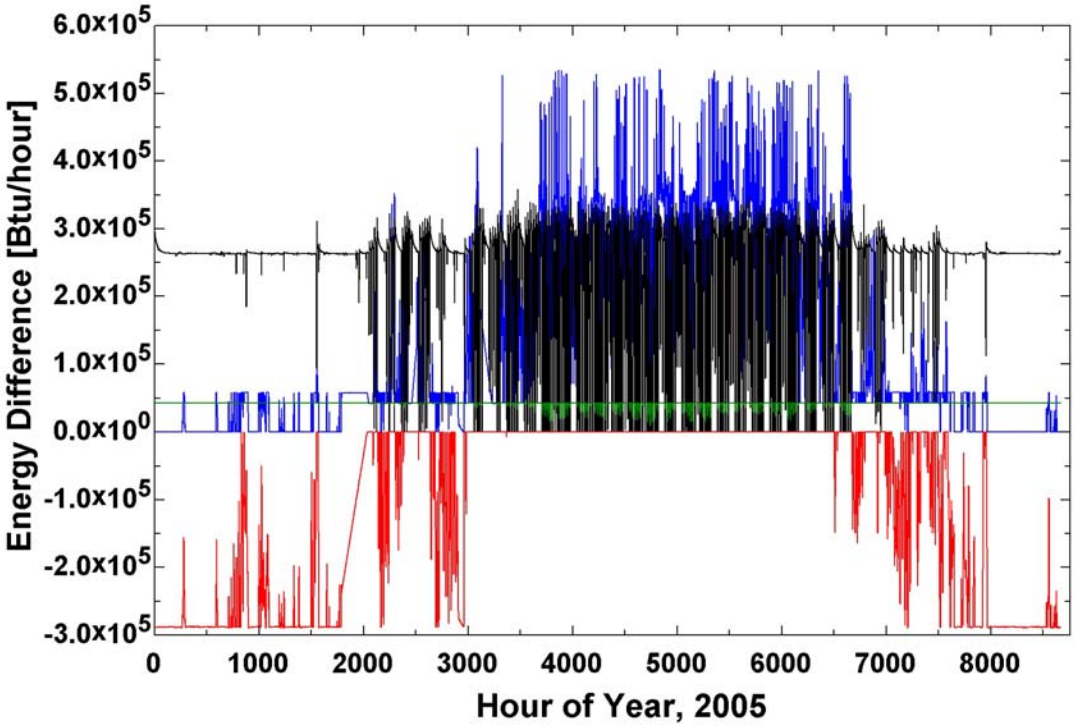

Figure 5.11 AHU3 Energy Differences, Baseline minus Design Minimum Air Flow Conditions

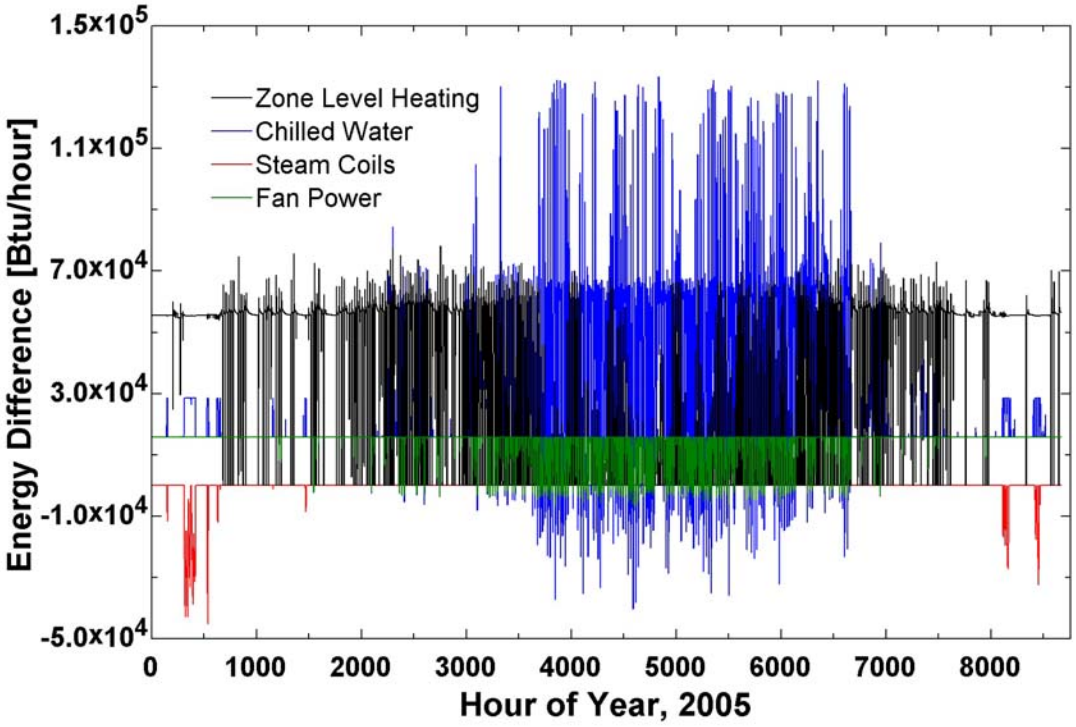

Figure 5.12 AHU5 Energy Differences, Baseline minus Design Minimum Air Flow Conditions

When an AHU is in heating mode and other zone variables such as the zone temperature, internal gains, and supply air flow rates remain constant, increasing the discharge air temperature does not have any net benefit. As the increased supply air temperature is achieved by increased steam heating coil energy usage, heat can either be added to the air stream by the steam coil in the AHU, or to the zone in the form of terminal reheat or radiant heating. However, in cooling mode, increasing the discharge air temperature can make a big difference to the amount of cooling energy required and to the amount of zone level heating required. The changes in heating and cooling energy due to an increase in discharge air temperature are illustrated in Figure 5.13 and detailed in Table 5.2.

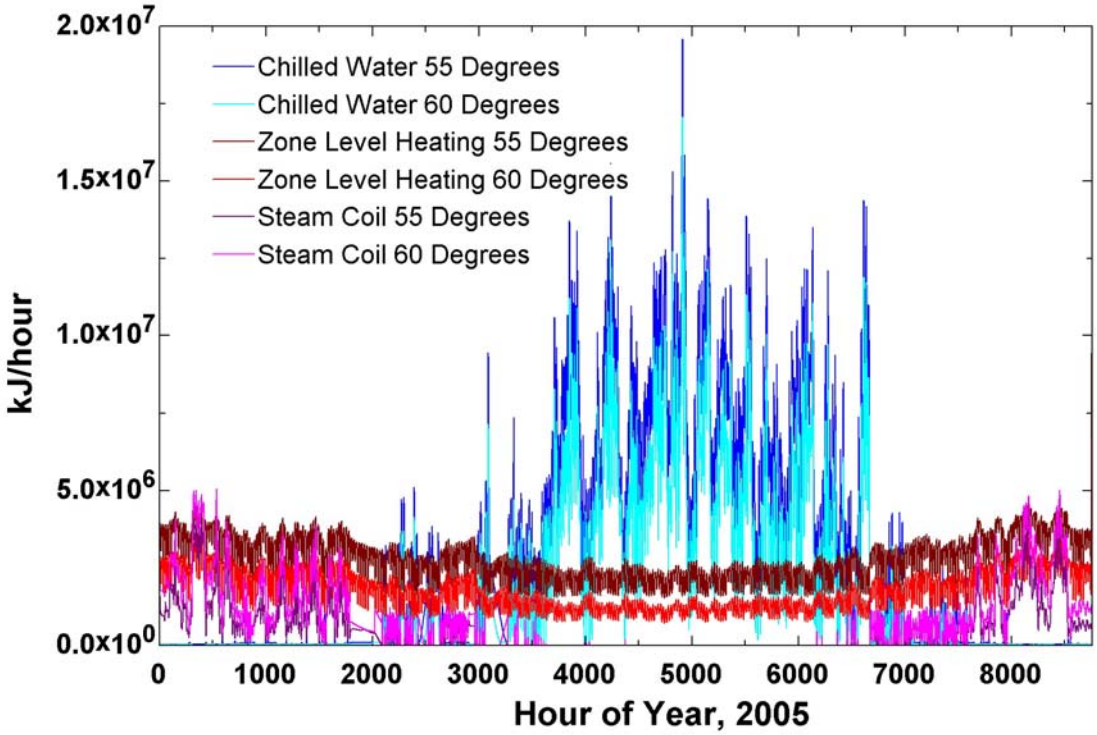

Figure 5.13 Simulated Energy Usage at Discharge Air Temperatures of 55° F and 60°F

Table 5.2 Simulated Energy Usage Comparison for Discharge Air Temperatures of 55° F and 60° F

	55° F Discharge Temperature [Btu]	60°F Discharge Temperature [Btu]	Savings [Btu]	Percent Savings[1]
Chilled Water	2.225 E10	1.495 E10	7.295 E09	32.8%
Zone Heating	2.316 E10	1.465 E10	8.505 E09	36.7%
Steam Coil	4.158 E09	6.632 E09	-2.474 E09	-59.5%
Total	**4.956 E10**	**3.624 E10**	**1.332 E10**	**26.89%**

[1]Percent Savings calculated as $\frac{55^{\circ} SupplyAir - 60^{\circ} SupplyAir}{55^{\circ} SupplyAir}$

While increasing the discharge air temperature appears to save a significant amount of energy annually, this control change may negatively affect occupant comfort. A higher discharge air temperature raises the humidity level of the supply air and therefore raises the humidity level of the zone because less moisture is removed from the air by the cooling coils. Also, it must be verified that the cooling load can still be met, even at a higher supply air temperature, without substantial increases in supply air flow rates.

The effect of a supply air temperature increase on zone relative humidity levels was investigated. In general, the zone relative humidity did increase, as illustrated in Figure 5.14 and Figure 5.15. However, it is unclear whether this increase would have a negative impact on comfort. Generally, a zone relative humidity of 60% is considered the maximum acceptable level for occupant comfort. The simulated humidity levels exceeded the 60% level at some points during the summer months, with maximum peak values reaching near 70%. While 70% relative humidity is too high for occupant comfort, as described in Section 4.3, the simulated zone relative humidity was consistently higher than the measured zone relative humidity (generally close to 10% higher). As described in Section 4.3, the simulated humidity and cooling energy results should be used to examine relative changes, rather than absolute values.

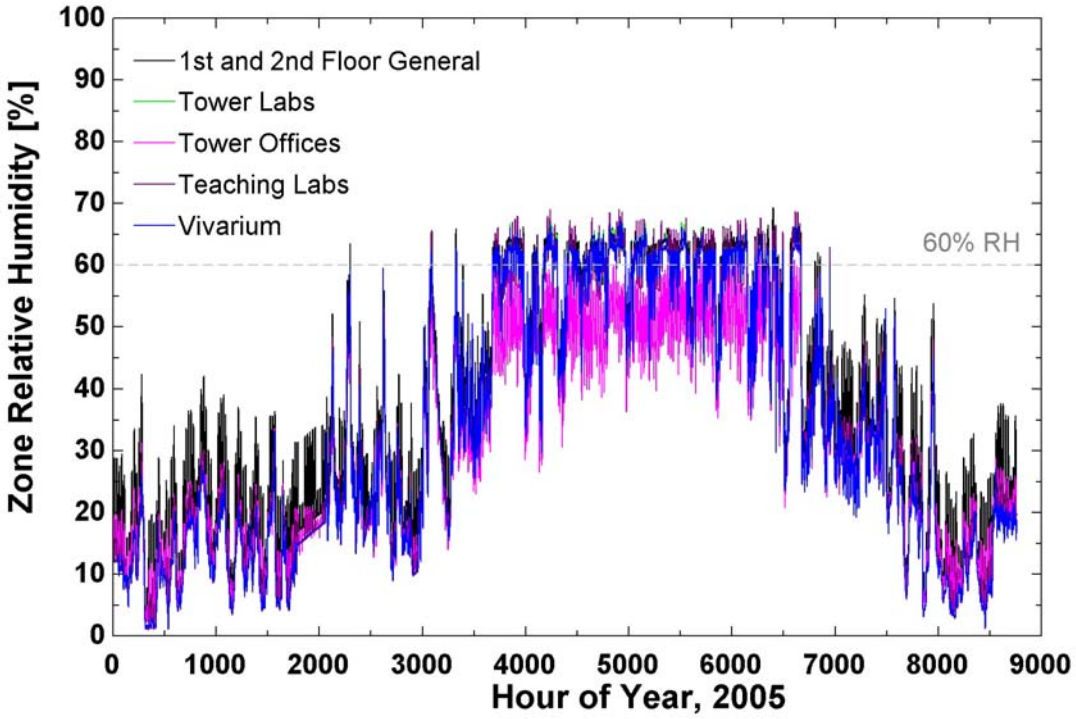

Figure 5.14 Zone Relative Humidity at a 60° F Discharge Temperature for All AHUs

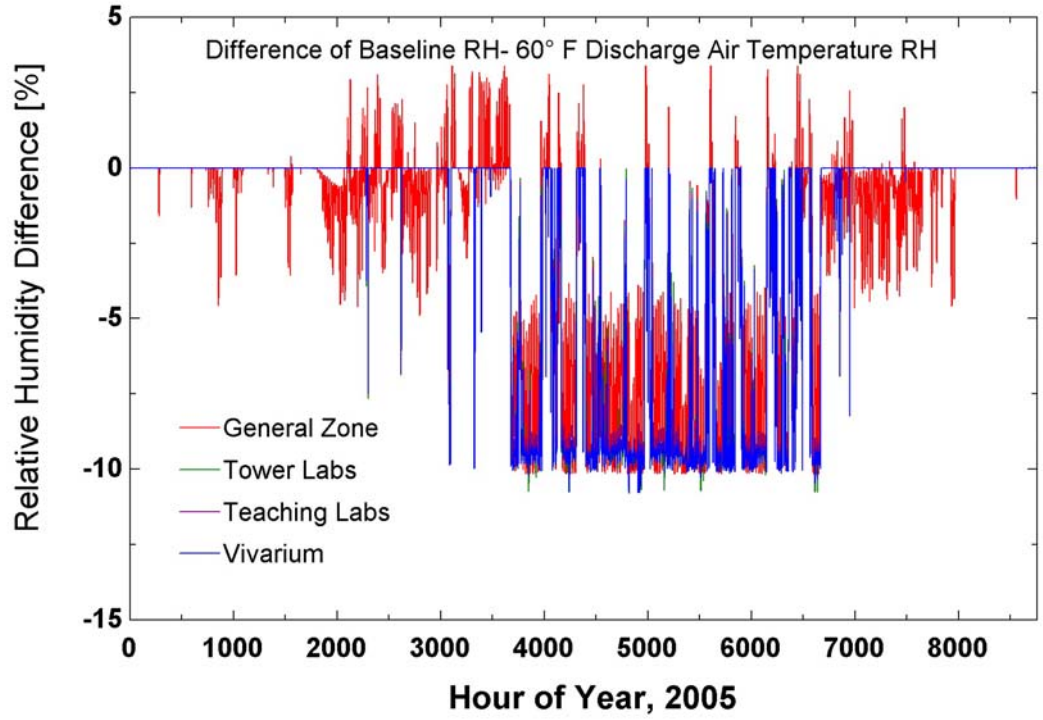

Figure 5.15 Difference in Zone Relative Humidity, Baseline Minus Increased Temperature Supply Air

As illustrated inFigure 5.15, the TRNSYS simulation likely predicts a higenerally predicts approximately 10% higher zone relative humidity level at the higher discharge air temperature than at the design discharge temperature. In the measured data, zone relative humidity occasionally peaks at values near 60%, but more often remains below 50%. Thus, while zone humidity level is a concern, this analysis does preclude further investigation into the benefits of increasing the discharge air temperature.

5.3 Reduction of Discharge Air Temperature for Tower Office Zone

The Tower Office zone, as shown in Figure 5.14, has a lower relative humidity than the others, due to an increased zone temperature. As indicated in Section 5.1, and Section 4.1, AHU5 often operates at its maximum flow rate both in the baseline simulation and in the actual BAS data. It is possible that the cooling load for this zone may exceed the capacity of AHU5 at baseline conditions, and it is likely that the cooling load exceeds the capacity of AHU5 for the increased discharge air condition. Figure 5.16 shows the Tower Office zone temperature difference and air flow rate difference due to the increased discharge air temperature. These results indicate that occupant comfort in this zone would be negatively affected by the higher discharge air temperature.

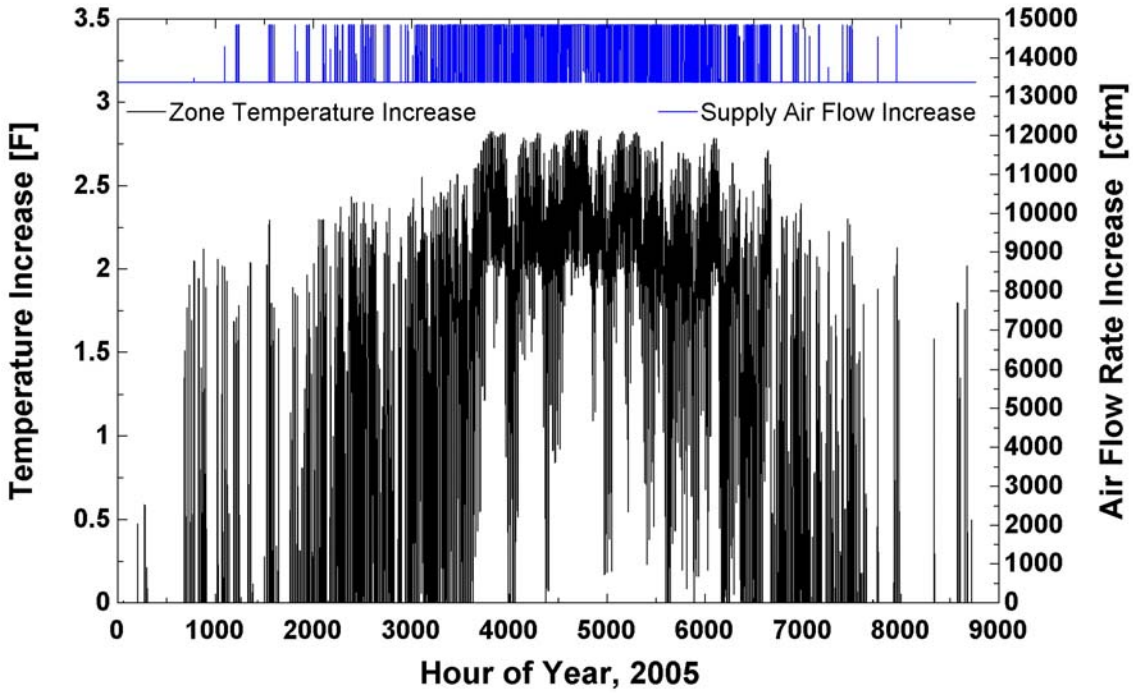

Figure 5.16 Increase in Tower Office Zone Temperature and AHU5 Supply Air Flow Rate with Higher Discharge Air Temperature

The Tower Office zone is the only zone in the building that may not have ample capacity to meet the zone cooling load. So, energy and comfort implications were investigated for this zone for lowering the discharge air temperature from 55° F to 50° F combined with the reduction in design minimum supply flow rate as described in Section 5.1. The reduction in temperature, when combined with a reduction in air flow rate showed a net energy savings for the zone, as detailed in Table 5.3.

Perhaps more importantly, this zone showed better temperature control for improved occupant comfort at the reduced discharge temperature as shown in Figure 5.17.

Table 5.3 Energy Usage for AHU5 with Reduced Minimum Flow Rate and Reduced Discharge Air Temperature

		Baseline [Btu]	Design Minimum 50°F Discharge [Btu]	Energy Savings [Btu]	Percent Savings[1]
AHU5	Zone Level Heat	9.670 E08	8.938 E08	7.318 E07	7.6%
	Steam Coil	0	0	0	0%
	Chilled Water	1.502 E09	1.508 E09	-6.061 E06	-0.4%
	Fan Power	2.923 E08	1.366 E08	1.557 E08	53.25%
	Total	**2.761 E09**	**2.538 E09**	**2.228 E08**	**8.1%**

[1]Percent Savings calculated as $\frac{55^{\circ} SupplyAir - 50^{\circ} SupplyAir}{55^{\circ} SupplyAir}$

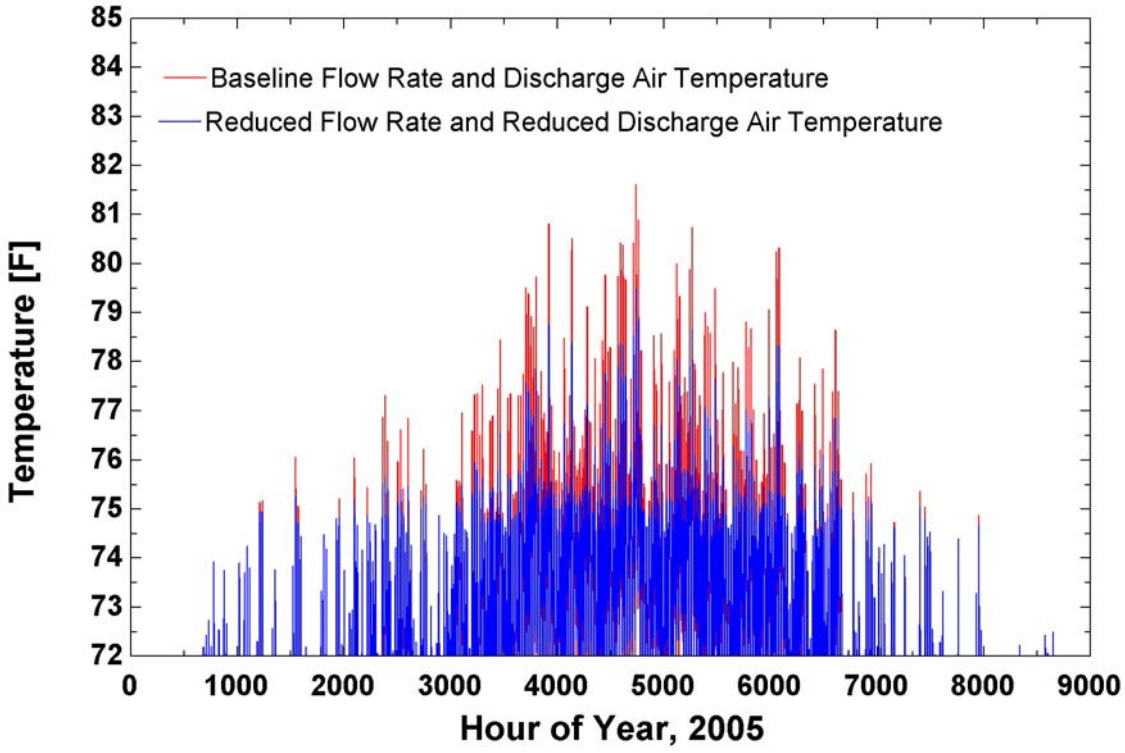

Figure 5.17 Simulated Tower Office Zone Temperatures at Baseline and With Reduced Flow Rate and Reduced Discharge Air Temperature

5.4 Combined Building Temperature and Flow Rate Adjustment

A new simulation was completed combining the above findings. The minimum flow rates for both AHU3 and AHU5 were reduced to the levels described in Section 5.1, the discharge air temperatures were increased for all zones except the Tower Office (AHU5) zone as described in Section 5.2, and the discharge air temperature for AHU5 was reduced as described in Section 5.3. The results for these changes are shown in Table 5.4. The potential savings in heating and cooling costs is about 25%.

Table 5.4 Simulated Energy Usage with Discharge Air Temperature for the Tower Office Zone at 50° F, All Other Zones at 60° F, Design Minimum Flow Rates for AHU3 and AHU5.

Design Minimum Flows	55° F Discharge Temperature [Btu]	50°/60°F Discharge Temperature [Btu]	Savings [Btu]	Percent Savings[1]
Chilled Water	2.233 E10	1.502 E10	7.306 E09	32.7%
Zone Heating	2.322 E10	1.396 E10	9.253 E09	39.9%
Steam Coil	4.158 E09	7.514 E09	-3.356 E09	-80.7%
Total	**4.971 E10**	**3.650 E10**	**1.320 E10**	**26.56%**

[1]Percent Savings calculated as $\frac{55^{\circ} SupplyAir - 50/60^{\circ} SupplyAir}{55^{\circ} SupplyAir}$

Verification that comfortable humidity levels can be maintained for zones with increased discharge air temperatures is important. However, this simulation suggests the potential for substantial energy savings and improved occupant comfort in the Tower Office zone.

Chapter 6: Fault Detection and Continuous Energy Monitoring

While fault detection was not a primary goal of this project, the model calibration process for Rennebohm Hall revealed a number of operational faults related to the building's space conditioning systems. As a result, some simple data verification and fault detection techniques were employed using the existing BAS. The estimated energy savings associated with correcting the mechanical system operational faults for this one building suggest that significant energy and energy cost savings could be accrued by applying similar techniques to other energy intensive buildings on campus.

A pre-requisite to evaluating the operating cost impacts associated with mechanical system related faults is identifying their presence. In this project, relatively simple field data verification and fault detection techniques were developed to uncover potential problems. Site visits, interviews with facility staff, and modeling were used to verify the faults that had the greatest operating cost impacts. None of the faults discovered appeared to compromise the safety of the building.

Data used for driving the fault detection were obtained using the existing building automation system (BAS). While the focus of the methods outlined here is on techniques that can be implemented using the existing building instrumentation and equipment, it should be noted that selectively sub-metering steam, chilled water, and electricity could further enhance energy monitoring and fault detection capabilities.

The types of building faults that these methods were designed to detect include simultaneous heating and cooling (either due to control problems or to leaking valves);

excessive outside air (during heating or cooling seasons); inadequate outside air (during economizer mode); and potential control problems (that can lead to unstable valve positions and fan speeds). The methods described here involve the compilation of key measures of performance for review by a person with some knowledge of the building mechanical system design and operation. However, by incorporating fault detection and diagnostic methods described in the literature (Braun, 2003; Chen & Braun, 2001; House et al, 2001; Gremmelius et al., 1999), the possibility exists to automate this fault detection process.

6.1 Role of Building Simulation in Fault Detection

Building simulation is required to determine a baseline energy usage for the building at a particular time given the mechanical system design, operating parameters and set points, occupancy, and weather conditions. Variables with values dependent on building loads – either on transmission losses or gains through the building shell, or on internal building gains related to building occupancy and usage – require some level of simulation to estimate their values. The airflow in a VAV system, for example, will often be directly proportional to the zone gains and losses; however, the exception occurs during heating mode operation. The volume flow rate of air in a VAV system serving perimeter and interior zones will be reduced to its minimum and modulate upward during cooling to meet the load requirements. The building reheat load is similarly dependent on building gains and losses. The variables that depend on building gains and losses can be categorized as *building-coupled*.

There are other state variables and parameters that do not require a building simulation to determine their values (or ranges of values). For these independent variables and parameters, a design energy usage relationship can be developed that will depend only

on outside air conditions. Since outside air conditions can be easily measured, the independent variables can be monitored and compared directly to a design energy consumption level. These independent variables can be categorized as *uncoupled* with respect to building gains and losses. Examples of uncoupled building variables and parameters include the volumetric airflow in a CAV system or the energy required to heat (or cool) a 100% outside air constant volume system. Examples of building-coupled and uncoupled variables are detailed in Table 6.1.

Table 6.1: Examples of Building-Coupled and Uncoupled Variables in Rennebohm Hall

Rennebohm Hall Building-Coupled Parameters	Rennebohm Hall Uncoupled Parameters
VAV Air Flow Rate	CAV Air Flow Rate
Terminal Reheat Energy	Outside Air Flow Rate
Humidification Steam Flow Rate	Cooling energy for 100% Outside Air Systems
	Heating energy for 100% Outside Air Systems
	Energy Recovery in a CAV System (With Constant Zone Air Exhaust Temperature)

As demonstrated in Chapter 5, simulation can be used to approximate the design levels for building-coupled variables and to estimate the energy impact of changes in those variables. But, building simulation is time consuming and a more simple approach may be sufficient for detecting faults. In many cases, useful information about the behavior of a system can be attained through examination of relative trends among building-coupled state variables and by verifying data values through alternative measurements or calculations. For example, in a VAV system, the supply air flow required to meet the building loads can be expected to be higher for a very hot day than for a very cold day. Also, the airflow should be higher on a day with high building occupancy levels than on a day when the building is essentially unoccupied. Airflow magnitudes as measured using velocity pressure

measurements should be approximately equal to the airflow magnitude calculated from the system fan speed. By looking at data trends and independently verifying data values, system faults can be flagged or detected in many cases without detailed knowledge of actual building loads.

While it is often possible to detect faults in building-coupled parameters without the use of simulation, it is difficult to quantify the energy and fiscal impact associated with one or more building mechanical system-related faults. For an uncoupled variable, it is possible to calculate a specific design value and the difference in energy impact between the two values can be calculated. Thus, ranking these faults by financial impact is feasible. However, if the design values of variables are not easily determined, it may be difficult to establish the energy impact of a fault without some level of simulation.

6.2 Fault Detection and Energy Monitoring Methods

The methods that have proven useful for detecting faults in Rennebohm Hall involve examination of flow rates and system temperatures using some simple rules to evaluate the system behavior. The system evaluation is, essentially, an application of the *Data Validation* methodology described in ASHRAE Guideline 2-2005 (ASHRAE, 2005), and is very similar to the rule-based approach described in House et al., 2001.

For the method to be effective, a reasonable time period for evaluating system behavior must be selected. If the time period is too short, outlying data points may trigger too many *false positives* in the search for building faults. However, if the time period is too long, a costly building fault may go unnoticed. Building operational faults that impact occupant comfort are generally noticed and repaired very quickly. One of the benefits of

energy monitoring is the potential for detecting operational faults that result in increased energy consumption without affecting comfort. A long time period for evaluating system behavior also causes data processing issues to become more onerous.

One month seems to be a reasonable time period for evaluation. The volume of data collected in 10 minute to 1 hour intervals over a one month period is still manageable by most analysis packages. Monthly time periods are also able to capture multiple low occupancy periods (i.e. weekends), representative high occupancy periods, and a range of weather conditions.

To evaluate the airflows for each AHU, multiple means of assessing the each flow should be evaluated each month. When flows are measured directly, the measured value should be compared to a calculated flow based on the fan VFD command and the fan design flow. With further research to determine an appropriate measurement uncertainty band, this comparison could be done numerically. However, the comparison can also be made graphically, as demonstrated in Section 6.3.

If airflows are consistently lower than design in a CAV 100% outside air system the system should be rebalanced, or, an investigation into air quality issues and zone usage could be conducted if zone loading or occupancy changes indicate the need for less supply air than mandated by the original design. The additional cost for operating with airflows that are consistently higher than design can be calculated by including the additional electric power required for higher fan speed, as well as the additional heating and cooling required for the incrementally higher air flow rates.

In systems utilizing return air, the relative flow rates for the outside airflow ($\dot{V}_{OA}$), mixed supply airflow ($\dot{V}_{SA}$), and return airflow ($\dot{V}_{RA}$) can be evaluated for internal consistency. A simple mass balance suggests:

$$\dot{V}_{OA} + \dot{V}_{RA} = \dot{V}_{SA} \tag{6.1}$$

This balance can be verified by plotting the sum $\dot{V}_{OA} + \dot{V}_{RA}$ on the same plot as the measured supply air flow rate.

The temperature distribution of the air through each air-handling unit can provide further insight into its functionality. When all available temperature data are plotted from the AHU inlet to discharge, the air temperature should reflect energy additions and extractions. Because of the ordering of the heat recovery, steam, and chilled water coils in the AHUs in Rennebohm Hall a progression should be seen from colder to hotter when the inlet condition (outside air temperature or mixed air temperature) is less than the discharge air set point, and from hotter to colder when the inlet condition is greater than the discharge air set point. In addition to the direction of the temperature progression, temperatures should be evaluated for unusual oscillation patterns and for unexpected energy changes.

Ideally, temperatures should be measured and evaluated at each point where there is the possibility for an energy exchange. For the Rennebohm Hall AHUs, temperature measurements should have been available: at the inlet (outside air or mixed air temperature), after the heat recovery coil, after the fan, after the steam coil, after the chilled water coil, after humidification, and at the discharge. Valve positions for the heat recovery coil, steam coil, and chilled water coil should be plotted on the same plot as the temperatures.

Generally, not all of these values will be available in a given AHU but some, such as the temperature after the fan, can be estimated.

6.3 Fault Detection Results

Using the techniques previously described, an airflow fault was detected in AHU3, a unit that uses return air and serves the general 1st and 2nd floor office and classroom spaces. The specific fault identified was a flow measurement station providing incorrect supply flow data. This problem is illustrated by first examining an airflow plot for the unit when it is functioning as expected. Figure 6.1: Air flow data for AHU3 operating when no faults Figure 6.1 shows three supply air flow values – the measured value, the value calculated from the VFD data, and the sum of the measured outside airflow and measured return airflow. These three values are similar in magnitude. In addition, the two return air values – measured and calculated from VFD data – are similar in magnitude. There is only one value available for the outside airflow, but as the sum of that value and the return airflow seem reasonable, it can be concluded that the flow measurement station is functioning as designed.

Figure 6.2 illustrates the airflows for AHU3 when the supply air flow measurement is faulty. The measured supply flow is close to zero for the entire month. While the unit was actually providing the flow indicated by the VFD calculated value (close to 40,000 cfm), the measured flow reading is the variable used to control the return fan unit. The return fan speed is controlled to maintain a return airflow of either the measured supply airflow minus the minimum outside air value, or the return fan minimum speed, whichever is greater. For this zone, the minimum outside airflow is a constant 19,500 cfm. As the difference between the outside air flow and the measured supply flow is less than zero, the return fan reverts to

its minimum setting VFD command of 14.6 Hz, resulting in approximately 13,500 cfm of return air. During the month of February shown in Figure 6.2, the impact of this fault was small. There may have been a small amount of extra outside air brought into the building, but for this month, that likely totaled only a few thousand cfm.

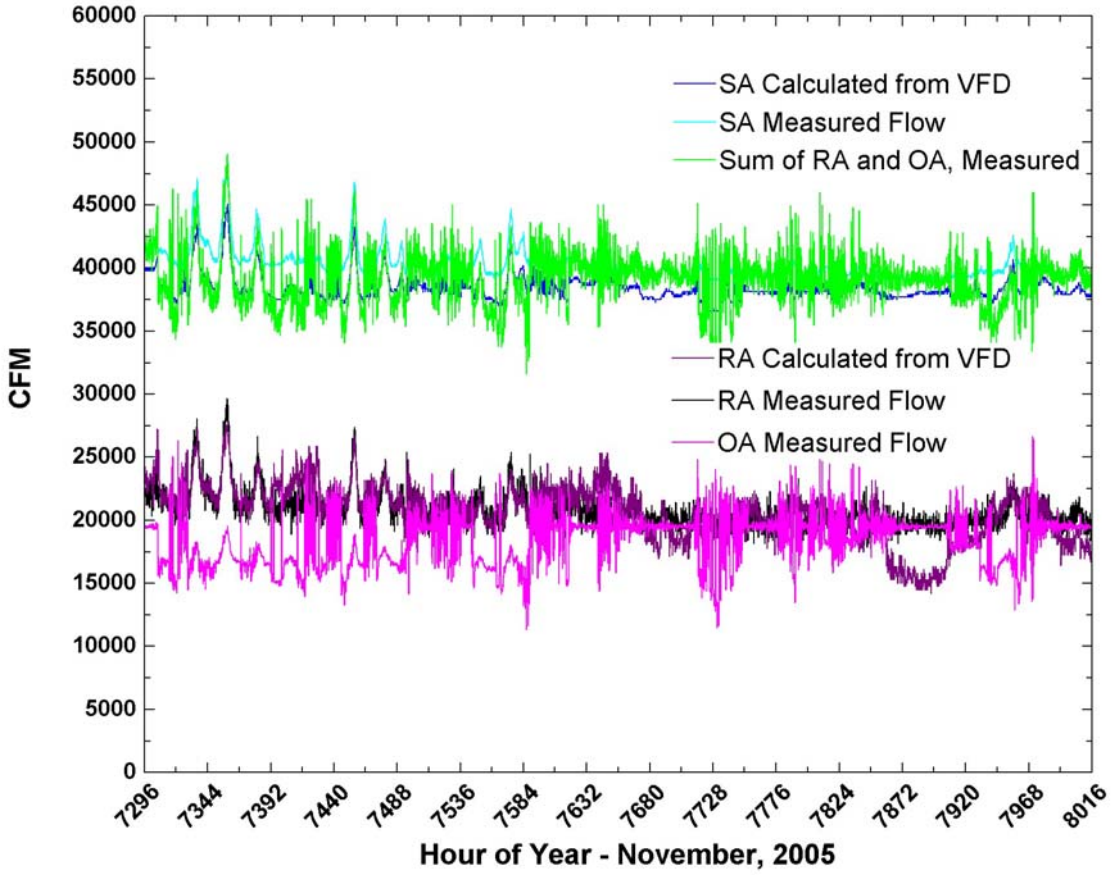

Figure 6.1: Air flow data for AHU3 operating when no faults were detected.

A larger impact of this fault was apparent during the summer months when the flow measurement became more sporadic, as shown in Figure 6.3.

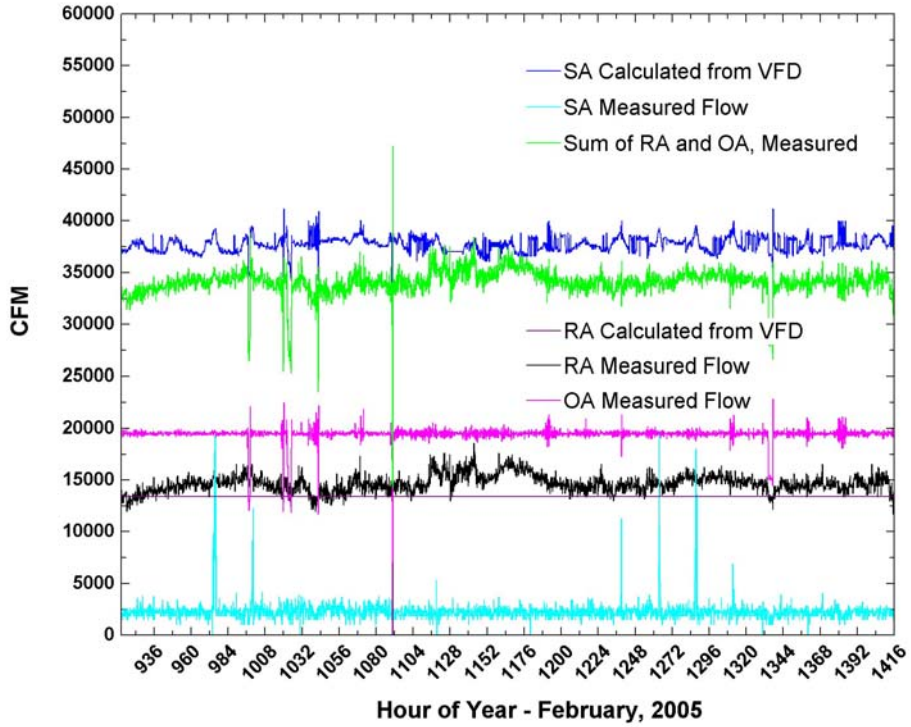

Figure 6.2 AHU3 Airflows, Faulty Supply Air Measurement.

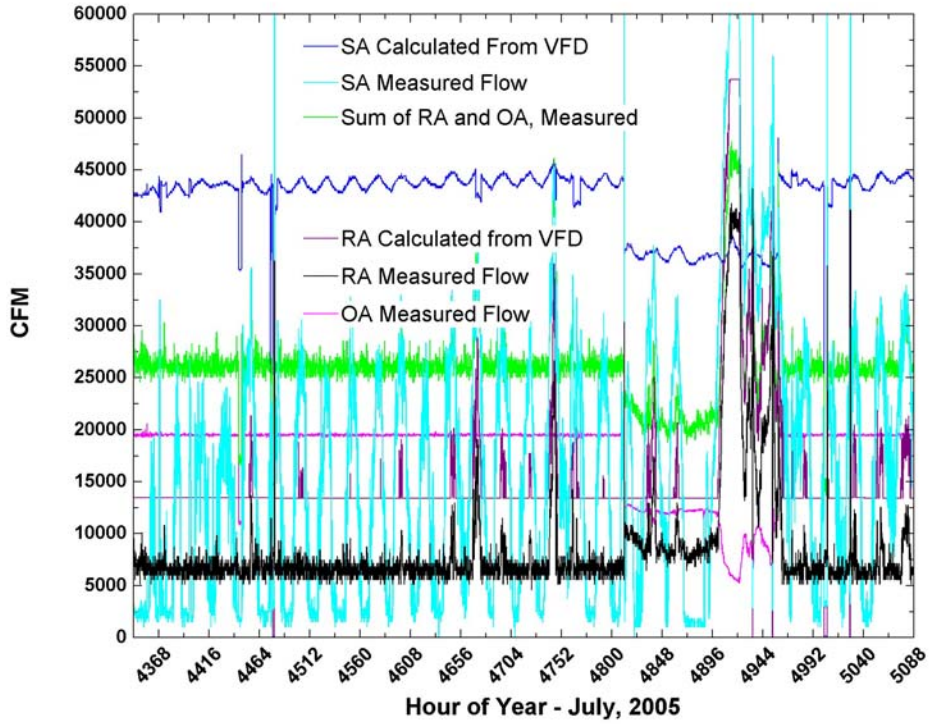

Figure 6.3 AHU3 Airflows, Faulty Supply Air Measurement Resulting in Loss of Control of the Unit

According to the technician that repaired AHU3, the root cause for the fault was due to a bad pressure transducer providing an erroneous, non-linear, velocity pressure reading. As the voltage output of this transducer oscillated, it occasionally produced a large enough signal for the return fan to revert from its minimum setting to its design setting. With the supply fan operating at its typical speed to induce a flow of approximately 43,000 cfm, and the return fan operating at its minimum speed, the static pressure in the mixing box of this unit was measured by the technician was a highly negative gage pressure. When the return fan occasionally ramped up to provide more return air, the sides of this AHU were expanding and contracting resulting. This created a significant volume of noise. When the pressure transducer was replaced and the air flow rate proportional gain reduced, the airflows in this unit came back under control as shown in Figure 6.4.

The AHU3 flow measurement fault illustrates the importance of completing repairs on sensors with signals that are used for system control. It is difficult to identify the energy cost associated with this fault as it occurred in a building-coupled variable. Further, there is likely a maintenance impact associated with this fault; however it is difficult to quantify the additional wear and tear inflicted on the fan motors, shafts, and bearings. It is also difficult to determine the actual supply air, outside air, and return air flow rates induced during the summer months when the unit was oscillating due to the lack of agreement among the various flow approximations. This fault is one that was implicated in affecting occupant comfort due to the noise produced by the unit. With the occupant comfort and acoustic signature, such faults tend to be identified more quickly.

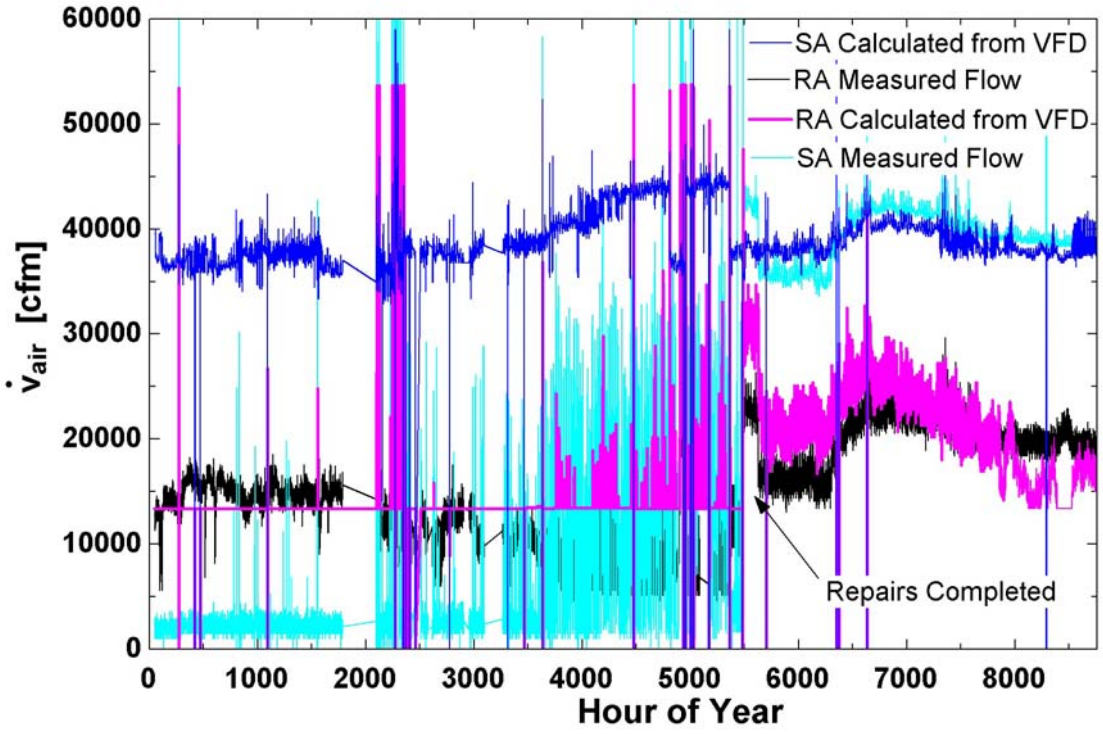

Figure 6.4 Airflow in AHU3 for 2005, Repairs Indicated

Evaluating the temperature distribution through AHU6 resulted in the identification of a leaking steam valve. All available temperatures in AHU6 are plotted in Figure 6.5. In addition, two calculated values are plotted: the temperature after the heat recovery coil plus an estimate of the fan heat added, and the heat recovery-fan heat sum plus an estimate of the heat added due to humidification. Both values were calculated for the worst-case limits. The fan heat was calculated assuming that 100% of the fan power was added to the air stream. The humidification value is a building-coupled variable, so the amount of humidification was calculated based on bringing the measured outside air humidity ratio to the target zone humidity ratio (based on the space relative humidity and zone conditions) assuming no latent gains. Unfortunately, there are no temperature measurements in this unit between the steam coil and the chilled water coil.

As shown in Figure 6.5, the AHU6 steam coil is commanded shut during the entire month. The fan heat addition and humidification heat addition are estimated. With the steam coil and chilled water coil command shut, there should be no other energy additions to the air stream between the measured heat recovery temperature and the measured discharge air temperature. The temperature measurements were independently verified with data collected during a building site visit and found to be accurate. Thus, the best explanation for the evident consistent temperature increase is a leaking steam valve. During heating mode, this fault does not have substantial impact, as steam heat added to the air stream in the AHU will be offset by a lower heat addition from the reheat coils in the terminal units; however, it increases the energy use of the building during cooling mode operation.

The April data presented in Figure 6.6 provides evidence of simultaneous heating and cooling, a more serious fault in terms of energy and cost impact. As indicated in Figure 6.6, a temperature increase that can not be explained by other energy inputs is present whenever the cooling coil is commanded shut. However, when the cooling coil opens, the discharge air temperature drops to its design value of 55º F. When the cooling coil closes, the discharge air temperature increases again with no documented heat addition.

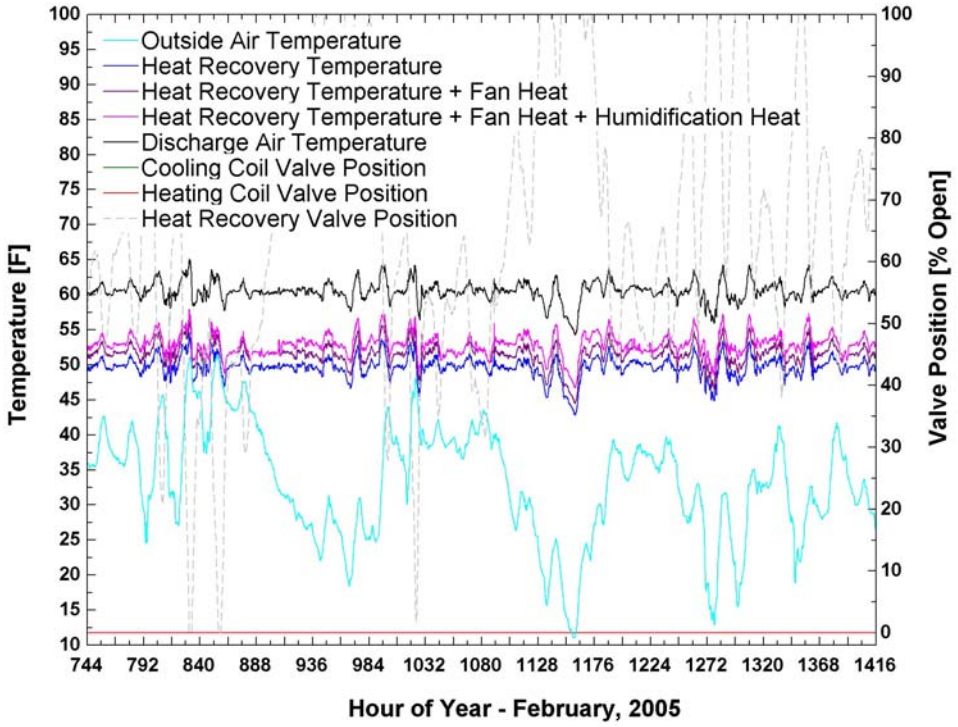

Figure 6.5 AHU6 Temperature Distribution Indicating a Leaking Steam Valve

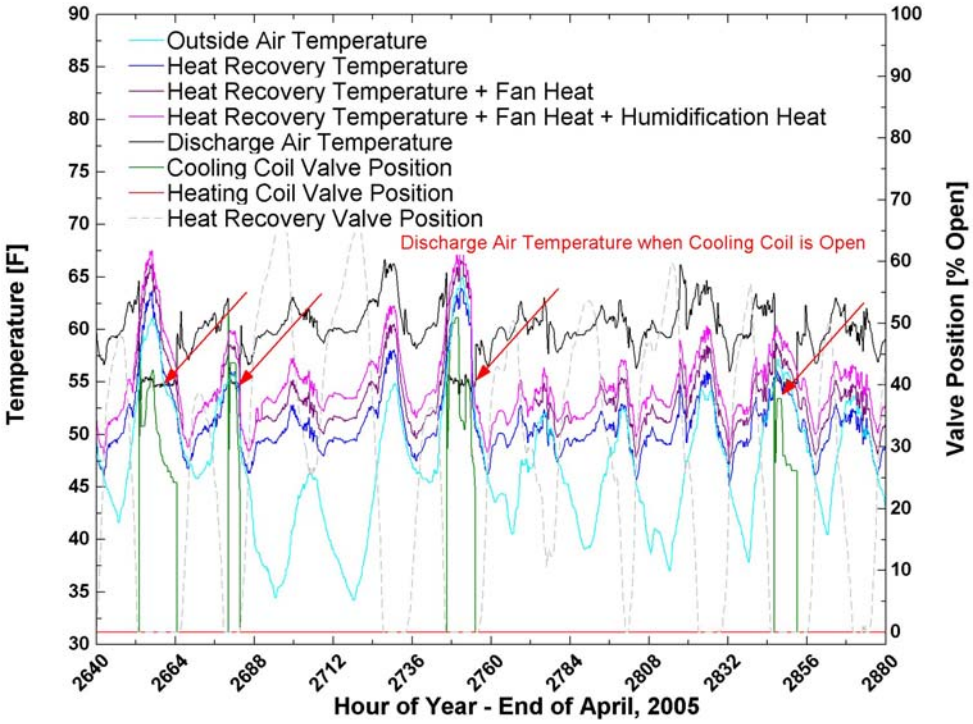

Figure 6.6 AHU6 Temperature Distribution, Probable Simultaneous Heating and Cooling

The temperature increase apparent in AHU6 is relatively constant over a period of months, indicating that the steam valve is likely stuck open or leaking at a constant rate. When the cooling coil down stream of the steam coil opens, it has ample capacity to cool the heated air. As there is no temperature measurement between the coils, a steam leak is undetectable when the cooling coil is in use.

Low building pneumatic pressure was discovered when AHU1 and AHU2 were undergoing testing and balancing for an unrelated issue. It was determined that the cause of the low pressure was multiple leaking pneumatic actuators on terminal units throughout the building. After a technician installed a new compressed air line dedicated only to the building mechanical equipment, the steam leak was resolved.

In order to quantify the cost impact of the leaky steam valve identified in AHU6, it is important to note that the leak probably does not have a net energy loss when the AHU is in heating mode. Extra heat added to the air stream by the AHU steam coil means less heat needs to be added at the zone level in the form of reheat or perimeter radiant heat. Thus, it is only when the chilled water coil is open that there is an associated energy and financial cost of the leaking valve. A discussion with the technician who performed the repair on the pneumatic control line estimated that the repair was completed in early fall. The chilled water coil is open continuously throughout the summer until it closes briefly in late September. At that point in late September, the leak is no longer apparent.

The energy addition due to the steam leak was calculated for each time step in the data with both the steam coil and the chilled water coil commanded shut. The energy addition was then averaged over the number of hours that both coils were shut. This procedure produced an average energy addition of 314,042 Btu/hour. It was assumed that

this energy addition was constant over the time when the cooing coil was open, so this average energy was multiplied by the number of hours that the cooling coil was open between January, 2005 and September, 2005 (4277 hours). This calculation results in an energy addition of 1.343 E09 Btu from the steam valve and an equal amount of cooling to return the air to its original temperature. The financial impact of this fault will be discussed further in Chapter 7.

Figure 6.7 illustrates the temperature distribution in AHU6 after repair of the compressed air system. There are two other items to note in Figure 6.7. The first is that the elevated discharge air temperature when the chilled water coil control valve signals that it is fully open suggests that the water-side for this cooling coil may have already been drained for the winter. The second is the onset of a fault in the heat recovery system. Mid month, the heat recovery valve is fully open without any corresponding heat gain for the air stream. Further investigation into the heat recovery system during this month revealed greatly elevated glycol temperatures in the runaround loop for the end of the month of November, with glycol supply temperatures gradually increasing to approximately 150°F. In January of 2006, the heat recovery system began functioning again–an explanation has yet to be determined for its failure.

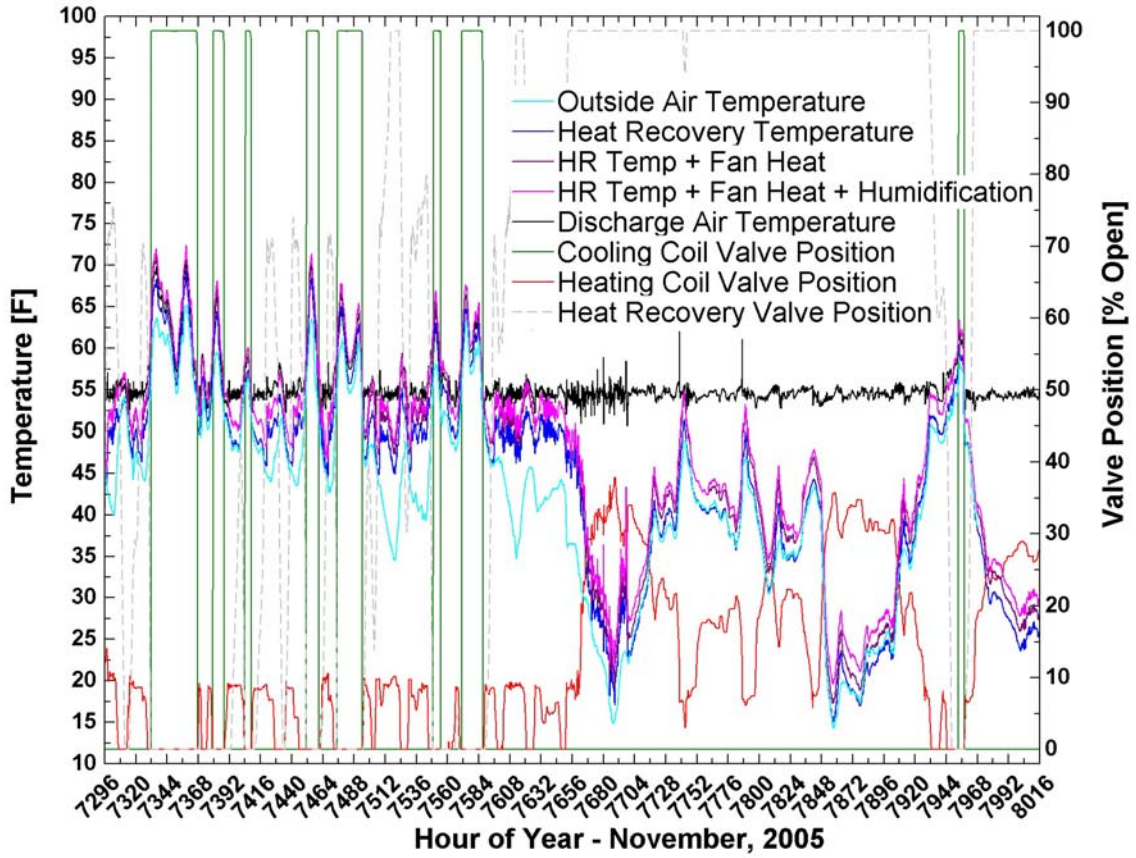

Figure 6.7 AHU6 Temperature Distribution, Steam Leak Repaired, Onset of Heat Recovery Fault

6.4 Barriers to Fault Detection

If temperature and airflow plots for each AHU could be generated each month in an automated process, an examination of these plots by trained staff (such as a capable building manager) could aid in the diagnosis of building faults. There are, of course, some significant barriers to these analyses. The primary barrier is time—both the time required for processing the data and time for analyzing the results.

In order for these procedures to be feasible, some initial programming and data processing are required. The logical path to provide data collection, pre-processing, and

analysis would be to utilize the existing building's energy management system but currently, this approach is far from being implemented. The data, as archived by the BAS system, are stored in separate, identically named files, in different time steps, and usually with some missing data. Some processing is required to match data by time and to extract the useful data from the files. It may be possible to program the BAS to generate these monthly reports. If not, then a data processing program could be written in practically any computer language. In addition, if temperature measurements are not available after each energy exchange in the AHU, some programming is required to estimate missing measurements. For the current project, a program was written in Visual Basic to compile monthly data for each AHU, and EES was used to interpolate and analyze the data. These data processing steps require an initial time investment and would need to be tailored to fit the mechanical system for each building.

The time required to analyze all the AHUs on campus each month would be too large to add to the job description of an existing single campus employee. Perhaps an effective strategy would be to invest some time into training the building managers to review the performance of their own building. When there are no building faults, this review would be very quick (for someone who knows the building mechanical systems). When there is a fault, its diagnosis will naturally take longer. The building manager would be able to provide the Physical Plant with information about the system in fault and the Physical Plant could judge the severity of the problem and could schedule repairs accordingly.

Chapter 7: Conclusions and Recommendations

Building mechanical systems are complex, consisting of numerous interdependent systems. Building simulation can be an important tool for understanding the systemic effects of new control or building design strategies. However, simulation can also be time intensive, and therefore quite costly. While simulation can be useful for fault detection and energy monitoring, it is not always required. It is important to differentiate among issues requiring simulation to resolve, and issues that could be resolved with a simplified approach, so that the most cost effective tool can be used.

This project has explored energy saving opportunities for one campus research facility, including exploration of the roles that building simulation, fault detection, and energy monitoring may play in achieving building energy savings. The findings of the project underscore the benefits of archiving BAS data to support conducting a systematic monthly review of building energy systems. While the focus here was on a single campus building, some of the findings may be generalized to other facilities.

It has been demonstrated that state-of-the-art buildings, such as Rennebohm Hall, could benefit from systematically monitoring their energy consumption patterns as a means of identifying common operational faults that lead to increased building energy consumption. In fact, because many of the new buildings on campus are energy intensive research facilities, it may be the new buildings that benefit most from energy monitoring and fault detection. Most new research facilities utilize sophisticated control designs, particularly facilities that are designed for energy efficiency and conservation. It has been previously demonstrated in the literature that faulty controls are among the most prevalent faults in

AHUs, and among the most costly to repair (Breuker and Braun, 1998b). Further, some of these faults can be difficult to detect if there is not an immediate impact on occupant comfort.

The operational faults identified in this project were often detectable before they had a significant impact on energy consumption or occupant comfort. In fact, a leaking pneumatic steam valve in AHU6 was *only* detectable in heating mode operation when there was no net energy penalty. An energy monitoring program could be as simple as configuring the building automation system, or another computer system, to prepare a set of monthly temperature and air flow reports for review by the building managers trained to interpret the reports. Faults identified in this manner could aid in planning and prioritizing system maintenance.

7.1 Energy and Cost Impact of Operational Faults Identified Using Simple Energy Monitoring Techniques

This project identified several operational faults that could be identified without building simulation, but that would be difficult or impossible to detect without some sort of systematic energy monitoring and evaluation protocol. In order to illustrate the potential cost effectiveness of a simple energy monitoring program, it may be useful to assign costs to some of the faults detected in this project. Modeling and simulation are used as tools to estimate the operating cost impact associated with allowing mechanical system faults to persist. The estimated savings associated with correcting the mechanical system operational faults for this one building suggest that significant energy and energy cost savings could be accrued by applying similar techniques to other energy intensive buildings on campus. It should be noted that while some simulation or energy modeling is required to quantify the

associated cost impacts of these faults, their presence was detected without the use of modeling or simulation.

The utility cost assigned to campus steam and chilled water is based on estimates provided by the Physical Plant in April, 2006. The present variable energy cost is $6.44 per million Btu of steam and $0.1492 per ton-hour of cooling ($12.43 per million Btu of chilled water). Steam and chilled water rates with capital costs included were also estimated based on information from the University of Wisconsin Physical Plant. The rates including capital costs were estimated at $8.59 per million Btu of steam and $0.2585 per ton-hour of cooling ($21.54 per million Btu of chilled water).

Using the above utility rates and the cost estimation method detailed in Section 6.3, the 9 month cost penalty of the leaking steam valve in AHU6 (calculated from January, 2005 through repair in September, 2005) is estimated at $40,471 (see Table 7.1). A similar, but significantly smaller steam leak was also discovered in AHU7. Estimating the cost by the same procedure as with AHU6 resulted in an estimated cost of $3,550 for the second leak during the same 9 month period. The combined cost of the two steam leaks is more than 80% of the net annual savings due to the building heat recovery system (see Table 7.2).

Table 7.1 AHU6 and AHU7 Steam Leaks, Estimate of Energy and Cost Impacts

Steam Valve	Energy [Btu]	Cost [$]	Cost, Capital Costs Included [$]
AHU6 Steam	1.343 E09	$8,650	$11,538
AHU6 Chilled Water	1.343 E09	$16,700	$28,933
AHU6 Total	**2.686 E09**	**$25,350**	**$40,471**
AHU7 Steam	1.178 E08	$759	$1,012
AHU7 Chilled Water	1.178 E08	$1465	$2,538
AHU7 Total	**2.356 E08**	**$2,224**	**$3,550**

Table 7.2 Heat Recovery Savings

Heat Recovered	Energy [Btu]	Utility Rate Assessed	Savings [$]	Savings, Capital Costs Included [$]
AHU1 Heat Recovered	9.243 E08	Steam	$5,952	$7,939
AHU1 Cooling	6.472 E07	CW	$805	$1,394
AHU1 Fan Power	27,323 kWh	Electric	-$1,366	-$1,366
AHU1 Pump Power	3,343 kWh	Electric	-$167	-$167
			$5,224	$7,800
AHU2 Heat Recovered	8.944 E08 Btu	Steam	$5,760	$7,683
AHU2 Cooling	8.916 E07 Btu	CW	$1,109	$1,921
AHU2 Fan Power	28,191 kWh	Electric	-$1,410	-$1,410
AHU1&2 Pump Power	3,316 kWh	Electric	-$166	-$166
Vivarium Net			$5,293	$8,028
AHU6 Heat Recovered	1.883 E09 Btu	Steam	$12,125	$16,173
AHU6 Cooling	1.464 E08 Btu	CW	$1,821	$3,154
AHU6 Fan Power	83,712 kWh	Electric	-$4,185	-$4,185
AHU6 Pump Power	14,399 kWh	Electric	-$720	-$720
AHU6 Net			$9,041	$14,422
AHU7 Heat Recovered	2.854 E09 Btu	Steam	$18,381	$24,517
AHU7 Cooling	1.380 E08 Btu	CW	$1,716	2,973
AHU7 Fan Power	90,175 kWh	Electric	-$4,509	-4,509
AHU7 Pump Power	14,399 kWh	Electric	-$720	-$720
AHU7 Net			$14,868	$22,261
Total			**$34,426**	**$52,511**

The heat recovery system serving AHU6 failed in November of 2005, as illustrated in Figure 6.7. During this time the glycol supply temperatures slowly rose to 150°F, and there was little or no heat transferred from the supply coil to the air stream. A definitive cause for this behavior has yet to be determined. The TRNSYS simulation predicted a total heat recovery (heating plus cooling energy) of 3.1074 E09 Btu for AHU6. Because of the heat recovery fault, a total of only 2.0294 E09 Btu was recovered by that system for the year, leaving a difference of 1.078 E09 Btu (heating) that could potentially have been recovered.

As calibration of the heat recovery coils revealed that the TRNSYS simulation tends to overestimate the heat recovered by the system, a more conservative value could be

assigned to the heat recovery fault by scaling the TRNSYS results by 90%. 90% of the TRNSYS result is 2.797 E09 Btu, leaving a difference of 7.673 E08. At the steam capital rate of $8.59 per million Btu of steam, that would total $9,260 in steam costs due to the failed heat recovery system. Using the more conservative energy impact estimate, the associated cost is $6,591.

It is harder to assign a cost to a malfunctioning pressure transducer that was discovered in AHU3. Most of the financial cost should be assigned to wear and tear on the motors and actuators in the unit, or to occupant discomfort. While a small amount of excess outside air was conditioned when the return fan reverted to its minimum setting, because of the supply fan setting and the minimum outside air flow requirement, the actual excess air likely only totaled a few thousand cfm. However, it is possible that the zone was over pressurized during this time and the oscillations of the supply and return fans and resulting noise were uncomfortable for the zone occupants.

Review of the air flow and temperature distributions for the AHUs in this one campus facility detected operational faults with an associated cost estimated at more than $50,000 per year. Compared to the facilities' operating budget, this is small. However, the faults detected here were common faults. With 54 buildings on campus classified as research facilities, it is likely that an energy monitoring program could be cost effective. It is important for such a program to be simple and to require very little time of the facilities management staff.

7.2 Energy and Cost Impact of Control Modifications Investigated Using Building Simulation

While building simulation is likely to be too time-consuming to be included in a campus wide energy monitoring program, it can be an extremely useful tool. If control or design conditions are being considered for existing campus facilities, simulation can provide insight into the systemic affects of the proposed alterations. Simulation can be used for new construction to compare designs and to demonstrate their functionality and energy efficiency.

Building simulations should be carefully calibrated. In the current project, some data that would have been most useful for calibrating the AHU chilled water coils (supply air relative humidity levels) were not archived. Thus, while it can be concluded that the increased discharge air temperature increases the zone relative humidity by up to 10%, it can't necessarily be concluded that the control changes would result in unacceptably high humidity levels. If 60% relative humidity is considered the upper limit for occupant comfort and the measured zone relative humidity rarely surpasses 50%, a 10% increase in relative humidity may be acceptable. Closer calibration of the amount of moisture removed by the chilled water coils would be useful for more closely modeling the actual humidity effects of the discharge air temperature change.

The estimated cost and energy impacts of reducing the minimum flow rates in AHU3 and AHU5 to their design levels, decreasing the discharge air temperature of AHU5 to 50°F, and increasing the discharge air temperature for all other building AHUs to 60°F are presented in Table 7.3. Because on the potential for saving over $200,000 annually, further investigation into the humidity effects of this temperature change are warranted.

Table 7.3 Energy and Cost Impact of Simulated Control Alterations

Design Minimum Flows	Difference [Btu]	Savings [$]	Savings, Capital Costs Included [$]
Chilled Water	7.306 E09	$90,839	$157,385
Zone Heating	9.253 E09	$59,592	$79,487
Steam Coils	-3.356 E09	-$21,614	-$28,830
Total	**1.320 E10**	**$128,816**	**$208,042**

7.3 Recommendations

7.3.1 Submeter Campus Building Steam and Chilled Water Usage

Rennebohm Hall was selected for study, in part, because it has whole-building steam metering. Many other campus buildings do not have such metering equipment installed. Identifying usage patterns and rates would allow for better energy monitoring which could save substantial amounts of energy.

In order for an energy monitoring program to be successful, the actual daily or monthly monitoring procedures must be simple and quick. The availability of measured heating and cooling energy flows to the building mechanical systems would allow comparison with energy flows calculated using temperature differences in the AHUs and air flow rates. Metered data would aid in verifying suspected leaking valves and simultaneous heating and cooling. By keeping historical data, unusual seasonal energy usage patterns can be monitored and investigated. And, the effects of efficiency improvements could be tracked.

In addition to aiding energy monitoring at the building level, steam and chilled water metering would allow better campus-wide energy monitoring. The buildings on the University of Wisconsin-Madison campus use significantly more fossil fuel energy per

square foot than at other University of Wisconsin campuses (see Figure 1.5). This number has changed very little from year to year, even with the Wisconsin Energy Initiative program the state participated in. It is likely that the lack of change in energy consumption per square foot under the Wisconsin Energy Initiative is due to the increasing ratio of research buildings to classroom and office buildings on campus. However, without careful metering of steam and chilled water distribution, this assertion cannot be verified.

It is important to individually meter process loads and building loads. Presumably, process loads are not to be targeted for efficiency improvements and energy monitoring. It is the building systems that should be monitored for opportunities to increase efficiency. While the whole building steam and chilled water consumption should be tracked for campus wide energy monitoring, it is also important to submeter the flows dedicated to the mechanicals.

7.3.2 Rennebohm Hall Recommendations

There are a few recommendations specific to Rennebohm Hall that could significantly improve the data monitoring potential for this building. Some of the most important improvements are those that would provide information to allow tracking of the energy flows in and out of the building. For example, it was discovered from the building control drawings that the chilled water return temperature sensor was not located appropriately. The chilled water return temperature should be measured after the flows to the equipment process load and to the building loads are merged. The process cooling load in Rennebohm Hall can be calculated separately from existing measurements. If this whole building load is measured, then the cooling load for the mechanical system could be calculated. This and other specific building recommendations are detailed in Table 7.4.

Table 7.4 Rennebohm Hall Recommendations for Improved Energy Measurement

Recommendation	Result
Replace or repair the steam condensate meter.	Allow verification of the steam flow measurement.
Measure the condensate temperature leaving the building.	Allow more accurate whole building steam energy usage calculations.
Measure the chilled water return temperature after the mixing of the equipment and building return flows	Allow calculation of the whole building cooling energy usage.
Submeter the building process steam flow and process condensate return temperature.	Allow separate tracking of the building mechanical system heating loads and process heating loads.
Measure the air temperature in each AHU between the steam coil and the chilled water coil.	Permit detection of leaking steam valves even when a unit is in cooling mode.
Measure the glycol return temperature for the heat recovery system after the three way mixing valve for each heat recovery loop.	Allow calculation of the fraction of glycol that bypassed the coil, and improve the system frost control.

7.3.3 Data Access and Archival

The data collected by the University building automation system are valuable and could be utilized more completely. This project has demonstrated that there can be a benefit to archiving and analyzing historical data. Currently, data that are not specifically selected for archival cycle out of the BAS system after 48 hours and are not saved. However, since there is a substantial initial cost for instrumenting each data point and data storage is relatively inexpensive, all data related to building energy and building functionality should be automatically archived. In addition, it could be beneficial to building managers and energy monitors to have read-only access to the BAS directly. Currently such access is restricted. However, allowing such access could increase knowledge of building functionality, and increase fault detection capability.

7.3.4 Directions for Future Work

The results of this project suggest potential directions for future research. Based on the estimated cost and energy savings of increasing the discharge air temperature for all but the Tower Offices zone, further investigation into the effects on zone humidity is warranted. This option may include investigation of the potential for adding desiccant dehumidification to the building or to select zones. Desiccant dehumidification could separate the building dehumidification and cooling needs. Research into the cost and parasitic loads of these systems is warranted.

The laboratory zones in Rennebohm Hall are designed to maintain large flow rates of 100% outside air constantly. The high flow rates and the lack of recirculating air are implemented out of concern for occupant safety and air quality. However, if the laboratory zone air flow rates could be reduced or varied based on occupancy or loading, the resultant energy savings would be substantial. It would be interesting to explore the energy implications and air quality affects of alternative laboratory air flow requirements and control strategies.

If research or experience indicate that laboratory air quality could not be maintained at reduced flow conditions or with variable air volume control, it would be interesting to explore the implications of restricting laboratory access and instituting a night set-back for the Tower Laboratory and Teaching Laboratory AHUs. Such a policy would not be possible for the Vivarium because of the animal research conducted in that zone. Restricting access to laboratory space would require changes in occupant behavior and would affect the way research is conducted in these zones. While the changes in behavior that would be required for such an energy conservation plan may not be acceptable for this building, zoning of

future laboratory space should be carefully considered to reduce laboratory ventilation requirements.

Lastly, this project has described the potential benefits to systematically monitoring campus building energy. To simplify the energy monitoring process, an automated system should be created to generate monthly building reports. Automated monitoring would involve programming the Johnson Controls Metasys system to compile the required data, or programming another computer system to mine archived Metasys data. In addition, a user interface for entering building system design information should be created. To further automate the fault detection process, research into the benefits of a rule-based algorithm or other statistical algorithms could be beneficial.

References

ASHRAE. 2000. “Fans”. 2000 *ASHRAE Handbook – Systems and Equipment.*. American Society of Heating, Refrigerating and Air-Conditioning Engineers, Inc.

ASHRAE. 1989. “Commissioning of HVAC Systems”. *ASHRAE Guideline 1-1989*. American Society of Heating, Refrigerating and Air-Conditioning Engineers, Inc.

ASHRAE. 2005. “Engineering Analysis of Experimental Data”. *ASHRAE Guideline 2-2005*. American Society of Heating, Refrigerating and Air-Conditioning Engineers, Inc.

ASHRAE “Standard Energy Efficient Design of New Buildings Except Low-Rise Residential Buildings”. ASHRAE 90.1-1989. American Society of Heating, Refrigerating and Air-Conditioning Engineers, Inc.

Balco Balancing Inc., 2001. School of Pharmacy Certified Test, Adjust, and Balance Report. 8/01. 3135 Sundew Way, Neenah, WI.

Braun, James E. 2003. “Automated Fault Detection and Diagnostics for Vapor Compression Cooling Equipment”. *Journal of Solar Energy Engineering.* Vol 125, August, 2003.

Breuker, Mark S., Braun, James E. 1998. “Evaluating the Performance of a Fault Detection and Diagnostic System for Vapor Compression Equipment.” *HVAC&R Research*. Vol. 4, No. 4, pp 401-425.

Breuker, Mark S., Braun, James E. 1998b. “Common Faults and Their Impact on Rooftop Air Conditioners”. *HVAC&R Research.* Vol. 4, No. 3, pp 303-318.

Chen, Bin, Braun, James E. 2001. “Simple Rule-Based Methods for Fault Detection and Diagnostics Applied to Packaged Air Conditioners”. *ASHRAE Transactions* Vol. 107, No. 1, pp 847-857.

Claridge D.E., Haberl, J., Liu, M., Houcek, J., and Athar, A., 1994. “Can You Achieve 150% of Predicted Retrofit Savings: Is It Time for Recommissioning?” *ACEEE 1994 Summer Study on Energy Efficiency In Buildings Proceedings: Commissioning, Operation and Maintenance*, Vol. 5. American Council for an Energy Efficient Economy, Washington D.C., pg 73-87.

Claridge, David E., Culp, Charles H., Liu, Mingsheng, Deng, Song, Turner, W.D., and Haberl, J.S.. 2000. “Campus-Wide Continuous Commissioning of University Buildings.” *ACEEE 2000 Summer Study on Energy Efficiency in Buildings Proceedings: Commercial Buildings: Technologies, Design, and Performance Analysis.* Vol. 3, American Council for an Energy-Efficient Economy, Washington D.C., pp 101-112.

Claridge, David E., Turner, W.D., Liu, Mingsheng, Deng, Song, Wei, Guanghua, Culp, Charles H., Chen, Hui, Cho, SoolYeon.. 2004. "Is Commissioning Once Enough?" *Energy Engineering*. Vol. 101, No. 4, pp 7-19.

DOA, 2005. *Energy Use in State-Owned Facilities, Fiscal Year 2004.* State of Wisconsin Department of Administration, Division of Energy. DOA-4701P(R10/04). February, 2005. http://www.doa.state.wi.us/docs_div_list.asp?divid=5&agencyid=68

Dodds, Debby, Baxter, Eric; Nadel, Steven, 2000. "Retrocommissioning programs: Current efforts and next steps". *Proceedings ACEEE Summer Study on Energy Efficiency in Buildings*, Vol. 4, pp 479-493.

ENERGY STAR Home Page. Nov. 18, 2005. http://www.energystar.gov/index.cfm?c=about.ab_index

Energy Information Agency (EIA) 2003. Table E.1 World Total Primary Energy Consumption (Quadrillion Btu), 1980-2003. *International Energy Outlook 2003*. Table Posted July 1 2005. http://www.eia.doe.gov/pub/international/iealf/tablee1.xls

Energy Information Agency (EIA) 2004. *Annual Energy Outlook 2004*. http://www.eia.doe.gov/oiaf/archive/aeo04/index.html

Energy Policy Act of 1992, Public Law 102-486.

European Commission, 2005. *Energy: Yearly Statistics 2003*. Luxembourg: Office for Official Publications of the European Communities, October 26, 2005. http://epp.eurostat.cec.eu.int/cache/ITY_OFFPUB/KS-CN-05-001/EN/KS-CN-05-001-EN.PDF

The European Parliament and the Council of the European Union, 2003. "Directive 2002/91/EC of the European Parliament and of the Council of 16 December 2002 on the Energy Performance of Buildings". Official Journal of the European Communities Vol 4, No. 1, pp 65-71.

Executive Order 99-13123 (1999).

GAO 2005. *Energy Savings Performance Contracts Offer Benefits, but Vigilance is Needed to Protect Government Interests.* United States Government Accountability Office Report to Congressional Requesters. GAO-05-340. June, 2005.

Gregerson, Joan, 1997. "Cost Effectiveness of Commissioning 44 Existing Buildings" *Proceedings of the 5th National Conference on Building Commissioning*. PECI.

Grimmelius, Hugo T., Meiler, Peter P., Maas, Hans L.M.M., Bonneir, Bas, Grevink, Jasper S., van Kuilenburg, Robert F. 1999. "Three State-of-the-Art Methods for Condition Monitoring". *IEEE Transactions on Industrial Electronics*. Vol 46, No.2. pp 407-416.

Haasl, Tudi and Sharp, Terry. 1999. "A Practical Guide for Commissioning Existing Buildings." Office of Building Technology, State and Community Programs, U.S. DOE. ORNL/TM-1999/34

Hall, Dee J.. "Is State Really Saving Energy?" *Wisconsin State Journal* Jul. 10, 2005: 1, A12.

Herzog P. and Lavine L, 1992 "Identification and quantification of the Impact of Improper Operation of Midsize Minnesota Office Buildings on Energy Use: A Seven Building Case Study." *Proceedings from the ACEEE 1992 Summer Study on Energy Efficiency in Buildings*, Vol 3. ACEEE, Washington DC, August 1992.

Holowka, Taryn. "391 Million Square Feet of Building Space Going for LEED." *USGBC News* Nov. 18, 2005. Nov. 30, 2005. <http://www.usgbc.org/News/usgbcnews_details.asp?ID=1950&CMSPageID=161>

House, John M., Vaezi-Nejad, Hossein, Whitcomb, J. Michael. 2001. "An Expert Rule Set for Fault Detection in Air-Handling Units". *ASHRAE Transactions* Vol. 107, No. 1, pp 858-871

Incroprera, Frank P., Dewitt, David P., 2002. *Introduction to Heat Transfer*. John Wiley & Sons, New York. 4th ed.

Katipamula, Srinivas, and Brambley, Michael R. 2005. "Methods for Fault Detection, Diagnostics, and Prognostics for Building Systems—A Review, Part I". *HVAC&R Research*. Vol. 11, No. 1, pp3-25.

Lang, Bob. Memo to the Members of the Joint Committee on Finance, Legislative Fiscal Bureau, State of Wisconsin, June 30, 2004. http://www.legis.state.wi.us/lfb/Section1310/063004_uw_11.pdf

Lawrence Berkley National Laboratory (LBNL) 2005. Window 5.2a v5.2.17a

Mitchell, John W., Braun, James E. 2006. *Design, Analysis, and Control of Space Conditioning Equipment and Systems.* In Progress.

Rossi, T.M. and Braun, J.E. 1997. "A Statistical, Rule-Based Fault Detection and Diagnostic Method for Vapor Compression Air Conditioners". *International Journal of HVAC&R Research*. Vol. 3, No. 1, pp 19-37.

Thermal Energy System Specialists (TESS), 2004. "Type 684: Air Side Economizer". *TRNSYS 16 TESS HVAC Library Documentation.*

Thermal Energy System Specialists (TESS), 2004b. "Type 752: Simple Cooling Coil". *TRNSYS 16 TESS HVAC Library Documentation.*

Thermal Energy System Specialists (TESS), 2004c. "Type 754: Heater/Humidifier". *TRNSYS 16 TESS HVAC Library Documentation.*

Thermal Energy System Specialists (TESS) http://www.tess-inc.com. accessed May 14, 2006.

Solar Energy Laboratory (SEL), TRANSSOLAR, Centre Scientifique et Technique du Bâtiment (CSTB), 2004. *TRNSYS 16: a TRaNsient SYstem Simulation program, Volume 5 Mathematical Reference*. Solar Energy Laboratory, University of Wisconsin, Madison. http://sel.me.wisc.edu/trnsys.

United States Code (USC) Chapter 42, Section 8253

Werre, Rick J. 2005. University of Wisconsin – Madison: Annual Electrical Distribution Report for the Period of July1, 2004 through June 30, 2005.

Appendix I

Table AI.1: Data Collected in the Vivarium Zone

System	Data Name	Description	Units
PHR_AH1 AHU 1	C-VLV	Cooling Valve Position	% Open
	DA-T	Discharge Air Temperature	°F
	FILT-DP	Filter Differential Pressure	Inches H_2O
	GLS-T	Glycol Supply Temperature, Heat Recovery	°F
	HR-T	Air Temperature after Heat Recovery Coil	°F
	HR-VLV	Humidifier Valve Position	% Open
	HTG-C	Heating Coil Valve Position	% Open
	OA-T	Outside Air Temperature	°F
	SF-SPEED	Supply Fan Speed – VFD Command	Hz
PHR_AH2 AHU 2	C-VLV	Cooling Valve Position	% Open
	DA-T	Discharge Air Temperature	°F
	FILT-DP	Filter Differential Pressure	Inches H_2O
	GLS-T	Glycol Supply Temperature, Heat Recovery	°F
	HR-T	Air Temperature after Heat Recovery Coil	°F
	HR-VLV	Humidifier Valve Position	% Open
	HTG-C	Outside Air Temperature	°F
	SF-SP	Supply Fan Speed – VFD Command	Hz
PHR_AH12 AHU 1 & AHU 2	HUM-VLV	Humidifier Valve Position	% Open
	OA-HUM	Outside Air Humidity	RH
	SF-VFD	Supply Fan VFD	Hz
	SYS-SP	System Static Pressure in Duct	Inches H_2O
PHR_HRM1 HRM 1	LEF-DPR	Laboratory Exhaust Fan Damper Position	% Open

Table AI.2: Data Collected in the General Zone

System	Data Name	Description	Units
PHR_AH3 AHU 3	C-VLV	Cooling Valve Position	% Open
	DA-T	Discharge Air Temperature	°F
	DA-VP	Discharge Air Velocity Pressure	Inches H_2O
	HFR-VLV	Humidifier Valve Position	% Open
	HTG-C	Heating Coil Valve Position	% Open
	MA-T	Mixed Air Temperature	°F
	MOA-CFM	Air Flow–Minimum Outside Air Damper	cfm
	MPOS-VP	Min. Outside Air Damper Velocity Pressure	Inches H_2O
	RA-CFM	Measured Return Air Flow	cfm
	RA-H	Return Air Humidity	RH
	RA-T	Return Air Temperature	°F
	RA-VP	Return Air Velocity Pressure	Inches H_2O
	RF-SP	Return Fan VFD Command	Hz
	SA-CFM	Measured Supply Air Flow	cfm
	SF-SP	Supply Fan VFD Command	Hz
	SYS-SP1	System Static Pressure in Duct	Inches H_2O
	SYS-SP2	2nd System Static Pressure Measurement	Inches H_2O

Table AI.3: Data Collected in the Teaching Lab Zone

System	Data Point	Description	Units
PHR_AH4 AHU 4	C-VLV	Cooling Valve Position	% Open
	DA-T	Discharge Air Temperature	°F
	HFR-VLV	Humidifier Valve Position	% Open
	HMAN-VLV	Humidifier Manifold Valve	% Open
	HTG-C	Heating Coil Valve Position	% Open
	LEF-DPR	Laboratory Exhaust Fan Damper	% Open
	LEF-SP	Laboratory Exhaust Fan Static Pressure	Inches H_2O
	SF-SPEED	Supply Fan VFD Command	Hz
	SYS-SP	System Static Pressure in Duct	Inches H_2O
	SA-CFM	Measured Supply Air Flow	cfm
	SF-SP	Supply Fan VFD Command	Hz
	SYS-SP1	System Static Pressure in Duct	Inches H_2O
	SYS-SP2	2nd System Static Pressure Measurement	Inches H_2O

Table AI.4: Data Collected in the Tower Office Zone

System	Data Name	Description	Units
PHR_AH5 AHU 5	C-VLV	Cooling Valve Position	% Open
	DA-T	Discharge Air Temperature	°F
	HFR-VLV	Humidifier Valve Position	% Open
	HTG-C	Heating Coil Valve Position	% Open
	MA-T	Mixed Air Temperature	°F
	OA-T	Outside Air Temperature	°F
	RA-CFM	Measured Return Air Flow	cfm
	RA-H	Return Air Humidity	RH
	RA-T	Return Air Temperature	°F
	RET-FLOW	Measured Return Air Flow	cfm
	RF-SPEED	Return Fan VFD Command	Hz
	RF-VFD	Return Fan VFD percentage	%
	SA-CFM	Measured Supply Air Flow	cfm
	SF-SPEED	Supply Fan VFD Command	Hz
	SF-VFD	Supply Fan VFD Percentage	%
	SUP-FLOW	Measured Supply Air Flow	cfm
	SYS-SP	System Static Pressure in Duct	In H_2O

Table AI.5: Data Collected in the Tower Lab Zone

System	Data Name	Description	Units
PHR_AH6 AHU6	C-VLV	Cooling Valve Position	% Open
	DA-T	Discharge Air Temperature	°F
	GLR-T	Glycol Return Temperature, Heat Recovery	°F
	GLS-T	Glycol Supply Temperature, Heat Recovery	°F
	HFR-VLV	Humidifier Valve Position	% Open
	HR-T	Air Temperature after Heat Recovery Coil	°F
	HR-VLV	Heat Recovery Valve Position	% Open
	HTG-C	Heating Coil Valve Position	% Open
	HVLV-OV	Humidifier Override	T/F
	OA-T	Outside Air Temperature	°F
	SF-SPEED	Supply Fan VFD Command	Hz
PHR_AH67 AHU 6 & AHU 7	SYS-SP4	System Static Pressure in Duct	Inches H_2O
PHR_AH7 AHU 7	C-VLV	Cooling Valve Position	% Open
	DA-T	Discharge Air Temperature	°F
	GLR-T	Glycol Return Temperature, Heat Recovery	°F
	GLS-T	Glycol Supply Temperature, Heat Recovery	°F
	HR-T	Air Temperature after Heat Recovery Coil	°F
	HR-VLV	Heat Recovery Valve Position	% Open
	HTG-C	Heating Coil Valve Position	% Open
	SF-SPEED	Supply Fan VFD Command	Hz

Tower Labs			
System	**Data Name**	**Description**	**Units**
PHR_HRM23 HRM 2 & HRM 3	EHRM2-H	Entering Air Humidity, HRM 2	RH
	EHRM2-T	Entering Air Temperature, HRM 2	°F
	EHRM3-H	Entering Air Humidity, HRM 3	RH
	FANS-ON	Number of Lab Exhaust Fans On	#
	HRM2-DPT	Entering Air Dew Point, HRM 2	°F
	HRM3-DPT	Entering Air Dew Point, HRM 3	°F
	LEF-DPR	Lab Exhaust Fan Damper Position	% Open
	LHRM2-T	Leaving Air Temperature, HRM 2	°F
	LHRM3-T	Leaving Air Temperature, HRM 3	°F
	SYS-SP1	System Static Pressure Reading #1	Inches H_2O
	SYS-SP2	System Static Pressure Reading #2	Inches H_2O
	SYS-SP3	System Static Pressure Reading #3	Inches H_2O
	SYS-SP4	System Static Pressure Reading #4	Inches H_2O

Table AI.6: Data Collected on Systems Serving the Entire Building

System	Data Name	Description	Units
PHR_HW Hot Water System	HW-DP	Hot Water Differential Pressure	Inches H_2O
	HWR-T	Hot Water Return Temperature	°F
	HWS-T	Hot Water Supply Temperature	°F
	HX-VLV	Heat Exchanger Valve Position	% Open
	P1-VFD	Pump 1 VFD Command	Hz
	P2VFD	Pump 1 VFD Command	Hz
	COND-F	Condensate Flow Totalization	lb_m/hr.
PRV_PHR Steam System	HSTM-P	High Pressure Steam Pressure	Psig
	HSTM-T	High Pressure Steam Temperature	°F
	STEAM-F	Steam Flow	lb_m/hour
PHR_CHW Chilled Water System	CH-DP	Chilled Water Differential Pressure	Inches H_2O
	CHW-F	Chilled Water Flow Rate	gpm
	CHWR-T	Chilled Water Return Temperature	°F
	CHWS-T	Chilled Water Supply Temperature	°F
	ECHS-T	Equipment Chilled Water Supply Temperature	°F

In addition to these 117 data points, there are at least 885 data points collected for room-level data. Many of these points are replicated in the BAS, tabulated in different time steps, or duplicated to appear both under the point-history and trend classifications.